UNIVERSIDADE FEDERAL DE PERNAMBUCO
CENTRO DE CIÊNCIAS BIOLÓGICAS
PROGRAMA DE PÓS-GRADUAÇÃO EM BIOQUÍMICA E FISIOLOGIA

SHEILA DE MELO BARROS

PREPARAÇÃO E CARACTERIZAÇÃO DE NANOCÁPSULAS PEPTÍDICAS DESTINADAS À VEICULAÇÃO DE COMPOSTOS TERAPÊUTICOS

ORIENTADOR: PROF. DR. EDUARDO I. CARNEIRO BELTRÃO (UFPE)

CO-ORIENTADOR: PROF. DR. J. M. TOMICH (KSU)

RECIFE
2016

SHEILA DE MELO BARROS

PREPARAÇÃO E CARACTERIZAÇÃO DE NANOCÁPSULAS PEPTÍDICAS DESTINADAS À VEICULAÇÃO DE COMPOSTOS TERAPÊUTICOS

Tese de Doutorado apresentada ao Programa de Pós-Graduação em Bioquímica e Fisiologia da Universidade Federal de Pernambuco-UFPE, como um dos requisitos para obtenção do título de Doutora em Bioquímica e Fisiologia pela Universidade Federal de Pernambuco.

Orientador: Prof. Dr. Eduardo I. Carneiro Beltrão.
Co-orientador: Prof. Dr. John M. Tomich.

RECIFE
2016

Catalogação na fonte:
Bibliotecário Rubens Leal de Azevedo Filho, CRB4-1432

B277p Barros, Sheila de Melo.
Preparação e caracterização de nanocápsulas peptídicas destinadas à veiculação de compostos terapêuticos / Sheila de Melo Barros. – Recife, 2016.
99 f.: il.; fig.; 30 cm.

Orientador: Eduardo Isidoro Carneiro Beltrão
Tese (doutorado) – UFPE. Centro de Biociências. Programa de Pós-graduação em Bioquímica e Fisiologia, Recife, 2016.
Inclui referências, apêndices e anexos.

1. Nanotecnologia. 2. Peptídeos 3. Nanocápsulas. 4. Branched Amphiphilic Peptide Capsules (BAPCs). I. Beltão, Eduardo I. Carneiro. (Orientador). II. Título

620.5 CDD (22.ed.) UFPE (BC2017/076)

Preparação e caracterização de nanocápsulas peptídicas destinadas à veiculação de compostos terapêuticos

SHEILA DE MELO BARROS

COMISSÃO EXAMINADORA

Prof. Dr. Eduardo Isidoro Carneiro Beltrão
Departamento de Bioquímica; LIKA – UFPE
(Orientador)

Prof. Dr. Luiz Bezerra de Carvalho Júnior
Departamento de Bioquímica; LIKA – UFPE
(Membro interno)

Profa. Dra. Maria Tereza dos Santos Correia
Departamento de Bioquímica e Fisiologia – UFPE
(Membro interno)

Profa. Dra. Adriana Fontes
Departamento de Biofísica e Radiobiologia – UFPE
(Membro externo)

Dra. Dijanah Cota Machado
Departamento de Fisiologia e Farmacologia – UFPE
(Membro externo)

Profa. Dra. Maria Danielly Lima de Oliveira
Departamento de Bioquímica; PPGIT – UFPE
(Suplente interno)

Prof. Dr. Claudio Gabriel Rodrigues
Departamento de Biofísica e Radiobiologia – UFPE
(Suplente externo)

Aprovada em: 25 / 10 / 2016

À minha mãe Rosa, que provavelmente nunca irá ter paciência suficiente para ler a minha tese, mas que me ouvia com atenção e carinho sempre que eu falava de Ciência, o que de fato começou aos meus oito anos, quando passei a descrever-lhe em detalhes cada um dos episódios fantásticos de “O Mundo de Beakman”.

AGRADECIMENTOS

Primeiramente a Deus, a quem consigo enxergar tanto nos textos sagrados, quanto no "intrincado código de quatro bases criptografado na forma 3 bilhões de letras do código genético humano".

Às minhas amadas "mães": minha mãe Rosa e minha vó Luiza, que costuma dizer que por ser vó é mãe duas vezes, por sua compreensão em momentos de ausência e por seu apoio incomparável na busca por meus sonhos.

À minha querida mãe na ciência Liliya Yuldasheva por me aceitar como filha em casa e no laboratório.

Ao professor Dr. Oleg Vladimirovich Krasilnikov, "*In memorian*", que estará sempre presente em minhas conquistas científicas, por ser o primeiro a me ensinar que posso fazer do trabalho o meu hobby e que a falha de um experimento pode significar o caminho para uma grande descoberta.

Ao meu adorável mentor, o professor J. M. Tomich, por acreditar em mim e me ensinar que "uma descoberta é feita quando apesar de vermos o que todo mundo vê, somos capazes de pensar o que ninguém pensou".

Ao meu querido orientador Eduardo I. Carneiro Beltrão, por sua "coragem de desbravador" ao aceitar a minha proposta de pesquisa e por me apoiar nesse projeto que mudou a minha forma de enxergar o mundo ao meu redor. Muito obrigada por acreditar em mim!

Ao professor Cláudio Gabriel Rodrigues, por seu suporte e compreensão durante a transição dos projetos e por seu exemplo de pesquisador e professor dedicado.

Ao professor Luiz Bezerra de carvalho Júnior, por sempre me inspirar com seu exemplo de criticidade construtiva e me ensinar o significado real de um líder que influencia com entusiasmo.

À minha amada amiga, conselheira e de modo informal "mentora científica" Maria Seabra (Cida), por me apresentar ao "Biotechnology Core" e por seu constante apoio ao longo desse projeto.

A Susan Whitaker por sua paciência e detalhadas explicações em cada fase do meu treinamento.

A Adriana Avila, Benjamin Katz e Pinakin Sukthankar por sua fundamental contribuição para os experimentos e escrita deste trabalho.

A Dijanah Machado, Juliana Aguiar, Gisely Albertin, e Layse Malagueta que mesmo a distância estiveram sempre ao meu lado, dispostas a ajudar no que fosse necessário.

À minha querida "Salsa family", por me proporcionar grandes experiências de amizade e me ajudar com toda a endorfina que eu precisava para escrever esse trabalho.

A Rosilene Rocha, por sua alegria e entusiasmo marcante que me serviram de "combustível" para as longas horas de escrita da tese e por adicionar Hakuna Matata ao meu "repertório musical de pré-defesa".

A toda a equipe do Laboratório de Biofísica de Membranas e Células Tronco Dr. Oleg Krasilnikov (LBM-CT) pelo apoio essencial na área científica e por me ajudar a construir os alicerces da minha carreira como cientista.

À Universidade Federal de Pernambuco, especificamente ao Programa de Pós-Graduação em Bioquímica e Fisiologia, pela acolhida e interesse demonstrado na execução e conclusão deste trabalho, e por todo o apoio recebido por parte da coordenação nas figuras das professoras Patrícia Paiva a quem expresso minha gratidão pelo encorajamento e incentivo e à professora Vera Lucia de Menezes Lima por suas palavras de motivação; e por fim aos integrantes da sua secretaria, em especial ao Djalma Gomes da Silva pela atenção e dedicação sempre pronto ajudar mesmo em meio muito trabalho.

À CAPES (Coordenação de Aperfeiçoamento de Pessoal de Nível Superior) pelo apoio financeiro, relativos ao auxílio Nacional e da bolsa do Programa de Doutorado Sanduíche no Exterior (PDSE), por meio das quais tive a oportunidade de execução do atual projeto de pesquisa.

E a todos aqueles que de alguma forma contribuíram para a realização deste trabalho e por me ajudarem a me tornar quem hoje sou.

“Uma descoberta consiste em ver aquilo que todo mundo viu, porém com a habilidade de pensar o que ninguém pensou.”

Albert Von Szent-Györgyi

RESUMO

Cápsulas peptídicas anfifílicas ramificadas ou do inglês, “Branched Amphiphilic Peptide Capsules” (BAPCs), são nanocápsulas formadas pela organização de dois peptídeos de diferentes tamanhos $(Ac\text{-}FLIVI)_2\text{-}K\text{-}K_4\text{-}CO\text{-}NH_2$ e $(Ac\text{-}FLIVIGSII)_2\text{-}K\text{-}K_4\text{-}CO\text{-}NH_2$ capazes de encapsular um grande número de diferentes moléculas. O atual trabalho teve como ponto de partida um estudo no campo do estado da arte, comparando e contrastando os diferentes nanocarreadores de última geração com os estudos até então publicados sobre as BAPCs, resultando na publicação: *“A review of solute encapsulating nanoparticles used as delivery systems with emphasis on branched amphipathic peptide capsules”*, DOI: 10.1016/j.abb.2016.02.027. Posteriormente, a pesquisa se voltou para a caracterização das BAPCs a partir da variação das proporções de seus peptídeos constituintes (1:0, 0.8:0.2, 0.5:0.5, 0.2:0.8 e 0:1) no intuito de avaliar a viabilidade de formação das nanocápsulas e suas propriedades físico-químicas características. Os testes de encapsulamento realizados por supressão de fluorescência do corante eosina Y revelaram a formação das cápsulas em todas as proporções utilizadas e que as mesmas permanecem estáveis na faixa de temperatura de 4 °C - 95 °C, ao mesmo tempo em que as BAPCs preparadas a 4 °C evidenciaram uma maior eficiência de encapsulamento quando comparadas àquelas preparadas a 25 °C e 37 °C. A análise da estrutura secundária por dicroísmo circular (DC) mostrou que os peptídeos em diferentes proporções resultam em cápsulas com estruturas secundárias características, indicando que $(FLIVI)_2\text{-}K\text{-}K_4$ é responsável pela conformação aleatória, enquanto que $(FLIVIGSII)_2\text{-}K\text{-}K_4$ mostra ser responsável pelos arranjos em folha beta. Paralelamente, os tamanhos determinados por espalhamento de luz dinâmico (DLS) revelaram a formação de BAPCs com um valor médio de 10 - 45 nm de diâmetro. Já os dados de voltametria (VC) cíclica sugerem que as BAPCs formadas por $(FLIVIGSII)_2\text{-}K\text{-}K_4$ apresentam a bicamada de menor espessura. Esta mesma sequência mostrou ainda o menor valor de citotoxicidade nos testes de citometria de fluxo (CF) e a maior taxa de transfecção quando utilizadas na entrega de um plasmídeo de 4.7 kb usado para a expressão de EGFP *in vitro.* Tais resultados destacam a habilidade de formar cápsulas estáveis de tamanhos desejados e estruturas variadas tornando as BAPCs atraentes candidatas para o transporte de ácidos nucleicos e potencialmente úteis para a entrega de compostos farmacológicos. Os resultados foram publicados por meio do artigo: *“Branched amphipathic peptide capsules: different ratios of the two constituent peptides direct distinct bilayer structures, sizes, and DNA transfection efficiency”*, DOI: 10.1021/acs.langmuir.7b00912.

Palavras-chave: BAPCs. Cápsulas peptídicas. Nanocarreadores. Entrega de fármacos. Entrega de DNA.

ABSTRACT

Branched Amphipathic Peptide Capsules (BAPCs) are nano-capsules formed from the spontaneous assembly of two different sized peptides $(Ac\text{-}FLIVI)_2\text{-}K\text{-}K_4\text{-}CO\text{-}NH_2$ and $(Ac\text{-}FLIVIGSII)_2\text{-}K\text{-}K_4\text{-}CO\text{-}NH_2$ able to encapsulate different solute molecules. This work initially focused on comparing and contrasting different state of the art nano-carriers with an emphasis on earlier BAPCs studies. This resulted in a publication*: "A review of solute encapsulating nanoparticles used as delivery systems with emphasis on branched amphipathic peptide capsules"*, DOI: 10.1016/j.abb.2016.02.027. Subsequently, the research focused on BAPCs characterization studies varying the ratios of the two peptides (1:0, 0.8:0.2, 0.5:0.5, 0.2:0.8, and 0:1) aiming to evaluate the viability of the capsules formation and their physical-chemical properties. The encapsulation efficiency tests using the self-quenching fluorescent dye eosin Y revealed all the ratios produced capsules that remain thermally stable in a range of 4°C - 95 °C, at the same time that the 4 °C showed the highest encapsulation efficiency when compared to the ones prepared at 25 °C and 37 °C. The secondary structures analyses made by circular dichroism (CD) showed that the different peptide ratios produce capsules with specific secondary structures indicating that the $(FLIVI)_2\text{-}K\text{-}K_4$ is responsible to lead the random coil conformation, while the $(FLIVIGSII)_2\text{-}K\text{-}K_4$ seems to be responsible for the beta-sheet arranges. In parallel, the sizes were determined by dynamic light scattering (DLS) and revealed that the different ratios yielded BAPCs that varied in size ranging from 10 - 45 nm in diameter. In addition, results obtained using Cyclic Voltammetry (CV) revealed that BAPCs formed from just $(FLIVIGSII)_2\text{-}K\text{-}K_4$ have the thinnest bilayer. The same sequence also displayed the lowest cytotoxicity at the Flow Cytometry (FC) analyses and the highest transfection efficiency when used to deliver a plasmid of a 4.7 kb responsible for the expression of EGFP in vitro. These results highlight the ability to prepare stable capsules of desired sizes and varied structures making the BAPCs currently attractive as a delivery vehicle for nucleic acids and encapsulated pharmacological compounds. The results were published: *"Branched amphipathic peptide capsules: different ratios of the two constituent peptides direct distinct bilayer structures, sizes, and DNA transfection efficiency"*, DOI: 10.1021/acs.langmuir.7b00912.

Key-words: BAPCs. Peptide Capsules. Nanocarriers. Drug delivery. DNA delivery.

LISTA DE FIGURAS

LISTA DE ABREVIATURAS

BAPCs	Cápsulas peptídicas anfifílicas ramificadas (Branched amphiphilic peptide capsules)
CAC	Concentração de agregação crítica (Critical assembly concentration)
CD	Dicroísmo circular (Circular dichroism)
CMC	Concentração micelar crítica
CV	Voltametria cíclica (Cyclic Voltammetry)
DAB	1,4-diaminobutano
DLS	Espalhamento de luz dinâmico (Dynamic Light Scattering)
DMPC	1,2-dimiristoil-sn-glicero-3-fosfocolina
DPPC	1,2-dipalmitoil-sn-glicero-3-fosfocolina
EGFP	Proteína verde fluorescente (Enhanced green fluorescent protein)
FC	Citometria de fluxo (Flow Cytometry)
FDA	Agência Norte Americana reguladora de fármacos e alimentos (Food and Drug Admiosnistration)
Fmoc	9-Fluorenil_metiloxicarbonila
ISO	Organização Internacional de Normalização (International Organization for Standardization)
ITC	Calorimetria de titulação isotérmica (Isothermal titration calorimetry)
LUV	Vesículas unilamelares grandes (Large unilamellar vesicles)
MET	Microscopia eletrônica de transmissão
MEVT	Microscopia eletrônica de varredura e transmissão
MLV	Vesículas multilamelares grandes (Multilamellar large vesicles)

NNI	Iniciativa Nanotecnológica Nacional (National Nanotechnology Initiative)
NSVs	(Non-ionic surfactant vesicles)
PEG	Polietilenoglicol
PCL	Poli (caprolactona)
PGA	Poli (ácido glicólico)
PLA	Poli (ácido láctico)
POPC	1-palmitoil-2-oleoil-sn-glicero-3-fosfocolina
PPI	Poli(propilenoimina)
PVA	Polivinil álcool
PVP	Poli-N-vinilpirrolidona
SDS	Dodecil sulfato de sódio (sodium dodecyl sulfate)
SMF	Sistema mononuclear fagocitário
TFE	Trifluoretanol
siRNA	Pequeno RNA de interferência (Small interfering RNA)
SLS	Espalhamento de luz estático (Static Light Scattering)
SRE	Sistema reticuloendotelial
SUV	Vesículas unilamelares pequenas (Small unilamellar vesicles)
TFA	Ácido trifluoracético (Trifluoroacetic acid)

SUMÁRIO

1 INTRODUÇÃO

Embora não exista ainda um real consenso quanto à definição de tecnologia e termos afins, a Portaria nº 3 de Maio de 2015, emitida pelo Ministério da Ciência e Tecnologia define a Nanociência e Nanotecnologia, respectivamente, como sendo a compreensão e controle da matéria e dos processos na escala nanométrica, geralmente, mas não exclusivamente, abaixo de 100 nanômetros.

Quando voltada para o estudo ou desenvolvimento de sistemas que envolvem material biológico (DNA, lipídios, enzimas, peptídeos, proteínas etc.) a nanotecnologia passa a ser chamada de "bionanotecnologia", tendo dentre as suas muitas aplicações, a pesquisa de dispositivos de diagnósticos, o desenvolvimento de vacinas e sistemas de liberação de fármacos, sendo alguns dos mais comumente estudados as micelas, lipossomas, niossomas, dendrímeros, vetores virais e nanocápsulas poliméricas (HILL, 1993; THOMAS et al., 2001; BOAS; HEEGAARD, 2004; PARVEEN et al., 2012; PABST et al., 2014; YASAM et al., 2014).

Estruturas transportadoras à base de lipídios, tais como micelas e lipossomas têm sido tradicionalmente propostas como preferenciais para a entrega de compostos bioativos em sistemas vivos (ALLEN, 2004). Tal escolha se deve principalmente ao fato de serem quimicamente semelhantes às membranas celulares e, portanto, biocompatíveis, além de sua versatilidade de tamanho devido à possibilidade de manipulação do número de lamelas e composição lipídica a depender das propriedades físico-químicas do fármaco (TORCHILIN, 2005; EDWARDS; BAEUMNER, 2006).

Apesar de suas vantagens, no entanto, as vesículas lipídicas ainda possuem limitações quanto à estabilidade, solubilidade e variabilidade estrutural (TORCHILIN et al., 2003).

Em se tratando da entrega de material genético, os vetores virais constituem-se em um dos mais utilizados devido principalmente à sua alta eficiência de transferência do material genético para células-alvo. Sua utilização como vetor é viabilizada em função da deleção de genes indispensáveis para a proliferação viral no intuito de bloquear a replicação do vírus e a continuidade do ciclo infeccioso, ao mesmo tempo em que promove a substituição destes por genes de interesse terapêutico (ROMANO et al., 2000).

Apesar disso, a entrega de material genético mediada por vírus apresenta efeitos indesejados como imunogenicidade (KAFRI et al., 1998; THOMAS et al., 2001), inespecificidade e mutagênese insercional (BAUM, 2003).

Nesse cenário, nanocápsulas formadas a partir de arranjos peptídicos têm se mostrado ferramentas promissoras para o desenvolvimento de sistemas de liberação de fármacos potencialmente seguros, uma vez que prometem superar problemas comumente encontrados em sistemas de entrega viral ou vesículas lípidicas (DISCHER; AHMED, 2006; GUDLUR, 2012).

Gudlur e cols. (2012) descreveram, pela primeira vez, um sistema de entrega de fármacos formado por vesículas similares a lipossomas, mas constituído inteiramente por peptídeos, capazes de armazenar soluções aquosas em seu interior. Tais vesículas, chamadas também de BAPCs, do inglês “Branched Anphiphilic Peptide Capsules”, são delimitadas por uma bicamada formada a partir de uma organização espontânea em meio aquoso de dois peptídeos curtos ramificados e anfifílicos.

Estudos realizados nos últimos anos têm demonstrado que esse tipo de nanocápsula apresenta vantagens consideráveis quando comparada aos sistemas lipídicos tradicionais tais como facilidade de síntese, estabilidade, resistência a altas temperaturas, à digestão proteolítica e dissolução. Podem, também, ser internalizadas por células de diferentes linhagens por meio de vias endocíticas em questão de horas e são capazes de escapar da via endossômica, resistindo à maquinaria de degradação celular (GUDLUR, 2012; SUKTHANKAR et al. 2013; SUKTHANKAR et al. 2015).

No trabalho atual foram ampliados os estudos de caracterização das BAPCs avaliando-se a viabilidade de formação das nanocápsulas ante a variadas proporções dos peptídeos constituintes, variabilidade de tamanho, caráter citotóxico e habilidade de entrega de plasmídeos de DNA, no intuito de viabilizar sua utilização, de forma segura e eficiente, como mecanismo de entrega de fármacos e produtos bioativos, bem como na veiculação de material genético destinado a processos de terapia gênica.

2 FUNDAMENTAÇÃO TEÓRICA

2.1 NANOTECNOLOGIA: CONCEITO E DESENVOLVIMENTO

Embora a concepção de que a matéria seja formada por átomos seja conhecida há mais de 2 mil anos, a noção do potencial de manipulação de compostos numa escala atômica é algo consideravelmente recente (TANIGUCHI, 1974; GOMES et al., 2015).

De fato, foi somente no ano de 1959, que se iniciaram as discussões em torno dos conceitos nanotecnológicos, quando em uma das conferências realizadas na reunião da Sociedade Americana de Física, no Instituto de Tecnologia da Califórnia, o físico norte americano Richard Phillips Feynman afirmou: "... os princípios da física não falam contra a possibilidade de se manipular substâncias átomo por átomo...", levantando a possibilidade de manipulação direta da matéria na escala atômica e molecular e estabelecendo-se assim, as bases iniciais para os estudos na área da nanotecnologia (FEYNMAN, 1960).

O prefixo "nano" em nanotecnologia é derivado da palavra grega 'νάνος' que significa anão e faz correspondência com a medida em nanômetro (nm), que por sua vez corresponde à bilionésima parte de um metro. Talvez a definição mais restrita do termo seja a do "National Nanotechnology Initiative" (NNI, Iniciativa Nacional de Nanotecnologia) que sugere a nanotecnologia como sendo a ciência, engenharia e tecnologia conduzida em nanoescala **(FIGURA 1)**, com tamanho médio de suas estruturas variando entre 1-100 nm (SILVA, 2004; NIKALJE, 2015).

Mais comumente, a nanotecnologia tem sido utilizada para se referir ao conjunto de estruturas projetadas a partir de estratégias do tipo "top-down", onde um material macroscópico é reduzido até atingir o nível de partículas nanométricas ou pelo método "bottom-up" que busca obter o mesmo resultado, porém utilizando átomos e moléculas como blocos de construção até se chegar a estruturas com algumas centenas de nanômetros de diâmetro (FAROKHZAD, 2009).

FIGURA 1. Escala nanométrica para fins comparativos das dimensões de dispositivos tecnológicos.

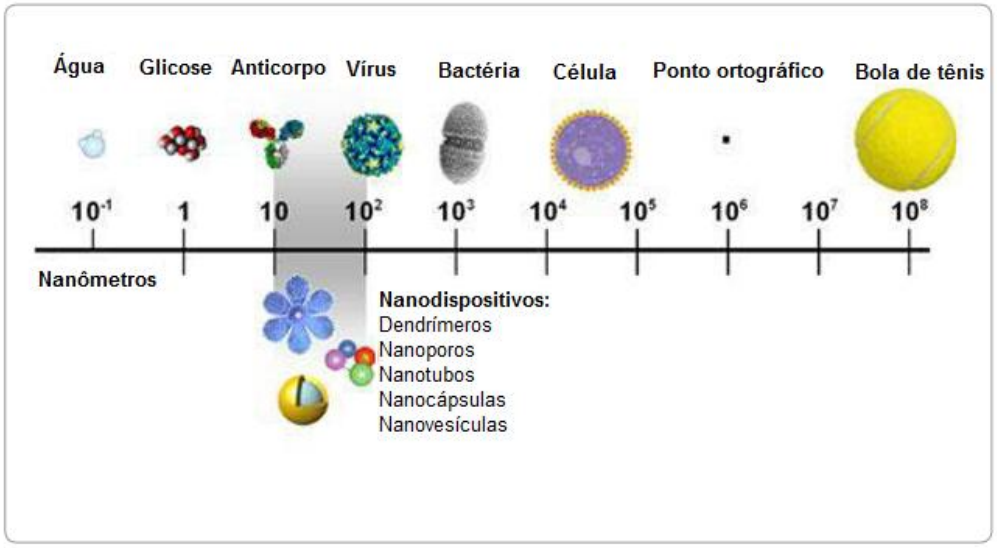

Fonte: Adaptado de YOUNG, 2007. Escala de comprimento variando de 10^{-1} nm a 10^{8} nm, exibindo em seus extremos as dimensões de uma molécula água e de uma bola de tênis. Na definição mais restrita (1-100 nm) os dispositivos manométricos se localizam na faixa que vai do tamanho médio de proteínas como os anticorpos (10 nm) a partículas virais (10^{2} nm). Quando considerada a definição mais ampla (1-1000 nm) tais estruturas podem chegar ao tamanho médio de uma bactéria (10^{3} nm).

Por se tratar, porém, de um campo multidisciplinar com produção de materiais de aplicações diversas, existe uma grande divergência quanto a uma definição precisa da nanotecnologia (PEREZ, 2012; NIKALJE, 2015).

Em 2014, o “Food and Drug Administration” (FDA), órgão governamental responsável pela regulação de fármacos e alimentos nos Estados Unidos, lançou um novo guia de avaliação utilizado na regulamentação de produtos de aplicações nanotecnológicas.

Nesse documento, o FDA deixe claro que não é de seu interesse estabelecer definições regulamentares de "nanotecnologia" ou termos afins. Em vez disso, a organização defende que baseado em sua compreensão técnica e científica do que seja nanomateriais e suas características, o FDA acredita que a segurança, eficácia, impacto na saúde pública ou o estado regulamentar dos produtos da nanotecnologia deve considerar todas as propriedades únicas e comportamentos que envolvam a aplicação da nanotecnologia e não apenas suas dimensões (FDA, 2014).

Dessa forma, o guia publicado identifica dois pontos a serem considerados nas etapas de avaliação da regulação de tais produtos, sendo considerados como critérios nessa avaliação:

(1) Se o material ou produto foi ou não projetado para ter, pelo menos, uma dimensão externa, ou uma estrutura ou superfície interna, na faixa da nanoescala (aproximadamente 1 nm a 100 nm);

(2) Se o material ou produto foi ou não projetado para apresentar propriedades ou fenômenos, inclusive propriedades físico-químicas ou efeitos biológicos, que possam ser atribuídos às dimensões nanométricas, ainda que estas fiquem de fora da faixa da nanoescala de até um micrômetro (1.000 nm).

Sob o ponto de vista do FDA, portanto, tanto um produto que se enquadre precisamente na escala de 1 a 100 nm, quanto um segundo que tenha uma dimensão superior à essa escala, mas que possua pelo menos uma de suas dimensões na escala nanométrica pode ser considerado um dispositivo nanotecnológico. Além disso, o documento emitido pelo FDA cita ainda o posicionamento da Organização Internacional de Normalização (ISO, do inglês “International Organization for Standardization”) que propõe que as considerações de saúde e segurança envolvendo nanomateriais não podem ser interrompidas à medida que simplesmente um produto atinge uma escala de dimensão de 100 nm. Segundo a ISO, como a produção de conhecimento é um processo de expansão constante, a definição de uma terminologia para a nanotecnologia precisa se adequar ao seu caráter amplo e multidisciplinar de aplicações, levando em conta fatores que consigam ir além de aspectos essenciais como forma e tamanho dos materiais nanoestruturados (ISO, 2010).

2.2 NANOTECNOLOGIA APLICADA À ÁREA DA SAÚDE

Devido ao seu caráter multidisciplinar, a nanotecnologia apresenta a possibilidade de aplicações em diversas áreas da ciência (MU; SPRANDO, 2010; NIKALJE, 2015), possibilitando a criação de materiais com características variadas. Sua utilização, porém, só é possível após uma avaliação específica de cada modelo criado na forma

nanoestruturada, de modo a permitir a disponibilidade de materiais seguros e de qualidade (DURAN et al., 2006; SUH et al., 2009).

Nos últimos anos, inúmeras pesquisas têm se voltado para a compreensão de processos biológicos e seus detalhados mecanismos de ação, a tradução desses achados em ferramentas terapêuticas eficientes, no entanto, é algo que ainda continua a desafiar a comunidade científica (DUNCAN, 2005; ALENCAR et al., 2013).

Dentre os muitos fatores a serem considerados no desenvolvimento de ferramentas tecnológicas de aplicação na área da saúde, encontram-se a preocupação com o tamanho, composição química e solubilidade, uma vez que tais características constituem-se em fatores decisivos nos processos de interações biológicas, bem como de seus subprodutos com o meio ambiente (MASSINI et al., 2014).

A razão pela qual a nanotecnologia é considerada uma ciência multidisciplinar se deve principalmente à sua complexidade e abrangência (CADIOLI; SALLA, 2006). Uma de suas muitas aplicações envolve o campo da nanobiotecnologia, que consiste em aplicar a nanotecnologia à manipulação de seres vivos ou de seus derivados biológicos, em geral no intuito de desenvolvimento de novos fármacos e ferramentas de diagnóstico e terapia de doenças, dando origem à chamada nanomedicina (DURÁN; DE AZEVEDO, 2002).

A nanomedicina pode ser definida como sendo a aplicação de recursos nanotenológicos no diagnóstico, tratamento e prevenção de doenças com a finalidade de promover e preservar a saúde humana (European Science Foundation's, 2005).

Dentre os muitos produtos desenvolvidos pela nanomedicina encontram-se os sistemas de liberação de fármacos, dos quais podemos destacar entre muitos, as micelas, lipossomas, niossomas, dendrímeros e nanopartículas poliméricas (polimersomas). Tais sistemas trazem consigo vantagens como a capacidade de reduzir o potencial tóxico e aumentar a eficiência terapêutica de muitas substâncias, principalmente devido ao aumento da estabilidade e solubilidade dos fármacos incorporados ao mesmo tempo em que podem viabilizar seu direcionamento ao sítio alvo da ação farmacológica (DUNCAN, 2005; TORCHILIN, 2006; CORTESI et al., 2007). Além disso, o tamanho bastante reduzido destes produtos lhes permite ultrapassar com menos dificuldade certas barreiras biológicas, facilitando a terapêutica de muitas patologias (FAHMY et al., 2005).

Nesse contexto, as pesquisas tecnológicas voltadas para o setor farmacológico enfrentam o grande desafio de desenvolvimento de métodos efetivos no que diz respeito à

liberação controlada de fármacos e sua aplicabilidade de um modo seguro e reproduzível (VASIR; LABHASETWAR, 2005; SHI et al., 2010).

Modelos convencionais de administração tais como: em gota, intravenosa, pílulas, pomadas, inalação etc., embora produzam bons resultados, a depender do local de ação e composição do fármaco podem apresentar uma eficácia reduzida, uma vez que podem culminar em uma metabolização antecipada da droga, além de gerar efeitos colaterais indesejados devido à ação inespecífica do medicamento (KIM et al., 2014). A via oral, por exemplo, comumente escolhida por ser menos invasiva, torna-se ineficiente em se tratando de medicamentos de natureza proteica ou peptídica, tendo em vista sua consequente degradação quando em contato com o ambiente ácido do estomago e rotas proteolíticas do trato digestivo (PAWAR et al., 2004; HAMMAN et al., 2005).

Durante a terapia sistêmica, os fármacos apresentam eficácia satisfatória, porém, frequentemente exibem inúmeros efeitos adversos (KINGSLEY et al., 2006).

Os sistemas de liberação controlada de fármacos são desenvolvidos no intuito de promover uma concentração plasmática ou tecidual do fármaco a uma velocidade controlada, de modo a se atingir o efeito terapêutico à medida que busca eliminar os riscos de inatividade farmacológica causada por dosagens inferiores (subterapêutica) ou ainda a superdosagem, responsável por causar efeitos tóxicos ao organismo **(FIGURA 2)** (TORCHILIN, 2005; PIMENTEL et al., 2007; CAMPOS, 2012).

FIGURA 2. Farmacocinética comparativa dos sistemas convencionais e sistemas de liberação controlada.

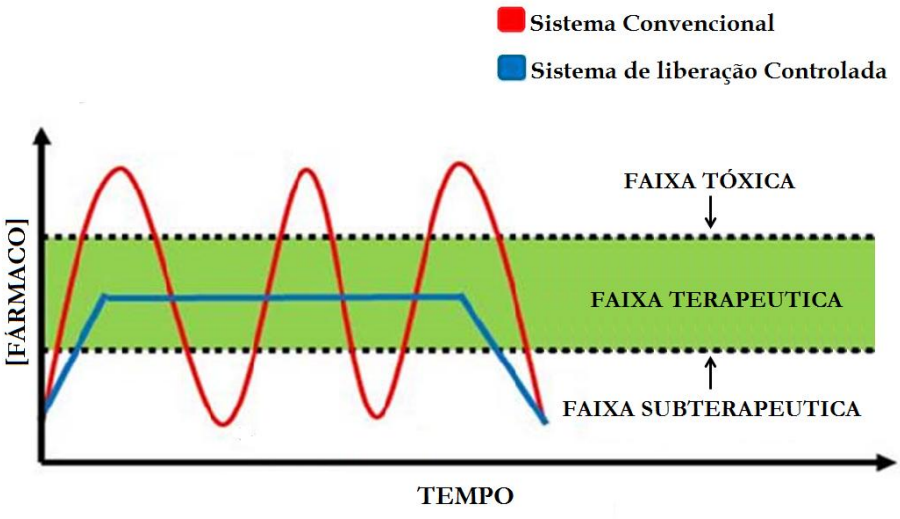

Fonte: Adaptado de CAMPOS, 2012.

Assim, embora tenhamos atualmente uma enorme gama de dispositivos e sistemas de carreamento de fármacos, a habilidade de alcance do sítio de ação específica do medicamento aliado à maximização do efeito terapêutico e redução dos efeitos colaterais ainda continua sendo um dos grandes desafios da indústria farmacêutica e comunidade científica atual (KINGSLEY et al., 2006).

2.3 NANOCARREADORES

2.3.1 Micelas

As micelas são estruturas formadas pela reunião de moléculas anfifílicas, cujas estruturas moleculares caracterizam-se por apresentar, no mínimo, duas regiões distintas, uma parte hidrofílica (polar) que tem afinidade com a água e uma outra hidrofóbica (apolar), com afinidade por lipídios **(FIGURA 3)**. Sua funcionalidade se deve à organização de suas cadeias, que se agrupam de modo a gerar um núcleo hidrofóbico, capaz de aprisionar moléculas igualmente hidrofóbicas em seu interior (DRUMMOND; FONG, 1999; LETCHFORD; BURT, 2007; XU et al., 2013).

FIGURA 3. Estrutura micelar resultante do arranjo de moléculas anfifílicas.

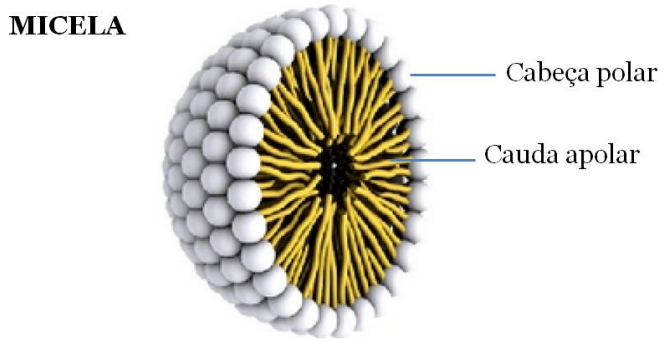

Fonte: Adaptado de BITOUNIS et al., 2012. Destaque na figura para a organização das moléculas anfifílicas, que se projetam de modo a exibir as caudas apolares (representadas em amarelo) unidas por meio de interações hidrofóbicas no centro, à medida que expõem as cabeças polares (representadas em branco) voltadas para a superfície onde interagem com o solvente hidrofílico na porção externa da micela.

Micelas naturais ocorrem de modo abundante na natureza e desempenham importantes papéis nos sistemas vivos, sendo as moléculas mais comuns a se organizarem seguindo esse padrão, os lipídios simples (constituídos apenas por ésteres de ácidos carboxílicos), lipídios complexos (fosfolipídios, esfingolipídios, etc.), ácidos biliares e derivados do colesterol (JOST et al., 1988).

Moléculas de surfactantes, como é o caso do detergente dodecil sulfato de sódio (SDS, do inglês "sodium dodecyl sulfate") podem se organizar formando uma variedade de diferentes nanoestruturas, dependendo da composição molecular e do sistema em que se encontram inseridas, sendo a organização micelar uma das mais comumente observadas (LIMA, 1998).

A transição da disposição das cadeias da forma monomérica para o estado de agrupamento é uma característica de micelas iônicas tanto de surfactantes aniônicos como catiônicos. Este fenômeno se deve principalmente à elevada organização das moléculas de água que induzem a associação das caudas hidrofóbicas, por sua vez, mantidas unidas por forças de Van der Walls à medida que tentam escapar da interação com as moléculas de água, na busca por conformações termodinamicamente estáveis (MARCONI, 1995; LIMA, 1998).

Quando, porém, dissolvidas em um ambiente apolar, a organização molecular ocorre no sentido de promover a minimização energética a partir de arranjos invertidos, ou seja, as caudas hidrofóbicas se voltam para o ambiente externo, consequentemente direcionando as cabeças polares para o interior e assim resultando nas chamadas "micelas reversas" (SANTOS, 2008).

Os primeiros estudos envolvendo sistemas micelares se voltaram basicamente para a indústria de detergentes e desinfetantes, bem como de agentes de flotação de minérios, estendendo-se posteriormente para a indústria metalúrgica e petroquímica, elaboração de aditivos alimentares, compostos farmacêuticos e cosméticos entre muitos outros (FENDLER, 1982; HILL, 1993).

As micelas lipídicas de um modo geral adotam um formato esférico e possuem um diâmetro médio de 1-100 nm, com um núcleo interno capaz de aprisionar fármacos lipofílicos em seu interior (LETCHFORD; BURT, 2007). O formato e o tamanho destas estruturas, porém, podem variar de acordo com a geometria molecular dos lipídios ou componente anfipático, bem como devido a fatores como concentração, temperatura, pH do meio e força iônica da solução, resultando em organizações

moleculares em forma de lamela, vesícula, ou tubo (cilindro) como demonstrado na **FIGURA 4** (SHEN et al., 1999; CHOUCAIR; EISENBERG, 2003; HSIAO et al., 2014).

FIGURA 4. Relação entre a geometria molecular do surfactante e suas respectivas estruturas de agregação.

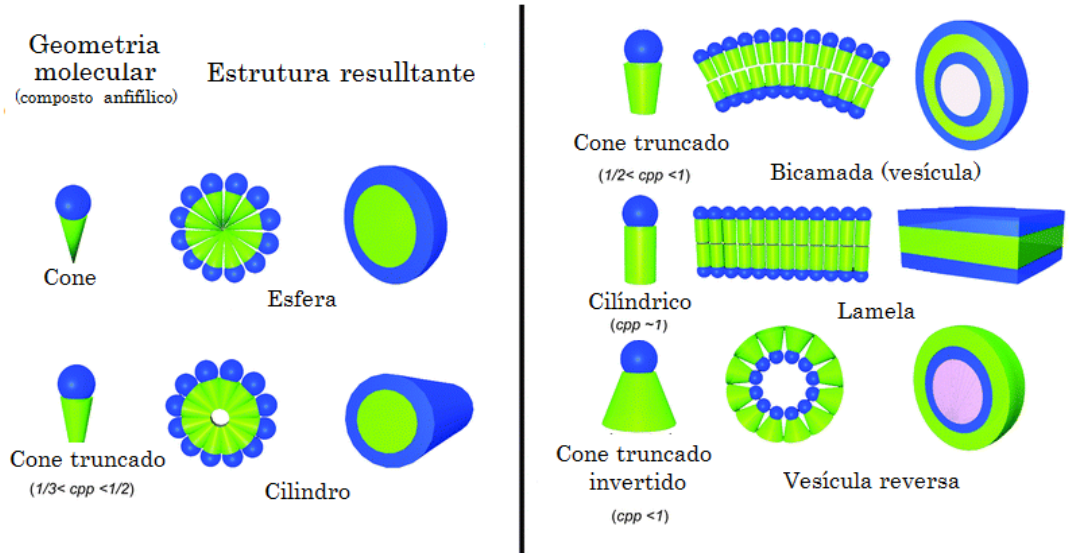

Fonte: Adaptado de RAMANATHAN et al., 2013.

É a partir do aumento da concentração, que as moléculas anfifílicas tendem a se agregar de uma forma mais organizada dando origem a bicamadas, micelas ou vesículas. Por se auto-organizarem de modo a gerar estruturas de caráter micelar, tal concentração é conhecida como concentração micelar crítica (CMC) e reflete, portanto, a concentração mínima em que as moléculas anfifílicas se organizam para formar micelas, sendo tal característica extremamente peculiar e dependente da constituição e propriedade de cada molécula (KATAOKA et al., 2001).

Quando em solução, os surfactantes iônicos atuam como eletrólitos fortes, a medida, porém que atingem a concentração micelar crítica, os monômeros se rearranjam espontaneamente de tal forma que adquirem uma conformação termodinâmica estável e solúvel ao mesmo tempo em que se observa uma série de mudanças nas propriedades físicas da solução. Desse modo, a formação de micelas pode ser detectada através de medidas da variação de propriedades físicas em função da concentração do surfactante, sendo as mais utilizadas: tensão superficial, condutividade elétrica, espalhamento de luz,

pH, pressão osmótica e solubilidade (FENDLER, 1982; SHAW, 1992; MANIASSO, 2001).

Micelas não poliméricas como as formadas por lipídios já são bem conhecidas e caracterizadas, as micelas poliméricas, por outro lado, são organizações micelares relativamente novas na área da pesquisa. Estruturalmente, seguem os mesmos parâmetros de agregação das micelas não poliméricas, diferindo apenas na incorporação de copolímeros em bloco de caráter biodegradável (LI; KWON, 2000; CHOUCAIR, 2003). Os copolímeros em bloco, por sua vez, são unidades de repetição linear de resíduos hidrofóbicos e hidrofílicos ligados covalentemente de modo a conferir um caráter anfifílico à molécula formada.

$K_{60}L_{20}$ é um exemplo de um copolímero dibloco, onde um polipeptídio composto por 60 resíduos de lisina é ligado covalentemente a um polipeptídio composto por 20 resíduos de leucina (HOLOWKA; POCHAN, 2005). Desse modo, o bloco de resíduos de leucina forma o segmento hidrofóbico do copolímero, enquanto os resíduos de lisina de carga positiva fornecem à molécula uma região de caráter mais hidrofílico.

Esta região da coroa hidrofílica externa tende a interagir com a camada de água ao redor, resultando numa aparência mais aberta das cadeias poliméricas de modo similar às cerdas de uma escova **(FIGURA 5)** (VONARBOURG et al., 2006). Tal organização confere às micelas uma aparência que lhes permite escapar do ataque fagocítico e possível destruição por parte do sistema reticuloendotelial (SRE). A finalidade do uso de micelas formadas por copolímeros em bloco surge, portanto, como uma forma de tentar minimizar problemas relacionados à solubilidade de fármacos hidrofóbicos, toxicidade e farmacocinética inapropriada (MIEDERER, 2008).

FIGURA 5. Modelo de uma micela polimérica.

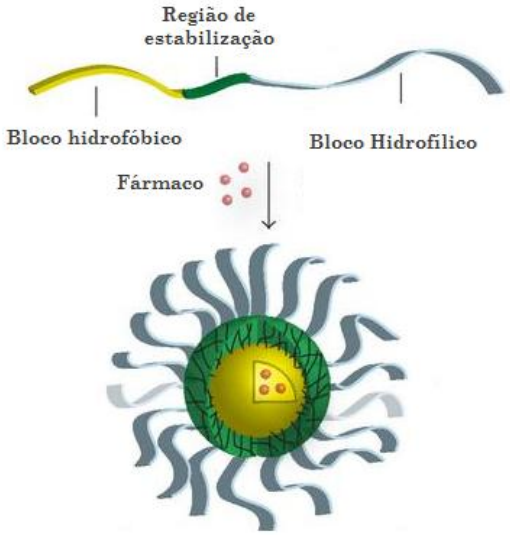

Fonte: Adaptado de RIOS-DORIA et al., 2012. O modelo descreve uma micela formada por um tribloco polimérico exibindo o núcleo hidrofóbico (em amarelo), uma região de estabilização micelar, formada por uma rede de polímeros intercruzados (em verde) e a região da coroa hidrofílica (em cinza).

Sem dúvida, um dos avanços mais significativos se deu com o desenvolvimento dessas estruturas acopladas a agentes anticancerígenos, seja a nível da composição das cadeias poliméricas constituintes da coroa ou mesmo por meio de moléculas sinalizadoras de superfície. Tal adaptação resulta em uma alteração positiva na biodistribuição e a farmacocinética de muitos compostos, o que significa um aumento do tempo de meia vida circulatória e da concentração do fármaco na região tumoral (BAE et al., 2005; MI et al., 2011).

Embora diversos copolímeros possam ser utilizados na formação de micelas, somente polímeros biodegradáveis e biocompatíveis encontram-se elegíveis para a produção de sistemas de aplicação terapêutica (ALLEN; CULLIS, 2004).

Existe atualmente uma grande variedade de polímeros utilizados para esse fim, sendo alguns dos mais empregados o Poli(etilenoglicol) (PEG), Poli(L-aminoácidos), poli(ácido lático) (PLA), poli(ácido glicólico) (PGA) e poli(ε-caprolactona) (PCL) (ADAMS; KWON, 2003; SINHA et al., 2004).

Sabe-se ainda, que micelas PEGuiladas apresentam o valor de CMC mais baixo que os surfactantes tradicionais resultando em baixa toxicidade celular e aumentam o tempo de

meia vida circulatória. Além disso, a elevada hidratação da região da coroa aliada à presença do núcleo hidrofóbico gera um gradiente de polaridade que auxilia na solubilização de uma variedade de compostos hidrofóbicos por mera associação física, sem que haja a necessidade de qualquer modificação na estrutura do composto farmacológico (LASIC et al., 1991; MOSES et al., 2003).

2.3.2 Lipossomas

Lipossomas são vesículas lipídicas esféricas formadas pela união de moléculas anfifílicas, em geral fosfolipídios, que se auto-organizam em água de modo a originar uma ou várias bicamadas lipídicas que se curvam sobre si **(FIGURA 6)**, acomodando as cabeças polares da camada lipídica interna de modo a gerar um compartimento aquoso no interior da estrutura esférica (DEMICHELI et al., 2005; SAMAD et al., 2007; XU et al., 2013). Os lipossomas são, possivelmente, o sistema de entrega de fármacos mais antigo e largamente utilizado, tendo sido estudado desde os anos 60 (SESSA; WEISSMANN, 1968) com a primeira administração tópica na década de 80 a partir do trabalho de Mezei e Gulasekharam (1980).

FIGURA 6. Estrutura esquemática de um lipossoma formado por fosfolipídios.

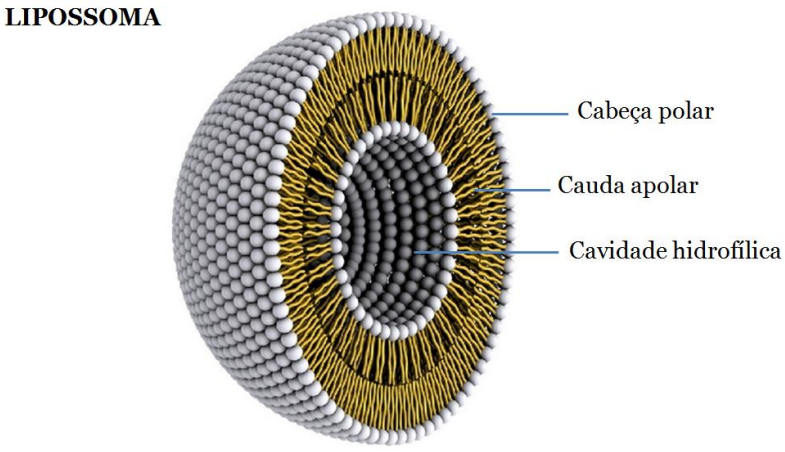

Fonte: Adaptado de BITOUNIS et al., 2012. De modo similar ao observado nas micelas, os lipossomas se formam a partir da organização das cabeças apolares dos lipídios (em branco) voltados para a superfície e em contato com o solvente hidrofílico, enquanto as caudas apolares

(em amarelo) se agrupam na porção interna, na tentativa de fugir da interação com o solvente, formando uma bicamada que se curva sobre si mesma e culmina com a formação de uma esfera com um núcleo hidrofílico em seu interior.

Lipossomas podem ser preparados com o emprego de uma grande variedade de fosfolipídios diacílicos incluindo: 1,2-dimiristoil-sn-glicero-3-fosfocolina (DMPC), 1,2-dipalmitoil-sn-glicero-3-fosfocolina (DPPC) e 1-palmitoil-2-oleoil-sn-glicero-3-fosfocolina POPC (ANDERSON; OMRI, 2004; SABÍNA et al., 2010; MIJAJLOVIC et al., 2013).

Dentre os vários aspectos considerados na classificação dos lipossomas, uma das mais tradicionais ocorre em função do tamanho e número de suas bicamadas constituintes. As SUV “small unilamellar vesicles”, são vesículas que possuem apenas uma bicamada, com diâmetro variando de 25 a 100 nm; enquanto que as LUV, “Large unilamellar vesicles” e MLV, “multilamellar vesicles” possuem diâmetro maior que 100 nm, sendo as LUV formadas por uma única bicamada lipídica enquanto que as MLV possuem múltiplas camadas (ANDREO-FILHO et al., 1999).

Em função de suas cadeias anfifílicas, os lipossomas podem armazenar o fármaco na camada lipídica ou em sua região hidrofílica, dependendo da afinidade da substância encapsulada (VEMURI; RHODES, 1995).

No interior da cavidade lipossomal ficam encapsulados os fármacos hidrossolúveis, onde são mantidos isolados do meio externo, ao mesmo tempo em que permanecem protegidos de reações com compostos do fluído orgânico, evitando degradação ou perca da atividade farmacológica. Já os fármacos de caráter lipofílico são aprisionados junto às cadeias apolares, agregando-se aos componentes estruturais da bicamada (ANDRADE et al., 2004).

Lipossomas possuem várias aplicações biológicas, cosméticas e farmacêuticas, sendo geralmente empregados em estudos relacionados à fisiologia celular, servindo como modelos de membranas celulares e veículos de entrega de fármacos (PABST et al., 2014).

Uma das grandes vantagens do uso de lipossomas como carreadores em sistemas biológicos diz respeito à sua capacidade de fusão com bicamadas lipídicas das membranas celulares bem como sua habilidade de penetração tecidual por meio de endocitose mediada por clatrinas (EWERT et al., 2005; HART, 2005; POLLOCK et al., 2010).

As vesículas do tipo lipossômica têm sido amplamente estudadas e moduladas para apresentar uma grande variação de características gerais, sendo as mais comuns, variações de tamanho, composição lipídica e carga superficial (SETHI, 2005).

Muitos desses estudos têm focado na modificação da superfície dos lipossomas clássicos como o objetivo de aumentar o tempo de meia-vida circulatória e sua capacidade de atingir alvos específicos. Tais modificações incluem a incorporação de polímeros dextranos lineares (NING et al., 2011), gangliosídios contendo ácido siálico (ALLEN; CHONN, 1987), polímeros hidrófilos como álcool polivinílico (PVA), (TAKEUCHI et al., 2001) polietileno glicol (PEG) (TORCHILIN, 2005) e poli-N-vinylpyrrolidona (PVP) (TORCHILIN et al., 2001), no intuito de estabilizar o sistema e proteger contra a degradação por parte do sistema mononuclear fagocitário (SMF).

Alguns desses estudos envolvem ainda a terapia alvo direcionada, tendo como exemplo a produção de lipossomas conjugados a anticorpos monoclonais por meio de moléculas de PEG e lipossomas a base de polímeros ligantes de proteases. Estes últimos podem ser enviados para o tecido alvo e ao entrar em contato com proteases associadas ao câncer sofrem desestabilização, permitindo a liberação do composto farmacológico no local do tumor (ZHANG, 2003; BASEL, 2011).

A entrega do conteúdo encapsulado pode seguir caminhos variados, dependendo do mecanismo ativado a partir da interação do lipossoma com a estrutura celular **(FIGURA 7).** O contato pode se dar tanto por meio de interação específica onde o lipossoma se liga à célula através de ligantes de superfície, quanto pela simples fusão dos lipossômicos à membrana celular. Outras possibilidades são: I) a de que ambas as membranas sofram desestabilização devido a algum componente membranar, resultando na liberação do conteúdo seguida da reestruturação da membrana ou II) a de que o fármaco entre na célula por micropinocitose, ou ainda por endocitose específica ou inespecífica. Uma vez dentro da célula, os lipossomas podem ser endocitados por lisossomas que ao liberar enzimas digestivas atuam rompendo a membrana do lipossoma permitindo assim a liberação de seu conteúdo no ambiente citoplasmático (TORCHILIN, 2005).

FIGURA 7. Representação esquemática da interação lipossoma-célula.

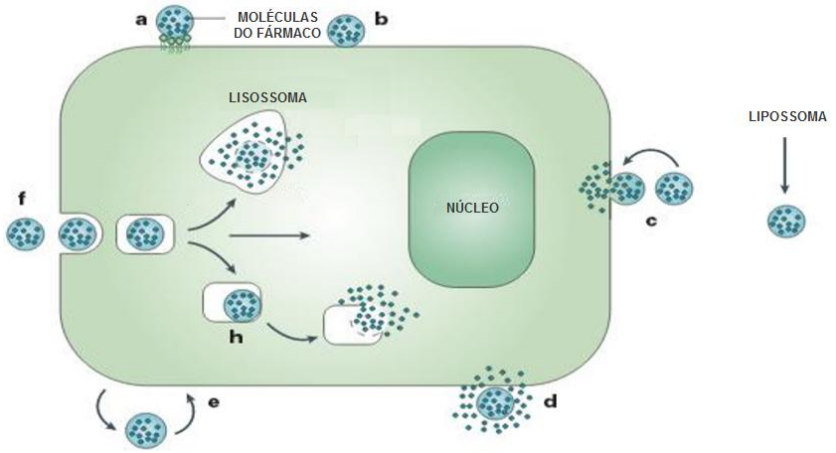

Fonte: Adaptado de TORCHILIN, 2005. **Representação esquemática da interação lipossoma-célula.** Interação de superfície a) de forma específica b) de forma inespecífica c) liberação do conteúdo encapsulado após desestabilização membranar d) liberação via micropinocitose e) endocitose específica f) material endossômico englobado no lisossoma g) desestabilização do endossomo seguida da liberação do fármaco no citoplasma.

Apesar da biocompatibilidade e ampla gama de aplicação dos liposomas, tem sido demonstrado que o transporte farmacológico por meio dessas vesículas pode levar a alterações nas propriedades farmacocinéticas e possíveis vazamentos da membrana com liberação do fármaco em áreas indesejadas do organismo. Por estes e outros motivos, novos estudos têm sido propostos no intuito de aprimorar o transporte por meio de vesículas lipídicas, bem como na elaboração de novos sistemas de carreamento capazes de promover a entrega segura e eficiente do conteúdo encapsulado (GABIZON et al., 2006).

2.3.3 Niossomas

Niossomas ou do inglês “non-ionic surfactant vesicles” (NSVs), são vesículas formadas por tensoativos não-iônicos de natureza natural ou sintética, capazes de originar estruturas lamelares nanoscópicas similares a lipossomas podendo, no entanto, apresentar ou não moléculas de lipídio em sua composição (UCHEGBU; VYAS, 1998; PARDAKHTY et al., 2007).

As primeiras vesículas formadas por niossomas foram desenvolvidas e patenteadas pela L'Oreal em meados da década de 70 e seus produtos introduzidos no mercado em

1987 por meio da Lacôme (VANLERBERGHE et al., 1978). Por se mostrarem mais estáveis que as vesículas formadas por fosfolipídios e apresentarem um baixo custo de produção aliado à facilidade de preparação e armazenamento, são candidatas bastante atraentes tanto para a indústria de cosméticos quanto farmacêutica, se mostrando como uma atraente alternativa para uso na liberação controlada de fármacos (KEMPS et al., 1988; UCHEGBU; VYAS, 1998; GIRIGOSWAMI et al., 2006).

As vesículas formadas por niossomas são capazes de armazenar tanto moléculas hidrofílicas quanto hidrofóbicas, podendo ser unilamelares ou multilamelares a depender dos compostos e métodos utilizados para a sua preparação (NASSERI, 2005).

Os niossomas são considerados vesículas elásticas capazes de sofrer deformação, fato que possibilita sua aplicação como carreador de fármacos para aplicação transdérmica, devido à sua habilidade de atravessar a camada córnea da pele (MISHRA et al., 2007). Já a inclusão de moléculas de colesterol na formulação, assim como é feita nos sistemas lipídicos, é capaz de fornecer uma maior rigidez à membrana ao mesmo tempo em que confere uma maior estabilidade ao sistema vesicular (NASSERI, 2005).

Os trabalhos publicados envolvem testes de diferentes tipos de tensoativos não-iônicos estando entre eles os éteres alquílicos de polioxietileno (PARDAKHTY et al., 2007), polissorbatos e ésteres de sorbitano (GIRIGOSWAMI et al., 2006).

De um modo geral, os niossomas possuem uma grande similaridade com os lipossomas, até mesmo no quis diz respeito à sua preparação, seguindo etapas de sonicação e aumento de pressão e temperatura, em uma metodologia bastante similar à aplicada na síntese lipossômica (KAZI et al., 2010).

Considerando, porém, que os surfactantes não-iônico são mais estáveis, e mais resistentes à oxidação do que os compostos à de base fosfolipídios, a preparação de niossomas é geralmente considerada mais barata e menos trabalhosa do que a dos seus homólogos lipossomais (MARIANECCI et al., 2013).

Os surfactantes não-iônicos secos podem ser usados na confecção de uma película fina para o revestimento de biomoléculas de carreadores solúveis em água constituindo os chamados “proniossomas”. Os proniossomas apresentam-se como um pó seco, que pode ser facilmente aplicado na confecção de comprimidos, cápsulas ou drágeas para admninistração unitária conveniente, ao mesmo tempo em que aumenta a eficiência de aprisionamento do fármaco e reduz a agregação e vazamento dos compostos armazenados (MARIANECCI et al., 2013; YASAM et al., 2014).

2.3.4 Dendrímeros

O termo “dendrímero” é derivado das palavras gregas *dendron* (árvore) e *meros* (porção). De um modo geral, os dendrímeros **(FIGURA 8)** podem ser definidos como estruturas poliméricas altamente ramificadas que se organizam em torno de um núcleo central, com forma, tamanho e comprimento das ramificações controladas e bem definidas (VOGTLE et al., 2000; NAAHIDI et al., 2013).

A síntese do dendrímero é feita a partir de um núcleo polifuncionalizado, que permite a adição de camadas crescentes de ramificações conhecidas como gerações (G), através de reações repetitivas que multiplicam a cada etapa o número de grupamentos funcionais da superfície (MAJOROS, 2008; SVENSON, 2009).

FIGURA 8. Modelo de um dendrímero de terceira geração.

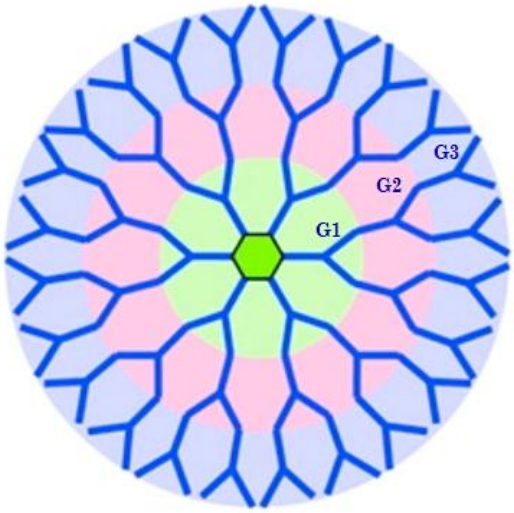

Fonte: Adaptado de ROSEN et al., 2009. O esquema exemplifica um dendrímero de terceira geração com destaque para o núcleo em verde e as sucessivas gerações (G1, G2 e G3) formadas a partir dos pontos de ramificação.

Dependendo do núcleo, sua estrutura tende a se organizar de modo a formar uma esfera com cavidades internas, dando origem a estruturas formadas por três partes constituintes: a) uma superfície multivalente, composta por um elevado número de sítios reativos, b) um extenso conjunto de ramificações localizado entre a superfície multivalente

e o núcleo e c) o núcleo central que serve como suporte para as ramificações poliméricas (HAWKER et al., 1993).

As estratégias de síntese usualmente empregadas envolvem os métodos de convergência ou divergência **(FIGURA 9).** No método divergente **(9A)**, desenvolvido por Tomalia (TOMALIA et al., 1986), os dendrímeros são sintetizados a partir do núcleo e aumentam pelo acréscimo sucessivo de novas gerações. O elevado número de reações realizadas por moléculas individuais em cada ponto de ramificação, no entanto, resulta em modificações moleculares que por sua vez acabam por gerar deformação na estrutura final do dendrímero (BOAS; HEEGAARD, 2004). A fim de contornar tal problema foi desenvolvida uma técnica que segue o caminho inverso, ou seja, o método convergente **(9B)**, sugerido por Hawker e Fretchét (HAWKER; FRETCHÉT, 1990) no qual o dendrímero é sintetizado a partir das extremidades em direção ao núcleo e consequentemente com um menor número de sítios reativos expostos.

FIGURA 9. Estratégias de síntese de dendrímeros.

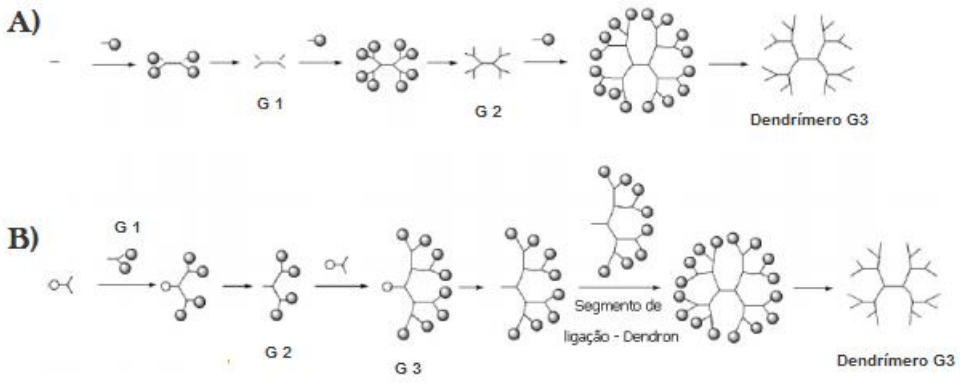

Fonte: Adaptado de BOAS; HEEGAARD, 2004. Os modelos descrevem em etapas, os métodos de síntese dendrimérica, ilustrando em A) O método divergente, no qual o dendrímero cresce a partir do centro em direção às extremidades e em B) O método convergente, onde o crescimento ocorre das extremidades para o centro da estrutura.

As cargas positivas presentes nas ligações de poliaminas e/ou poliamidas usadas para a construção dos dendrímeros indicam potencial para toxicidade celular e imunogenicidade. No entanto, a propagação parcial da superfície do dendrímero com moléculas de Polietileno Glicol (PEG) ou ácidos graxos exibe uma redução significativa na

toxicidade, protegendo as cargas positivas superficiais (JEVPRASESPHANT et al., 2003; NIGAVEKAR et al., 2004).

Foi somente a partir da década de 70 que se passou a ter a síntese laboratorial controlada de dendrímeros a fim de tornar possível a sua comercialização por empresas especializadas (TOMALIA, 1995). O primeiro tipo a ser produzido foram os dendrímeros a base de poliamidoamina, conhecidos como PAMAM e que passou a ser comercializado pela empresa Dendritech a partir da década de 80 (TOMALIA et al., 1985). Posteriormente novos polímeros passaram a ser testados, dando origem a marcas igualmente conhecidas no mercado como é o caso dos dendrímeros a base de poli(propilenoimina) ou PPI, também chamados de Astramol ou DAB-Am-X, comercializados pela SyMO, bem como os distribuídos pela POLYMER FACTORY, feitos a base de poliéster (BAREFIELD et al., 1980; ABHAY et al., 2003).

Entre os exemplos de estudos mais recentes demonstrando a eficiência de dendrímeros como sistemas carreadores, podemos citar os estudos que avaliam essas estruturas como mecanismos de transporte de fluorouracil (TRIPATHI et al., 2002) e indometacina (CHAUHAN et al., 2004).

2.3.5 Nanocápsulas poliméricas

De um modo cada vez mais frequente, nanocarreadores formadas a partir de arranjos de polímeros biodegradáveis têm sido propostos como promissores modelos de substituição de lipossomas e outros sistemas de entrega baseados em lipídios, como um meio para alcançar células ou tecidos alvos (DISCHER; AHMED, 2006; GUDLUR, 2012). Estas estruturas têm exibido maior estabilidade e especificidade quando comparadas àquelas baseadas em moléculas lipídicas (MENG et al., 2009) mostrando-se como atraentes candidatas para a liberação de fármacos.

De acordo com o método de preparação, os arranjos poliméricos podem dar origem a nanocápsulas ou nanoesferas **(FIGURA 10).** As nanocápsulas constituem estruturas circulares, variando entre 10 a 1000 nm de diâmetro (SCHAFFAZICK et al., 2003) que atuam como reservatório membranar para substâncias em seu interior, isolando o núcleo do meio externo e criando, assim, um uma cavidade central preenchida com meio lipídico ou aquoso, dependendo da solubilidade da substância a ser encapsulada. Já as nanoesferas são bastante semelhantes, diferindo pela presença de uma matriz polimérica que preenche

totalmente a esfera e onde o fármaco encontra-se disperso (WATNASIRICHAIKUL et al., 2000; PARVEEN et al., 2012).

FIGURA 10. Representação esquemática de nanocápsulas e nanoesferas poliméricas.

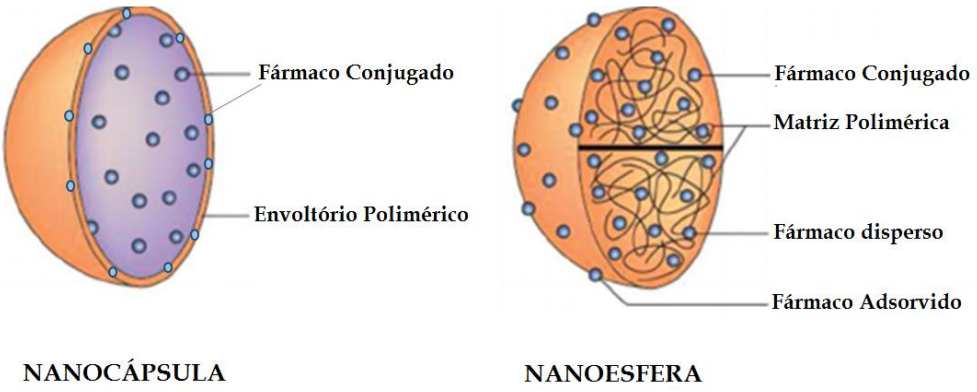

Fonte: Adaptado de VASHIST et al., 2014. Destaque para a diferença morfológica com as nanoesferas formadas por uma matriz polimérica sólida, diferentemente das nanocápsulas que formam um reservatório central de encapsulamento.

As nanocápsulas poliméricas, também chamadas de polimersomas se assemelham em constituição às micelas poliméricas, uma vez que também são formadas por copolímeros em bloco, porém, sem a presença de componentes lipídicos agregados. Os arranjos das cadeias do polímero, por sua vez se dão de modo semelhante aos dos lipossomas, com a formação de um invólucro membranar envolvendo a cavidade central de encapsulamento (PARVEEN et al., 2012).

A maior parte dos polimersomas e peptídeos anfifílicos apresentam um baixo valor de concentração crítica de agregação (CAC), do inglês “critical assembly concentration”, uma medida similar ao da concentração crítica micelar (CMC). A média de valores para CAC desses compostos gira em torno de 10^{-6} – 10^{-7} M, o que corresponde a um valor cerca de 1000 vezes menor que o CMC da maioria dos surfactantes (10^{-3} – 10^{-4} M) (MOGHIMI; SZEBEN, 2003; WANG et al., 2009).

Por apresentarem maior peso molecular que as cadeias lipídicas, os blocos poliméricos exibem cadeias mais espessas e de maior resistência, o que acaba por conferir aos polimersomas, uma maior estabilidade e variabilidade do que as das convencionais estruturas lipossômicas (MENG et al., 2009). Estudos demonstram ainda, que as membranas polimersômicas possuem uma resistência dilatacional membranar numa faixa

de 40-50 % enquanto que para as membranas lipídicas esse é valor corresponde a no máximo 5% (NEEDHAM et al., 2000).

Em um artigo de revisão publicado em 2008 por Levine e colaboradores, há um sumário geral do uso de vesículas poliméricas relacionadas ao diagnóstico e terapia do câncer.

Cada vez mais comum, esse tipo de nanocarreador tem sido empregado no transporte *in vitro* e *in vivo* de diversas drogas anticancerígenas como é o caso de Doxorubicina e Paclitaxil, proteínas como mioglobina, hemoglobina e albumina, moléculas fluorescentes, plasmídeos e siRNA (SHARMA et al., 1995; BEREZOV et al., 2001).

Ao serem injetadas, as nanovesículas são distribuídas pelo organismo de modo a permitir o monitoramento do conteúdo encapsulado por meio de métodos ópticos não invasíveis, eliminando assim a necessidade de sacrificar o animal (TANISAKA et al., 2008).

As nanocápsulas ou vesículas poliméricas podem ser obtidas a partir da estruturação de uma variedade de moléculas, dentre as quais, aquelas formadas a partir de copolímeros anfifílicos são até o momento as mais estudadas e em geral, apresentam diferentes segmentos hidrofóbicos e hidrofílicos, podendo ser obtidas tanto a partir de compostos naturais quanto sintéticos. Nos casos em que o polímero em questão é um polipeptídeo, as estruturas vesiculares formadas são denominadas “vesículas peptídicas ou peptossomos” (DISHER; EISENBERG, 2002).

2.3.5.1 Nanocápsulas Peptídicas

Embora já exista um número considerável de estudos envolvendo a preparação e caracterização de nanomateriais baseados em polipeptídeos, a quantidade de trabalhos abordando o uso de peptídeos formadores de vesículas é ainda relativamente pequena quando comparada com os diversos artigos publicados sobre o uso de outros arranjos poliméricos. Devido a isso, o campo de pesquisa envolvendo nanocápsulas peptídicas pode ser visto como em seu estágio inicial de desenvolvimento, mas ainda assim, detentor de um acelerado ritmo de crescimento (VANDERMEULEN et al., 2004; BARROS et al., 2015).

A característica estrutural comum à maioria dos materiais formados por polipeptídio sintético é a sequência de copolímeros em bloco de caráter anfifílico,

organizados de modo em que um ou mais dos domínios poliméricos seja peptídico (SCHLAAD; ANTONETTI, 2003).

VAUTHEY et al. (2002) foram os primeiros a demonstrar que resíduos peptídicos anfifílicos formados por 7 e 8 monômeros (A_6D, V_6D, V_6D_2, L_6D_2) formavam agregados capazes de originar nanotubos e nanovesículas peptídicas. Devido à sua característica estrutural e comportamento em solução, tais peptídeos foram a princípio chamados de "Surfactant-Like Peptides". Logo em seguida, um grupo formado por Santoso e colaboradores (2002), utilizou a ideia dos "Surfactant-Like Peptides" para testar a eficiência de sequências formadas por resíduos de 4 a 10 monômeros de glicina ligados a moléculas de ácido aspártico na formação de nanotubos e nanovesículas em água e pH neutro, sugerindo a aplicação dessas estruturas na confecção de “scaffolds” para diferentes aplicações, bem como para o encapsulamento enzimático.

Os peptídeos anfifílicos capazes de dar origem a nanovesículas podem constituir desde uma simples sequência polipeptídica até uma molécula mais complexa, desde que apresente uma estrutura caracterizada pela presença de uma cadeia hidrocarbônica hidrofóbica ligada a uma porção hidrofílica de propriedades semelhantes às moléculas comumente empregadas na formação de micelas e vesículas anfifílicas (TSONCHEV et al., 2004).

As forças de associação e estabilização que dirigem a formação de vesículas lipídicas também se aplicam a outras vesículas poliméricas, incluindo as formadas por peptídeos anfifílicos. Além das já citadas, são exemplos de algumas dessas sequências formadoras de vesículas (V_mK_n, G_mD_n, V_6D, KA_6, A_6K, I_3K, A_6K_2, $A_2V_2L_3WE_2$ e GAVILRR) (SANTOSO et al., 2002; ZHAO et al., 2010; JEONG et al., 2014).

O comprimento da cadeia hidrofóbica desses peptídeos desempenha um papel crucial na definição do arranjo final e definição da espessura da camada de revestimento. Tipicamente, o tamanho dessas cadeias corresponde a cerca de 3-9 resíduos hidrofóbicos. Tendo em vista que longas cadeias diminuem a solubilidade e que por outro lado, cadeias muito curtas embora mais solúveis apresentem o inconveniente de ter o potencial de agregação reduzido, faz-se de extrema importância o alcance de um equilíbrio adequado reduzindo ou aumentando a cadeia peptídica de acordo com as propriedades e objetivos almejados para cada sequência utilizada (ZHAO et al., 2010).

O comprimento das cadeias influencia ainda no diâmetro das estruturas formadas e como consequência da solubilidade, o que pode levar a diferentes graus de interação

resultando em valores diferenciados de concentração crítica de agregação ou CAC. De um modo geral, os estudos abordam sequências com tamanhos que vão de 2 a 9 monômeros peptídicos resultando em tamanhos entre de 60-250 nm de diâmetro e valores de CAC de 12 a 50 μM (VAN HELL et al., 2007; VAN HELL et al., 2010; JIAO et al., 2012).

2.3.5.1.1 Cápsulas peptídicas anfifílicas ramificadas (BAPCs)

As cápsulas peptídicas anfifílicas ramificadas ou do inglês, "Branched Amphiphilic Peptide Capsules" (BAPCs) representam uma nova classe de nanocarreadores formados por vesículas similares a lipossomas, mas constituídos inteiramente por peptídeos, capazes de armazenar soluções aquosas em seu interior.

Descritas pela primeira vez por Gudlur et al. (2012), são estruturas de auto-montagem onde uma cavidade hidrofílica (aquosa) encontra-se rodeada por uma bicamada peptídica anfifílica ramificada. Trata-se de nanocarreadores essencialmente estáveis, biocompatíveis e biodegradáveis, com estrutura e propriedades semelhantes aos lipossomas e polimersomas.

O sistema descrito por Gudlur e colaboradores refere-se a estruturas vesiculares formadas a partir da organização em meio aquoso, de duas sequências peptídicas formadas por 15 e 23 aminoácidos – $(FLIVI)_2$-K-K_4 e $(FLIVIGSII)_2$-K-K_4 – comumente referidos como $(h_5)_2$-K-K_4 e $(h_9)_2$-K-$_{K4}$ ou simplesmente h_5 e h_9 **(FIGURA 11).**

FIGURA 11. Sequência de peptídeos ramificados constituintes das BAPCs.

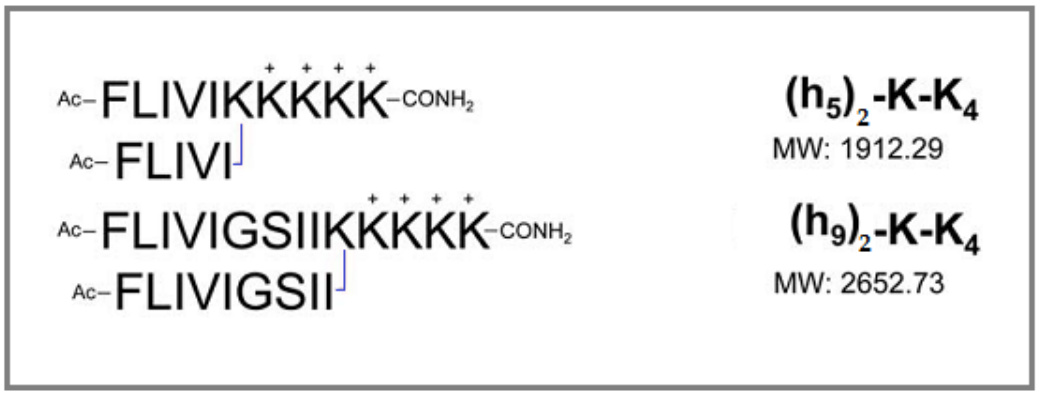

Fonte: GUDLUR et al., 2012.

Um estudo realizado por Gebhardt et al. (2008) descreve os detalhes de transição estrutural α-helix para folhas β observados em arranjos peptídicos formados por resíduos de poli(L-lisina) associados a moléculas de polibutadieno. No caso das micelas e vesículas formadas por essa sequência, a transição acontece em pH acima do pKa das cadeias laterais da lisina (ph=10) diminuindo a curvatura interfacial e resultando em uma interface mais plana e em um dicreto aumento no raio hidrodinâmico das vesículas, porém, sem afetar a agregação molecular. Desse modo, as partículas permaneceram intactas após a mudança como demonstrado por experimentos de espalhamento dinâmico de luz (DLS, do inglês "Dynamic Light Scattering") e espalhamento de luz estático (SLS, do inglês "Static Light Scattering") (FETTERLY; STRAUBINGER, 2003; PERCEC et al., 2010).

No caso das BAPCs, sabe-se que os resíduos de lisina carregados positivamente encontram-se nas duas fases aquosas, com os grupos polares expostos em ambos os lados da membrana em contacto com água, enquanto que as cadeias laterais aromáticas de resíduos de fenilalanina e outros aminoácidos anfipáticos encontram-se voltados para o interior da bicamada, mantendo-se unidos por meio de interações hidrofóbicas **(FIGURA 12).**

Além disso, experimentos de Dicroísmo circular (DC) e espectroscopia no infravermelho por transformada de Fourier (FT-IR) indicaram a presença de folhas β paralelas sugerindo a presença redes de pontes de hidrogênio que ajudam manter a estrutura organizada estável mesmo em concentrações muito baixas (sub-micromolar), conforme avaliado por estudos de diluição definidas por calorimetria de titulação isotérmica (ITC, do inglês "Isothermal titration calorimetry"), condições essas em que praticamente todos os agrupamentos de fosfolipídios de um sistema lipídico seriam totalmente dissociados (GUDLUR et al., 2012).

Com base em simulações computacionais, estes peptídeos se comportam de forma análoga a fosfolipídios em solução aquosa, de modo que as regiões hidrofóbicas destas moléculas sendo pouco solúveis em água buscam se proteger-se da interação com a água por formação de bicamadas com um valor aproximado de 4 nm de espessura (GUDLUR et al., 2012).

FIGURA 12. Modelo da formação das BAPCs obtido por meio de modelagem computacional do tipo Dinâmica Molecular (MD).

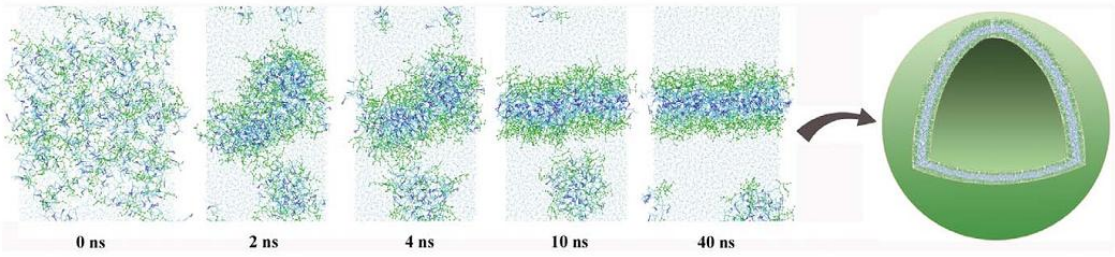

Fonte: GUDLUR et al., 2012. Os átomos expostos no modelo bastão e bola mostram os resíduos de lisina (verde) interagindo com a água, enquanto que as cadeias laterais aromáticas dos resíduos de fenilalanina (azul escuro) e os demais resíduos apolares (azul claro) se voltam para a face interna da bicamada. Os intervalos de agregação exemplificam o estado de organização a 0 ns, 2 ns, 4 ns, 10 ns e 40 ns onde a bicamada se dobra para formar a nanocápsula, mostrada à direita.

2.3.5.1.1.1 *Origem da sequência peptídica das BAPCs*

A sequência utilizada na formação das BAPCs ocorre na natureza como uma porção de um dos segmentos transmembrana do canal de cálcio tipo L sensível a dihidropiridina CAIVS3 (DPWNVFD**FLIVIGSII**DVILSE) (GROVE et al., 1993; IWAMOTO et al., 1994). Os estudos iniciais envolvendo tal sequência se voltavam, no entanto, para a avaliação de propriedades adesivas desse peptídeo e suas variantes (SHEN et al., 2006; VELICHKO et al., 2008).

Observou-se a princípio, que a liofilização da sequência DPWNVFD**FLIVIGSII**DVILSE quando produzida por síntese em fase sólida resultava em aglomerados insolúveis resistentes ao rompimento por agitação mecânica. Tal propriedade sugeria a presença de intensas forças de coesão que estariam dirigindo a associação. Nesse ponto, sugeriu-se que uma transição das cadeias da conformação α para β poderia ser controlada de modo previsível por meio da adição de um aminoácido carregado positivamente às duas extremidades da sequência marcada (h_9) e controle do pH (GROVE et al., 1993; Mo et al., 2008).

Os experimentos envolviam medidas da força de cisalhamento necessária para separar duas tiras de madeira de cerejeira coladas pelo tratamento com solução do peptídeo em água a 4% m /v. Ao longo do experimento, foi observado que ao se manter o núcleo

hidrofóbico com as sequências FLIVI (h_5) e FLIVIGSII (h_9) adicionando às suas extremidades resíduos de lisina, as imagens geradas por microscopia eletrônica de transmissão (MET) exibiam a formação de estruturas organizadas formando uma rede de nanofibras **(FIGURA 13)** (Mo et al., 2008).

FIGURA 13. Nanofibras peptídicas formadas por cadeias de h_9 em solução.

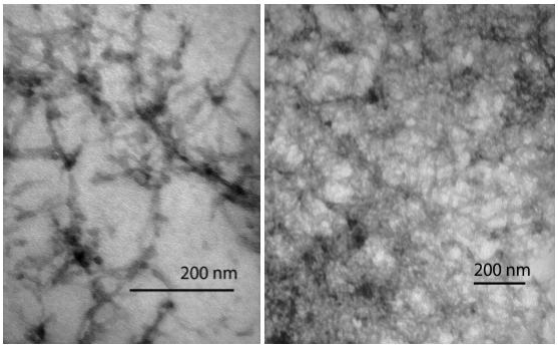

Fonte: GUDLUR et al., 2012. Imagens geradas por microscopia eletrônica de transmissão (MET).

Ao se perceber que as estruturas originadas se assemelhavam àquelas formadas por moléculas de surfactantes micelares, surgiu a ideia da síntese de uma sequência ramificada que se assemelhasse em estrutura e polaridade aos fosfolipídios constituintes dos lipossomas, originando assim os peptídeos ramificados anfipáticos responsáveis pela formação das nanocápulas peptídicas em meio aquoso (BAPCs) (GUDLUR et al., 2012).

2.3.5.1.1.2 Estudos iniciais caracterização das BAPCs

A fim de formar vesículas delimitadas por uma bicamada peptídica, a sequência utilizada incluía 5 resíduos de lisina ligados entre si, com o quinto resíduo gerando um ponto de ramificação na porção N-terminal, a partir da adição de dois segmentos hidrofóbicos simultâneos (h_5 e h_9) por meio da técnica de Fmoc **(FIGURA 14)**, cujo princípio geral consiste em ciclos repetitivos de acoplamento de aminoácidos ligados a uma resina ou suporte sólido polimérico. Para isso, a resina é inicialmente ativada, a fim de promover a exposição dos ligantes amino terminal livres e a retirada do grupo protetor Fmoc, facilmente removidos pela presença de uma base como a peperidina **(etapa 1a).** Várias técnicas de ativação são encontradas na literatura (CHAN; WHITE, 2000). Nesse ponto, procede-se então a ativação do primeiro aminoácido **(etapa 1b)** e então seu

acoplamento à resina por meio de sua extremidade C-terminal **(etapa 2),** enquanto seu grupamento amino permanece protegido pelo grupo Fmoc e suas cadeias laterais por grupos t-butila, garantindo sua integridade durante toda a síntese da cadeia peptídica. Após a ligação do primeiro aminoácido, o grupo amino deste é então desprotegido **(etapa 3a)** e um segundo Fmoc aminoácido ativado **(etapa 3b)** e acoplado **(etapa 4)**, gerando assim um novo grupo amino N-Terminal, que ficará disponível para uma nova ligação. As etapas de acoplamento e desproteção do grupamento N-Terrminal são repetidas alternadamente **(etapa 5)**, até que o peptídeo seja obtido, obedecendo a sequência desejada. Na etapa final, o peptídeo é liberado de seu suporte sólido e os grupos protetores das cadeias laterais também são removidos. Enquanto o grupo Fmoc é removido facilmente em meio básico, os demais grupos protetores **(Etapas 6a e 6b)** são removidos em meio ácido, geralmente por meio do TFA (MERRIFIELD, 1963; FIELDS; NOBLE, 1990; CHAN; WHITE, 2000; AMBLARD et al., 2006).

FIGURA 14. Esquema de síntese peptídica segundo a estratégia F-moc.

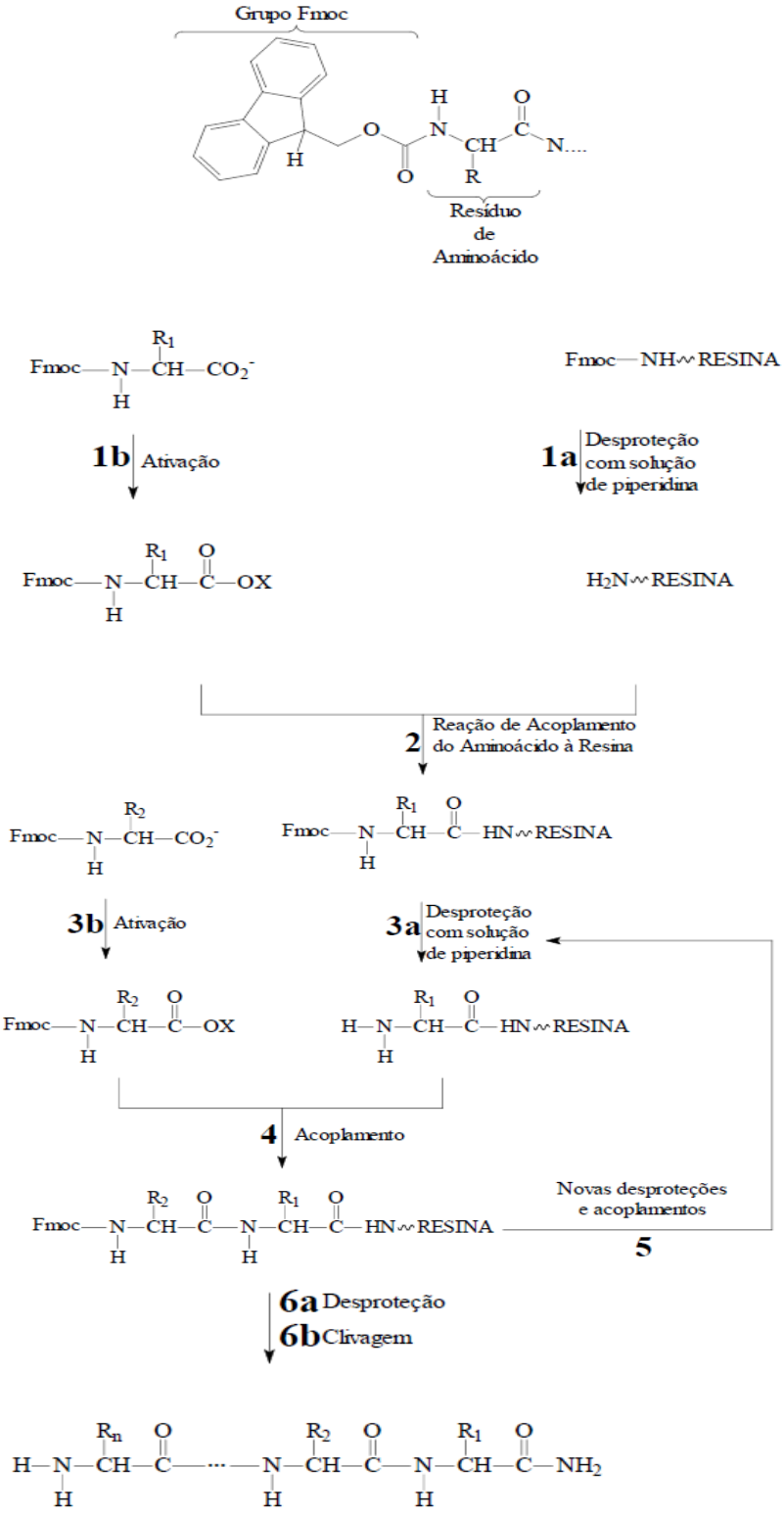

Fonte: CAPRINO; HAN, 1972.

Nos estudos iniciais, se decidiu utilizar uma mistura dos dois peptídeos de tamanhos diferentes (h_5 e h_9) de modo que a sequência mais curta poderia compensar qualquer tensão de curvatura durante a formação da nanocápsula, resultando em nanocápsulas com dimensões na faixa de 50-150 nm de diâmetro **(FIGURA 15)** (GUDLUR et al., 2012).

FIGURA 15. Nanocápsulas peptídicas formadas em meio aquoso.

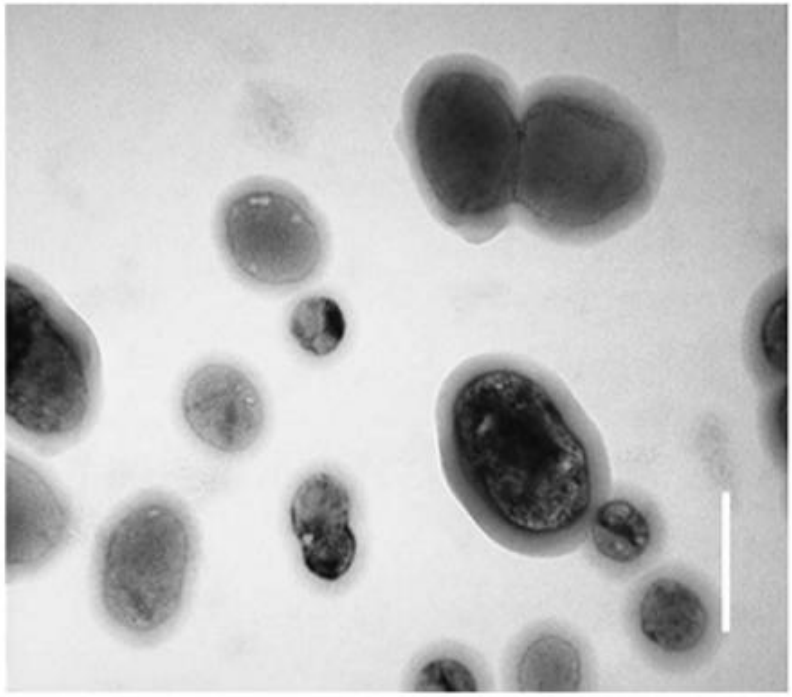

Fonte: GUDLUR et al., 2012. BAPCs (1.5 mM) formadas após um período incubação de 2h. Imagens geradas por meio de microscopia eletrônica de transmissão (MET). Barra de escala de 200 nm.

A fim de se obter uma maior compreensão do sistema, SUKTHANKAR et al. (2013) acompanhou as etapas do processo de formação das BAPCs **(FIGURA 16)**, demonstrando que após a hidratação dos peptídeos, as cadeias começam se organizar de modo a formar uma rede de nanofibrilas, que gradualmente se agrupam dando origem a nanocápsulas com tamanho médio de 20 nm. O mais interessante foi que se observou que

por volta de 60 minutos após a hidratação, as nanocápsulas formadas a 25 °C começam a se fundir, chegando a formar cápsulas de dimensões micrométricas.

FIGURA 16. Etapas de formação das BAPCs.

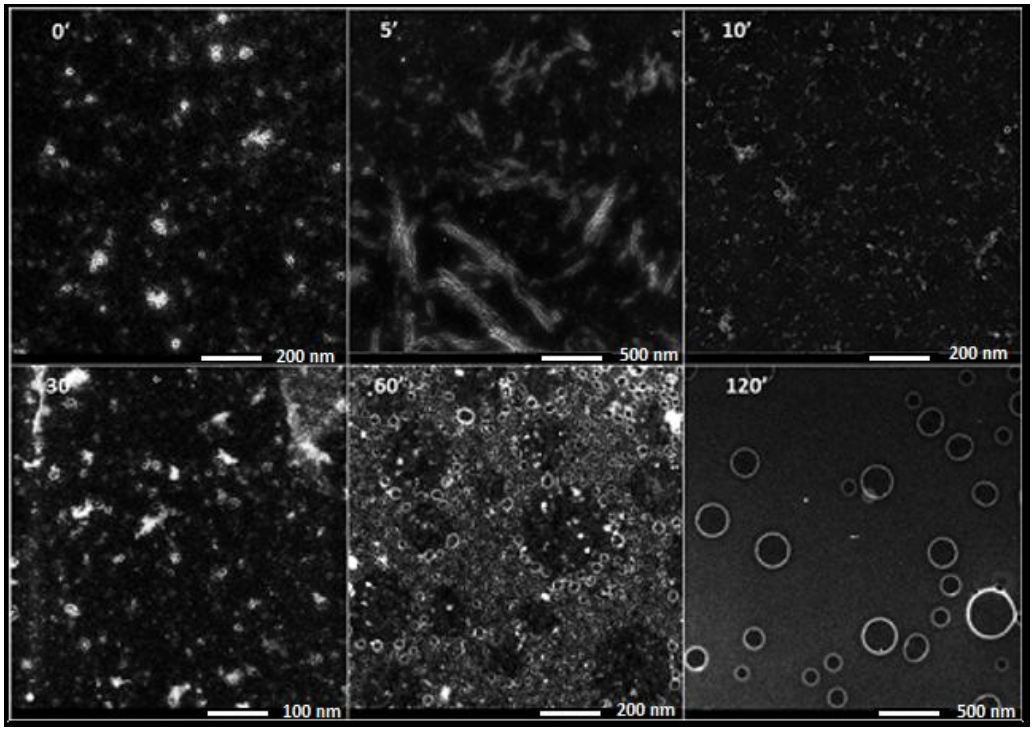

Fonte: SUKTHANKAR et al., 2013. Imagens geradas por meio de microscopia eletrônica de varredura e transmissão (MEVT). As imagens destacam o início da agregação peptídica de uma solução a (0.1 mM) no tempo 0, a formação de uma rede de nanofibrilas após o intervalo de 5 minutos, o início de formação das nanocápsulas por volta de 30 minutos, as BAPCs formadas após 60 minutos e o processo de fusão que culmina com BAPCs de dimensões variadas na faixa dos 120 minutos. As barras de escala são de 200 nm, 500 nm, 200 nm, 100 nm, 200 nm and 500 nm, para os correspondentes intervalos de tempo de 0, 5, 10, 30, 60, and 120 min.

Quando, porém, preparadas a 4 °C ou quando após a fusão são redimensionadas por meio de extrusão e então submetidas a submetidas 4 °C por pelo menos 1h, as BAPCs interrompem o processo de fusão e não apresentam mais tal propriedade, ainda que sejam levadas novamente à temperatura de 25 °C **(FIGURA 17 B).**

Além disso, ao promover a mistura de duas populações de BAPCs, com o primeiro grupo contendo o corante Eosina Y e o segundo contendo apenas água, as BAPCs se fundem levando a uma diluição do corante que pode ser registrado como um aumentando

da intensidade da fluorescência **(FIGURA 17 A)**, devido ao quenching carcterístico de Eosina Y (SUKTHANKAR et al., 2013).

FIGURA 17. Processo de fusão das BAPCs registrado por meio de espectroscopia de fluorescência.

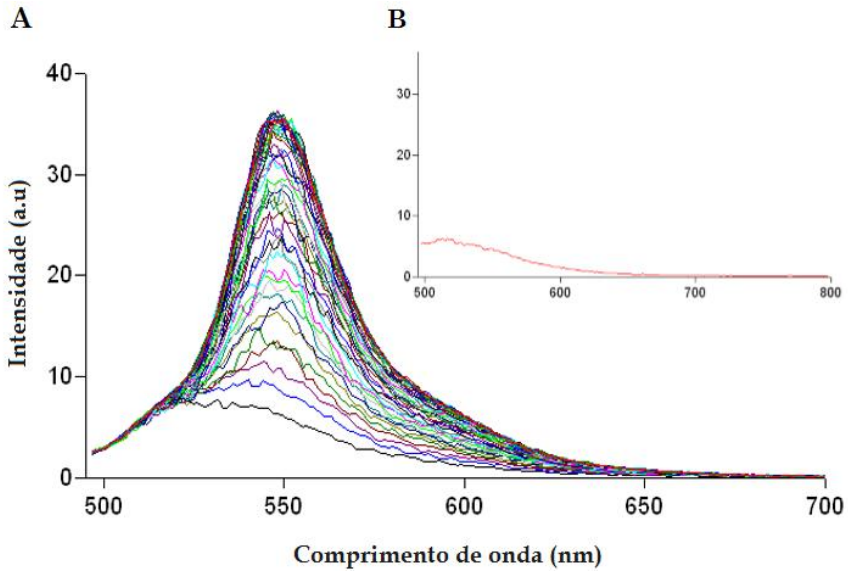

Fonte: SUKTHANKAR et al., 2013. A) Registros de intensidade de fluorescência da mistura de BAPCs contendo água e BAPCs encapsulando o corante Eosina Y (2,2 Mm) a 25 °C, com scans realizados a cada 5 minutos durante um intervalo de tempo de 235 minutos. Em B) o registro da fluorescência de uma amostra da mesma mistura de BAPCs mantida a 4 °C por 6.5 h, mostra o pico de intensidade na faixa registrada para a amostra inicial, antes do processo de fusão, evidenciando que quando mantidas a essa temperatura o processo de fusão das BAPCs pode ser interrompido.

Como demontrado por Sukthankar e colaboradores (2013), as BAPCs formadas possuem um diâmetro médio de 20-30 nm com um volume interno de 4.000 nm^3, fato que as torna possíveis candidatas para o encapsulamento de um grande número de diferentes moléculas, incluindo proteínas. Em 2015, Sukthankar e colaboradores demonstraram tal habilidade ao utilizar as BAPCs no encapsulamento de RNase A e citococromo c. Os resultados não apenas demonstraram um encapsulamento bem sucedido quanto uma eficiente distribuição para o interior de células HeLa **(FIGURA 18).** Além disso, embora o citocromo c e RNase A sejam conhecidos por sua ação apoptótica (KIM et al., 1995; ZHIVOTOVSKY et al., 1998), nos experimentos com as BAPCs como carreador, nenhum sinal de apoptose foi registrado.

FIGURA 18. Internalização celular de BAPCs encapsulando TRNase e Tcytc.

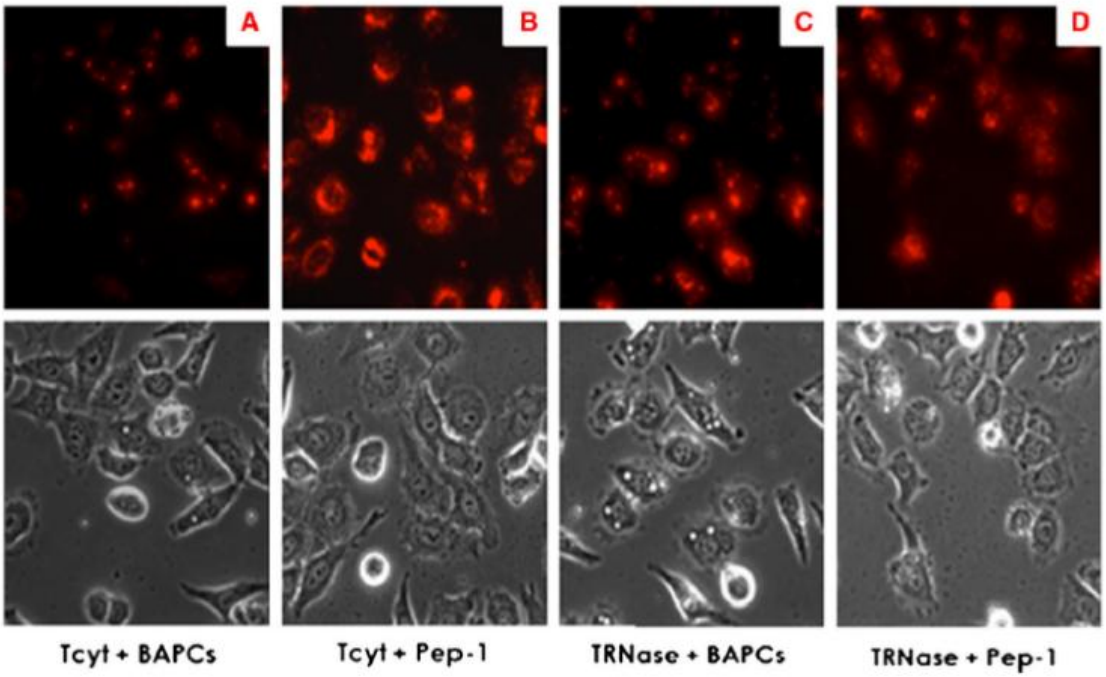

Fonte: SUKTHANKAR et al., 2014. Imagens geradas por microscopia de fluorescência de células HeLa após 3 h de incubação, com BAPCs encapsulando RNase e citococromo marcados com a sonda fluorescente TAMRA (TRNase A, 13.7 kDa e Tcytc, 12 kDa): A) Tcytc B) Tcytc e Pep-1 C) TRNAse e D) TRNase e Pep-1.

O estudo mostrou ainda, a habilidade das BAPCs em se manter intactas no interior das células HeLa por um longo período de tempo. Imagens geradas com o auxílio de microscopia confocal mostraram que mesmo após 14 dias, as BAPCs marcadas com rodamina B eram transferidas para novas células durante a divisão mitótica sem que houvesse degradação das estruturas de encapsulamento **(FIGURA 19).**

FIGURA 19. Internalização das BAPCs por células HeLa.

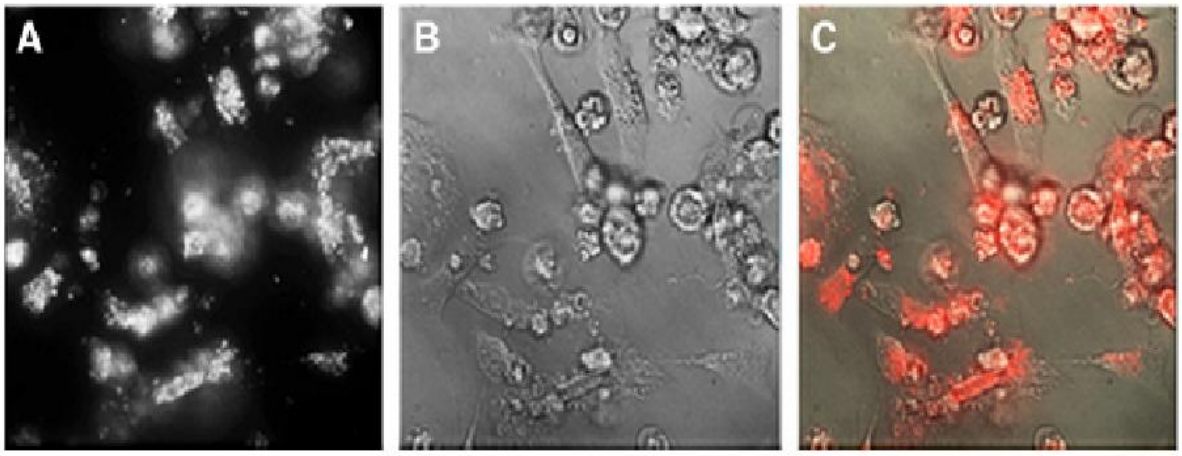

Fonte: SUKTHANKAR et al., 2014. Imagens geradas por microscopia confocal, obtidas duas semanas após a internalização celular das BAPCs.

A estabilidade térmica das BAPCs foi também avaliada por Gudlur et al. (2012), utilizando calorimetria diferencial de varredura (DSC, do inglês "Differential Scanning Calorimetry") numa escala de temperatura entre 20-95 °C. Este experimento foi confirmado em uma varredura por meio de espectroscopia de fluorescência na mesma faixa de temperatura com BAPCs contendo o corante eosina Y a 2.1 mM, sem que houvesse nenhum aumento de intensidade de fluorescência, indicando que as BAPCs não se rompem liberando seu conteúdo armazenado.

A inexistência de uma temperatura de transição indica a manutenção da estrutura membranar e integridade funcional. Essa informação é importante porque vesículas formadas por fosfolipídios exibem uma temperatura de transição entre 35-45 °C (BILTONEN; LICHTENBERG, 1993). A essa temperatura, as vesículas lipídicas tendem a se tornar permeável e tal propriedade pode ser vista como uma desvantagem devido à impossibilidade de retenção do conteúdo internalizado quando exposto a elevadas temperaturas.

A medicina nuclear molecular desempenha um papel importante no diagnóstico e tratamento de câncer. Dependendo das propriedades do radioisótopo eles podem ser utilizados tanto propósitos de diagnóstico quanto de terapia. Nessa perspectiva, partículas alfa alvo direcionadas têm uma vantagem significativa na radioterapia sítio específica por

conta da sua elevada energia, especificidade, bem como habilidade de matar células não proliferativas e não precisar de oxigenação (ELGQVIST et al., 2014).

Em muitos casos, a radioimunoterapia alvo direcionada se beneficia da especificidade de anticorpos conjugados a radionuclídeos para entregar radiação biocida para células cancerosas (COUTURIER et al., 2005).

Radionuclídeos emissores de partículas alfa como Ac ^{225} (Actínio-225) e Bi ^{213} (Bismuto-213) são comumente utilizados para esse propósito. Esse método, no entanto, possui alguns inconvenientes como o de que a alta energia proveniente das partículas alfa podem colidir e destruir as ligações covalentes entre a molécula ligante e o anticorpo. Além disso, a liberação de radionuclídeos livres pode levar ao acúmulo em áreas indesejadas do organismo resultando em potenciais danos biológicos (SOFOU et al., 2007).

Cálculos teóricos feitos por Sofou et al. (2007) sugerem uma retenção desprezível (<0.001%) para isótopos de Ac^{225} em lipossomas de 100 nm de diâmetro e 50% de retenção para lipossomas com tamanho maior que 650 nm.

Até mesmo liposomas gigantes (1 μm de diâmetro) possuem valores de retenção < 65% e de fato as medidas de retenção por parte de lipossomas de 650 nm tem se mostrado substancialmente mais baixa (11%) do que o valor predito (KEMPE & BARANY, 1996).

Enquanto isso, o encapsulamento de Ac^{225} por meio das BAPCs demonstrou uma absorção não letal de Ac^{225} por parte das células em cultura, com retenção estável de ≥ 95% ao longo de 7 dias **(FIGURA 20).**

FIGURA 20. Retenção de Ac^{225} encapsulado.

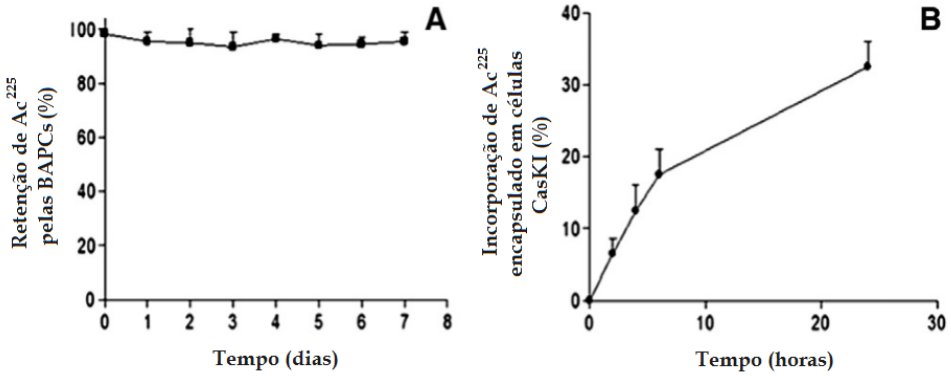

Fonte: SUKTHANKAR et al., 2014. A) Retenção de Ac^{225} encapsulado nas BAPCs durante 7 dias B) Internalização das BAPCs encapsulando Ac^{225} em células CasKI em cultura ao longo de 24 h.

Quando avaliados nos experimentos *in vivo,* os níveis de Ac^{225} livre e encapsulado nas BAPCs foram monitorados a nível dos ossos, fígado e rins durante um período de 24h.

Após 1h como ambos, Ac^{225} livre e Ac^{225} encapsulado nas BAPCs, encontram-se ainda saindo da cavidade peritoneal não havia nenhuma diferença significativa na integração desses componentes nos órgão avaliados, exceto no osso onde Ac^{225} livre tende a se acumular. O único órgão onde havia mais Bi^{213} presente comparado com Ac^{225} foram os rins, responsável pela eliminação de componentes resultantes do metabolismo.

Após o período de 24h, os resultados demonstraram um maior acúmulo de Ac^{225} livre no fígado e nos ossos quando comparado ao Ac^{225} encapsulado pelas BAPCs.

Uma vez que tanto o Ac^{225} quanto o seu produto Bi^{213} estavam presente juntos indicando retenção do Bi^{213} formado no interior das BAPCs, os resultados preliminares apontam para a habilidade das BAPCs de incorporar e reter estes elementos, indicando a possibilidade de desenvolvimento de BAPCs alvo direcionadas capazes de encapsular isótopos radioativos para o tratamento de câncer, com um aumento da eficácia terapêutica e consequente redução da dose letal tumoral.

2.3.5.1.1.3 Utilização das BAPCs no transporte de material genético

A habilidade de transferência de material genético para o interior celular com o objetivo de ativação, silenciamento ou introdução de genes específicos em alvos celulares apropriados para fins terapêuticos, constitui a essência da terapia gênica atual (ELSABAHY et al., 2011).

A terapia gênica tem sido proposta como uma eficiente alternativa de substituição de fármacos para o tratamento de diversas doenças (AZEVÊDO, 2009).

Diferentes estratégias têm sido propostas como possíveis alternativas para a administração ou entrega celular do material genético com veículos que vão desde os conhecidos vetores virais até uma gama de novos materiais nanoestruturados tais como lipossomos, lipoplexos (DNA complexado a vesículas lipídicas), poliplexos (DNA complexado a polímeros biodegradáveis), microesferas, nanocápsulas e outros, têm a capacidade de associar-se com ácidos nucleicos, possibilitando a liberação mais prolongada do que o uso de DNA livre e a redução da toxicidade em relação ao uso de vetores virais. A adição de outras moléculas, como polietilenoglicol ou anticorpos, pode ainda auxiliar no direcionamento e controle da liberação do material genético (WU; WU, 1988; DAVIDSEN et al., 2003; PARDRIDGE, 2003; VAN ZANTEN et al., 2004; WASUNGU; HOEKSTRA, 2006; ZHOU et al., 2013).

Recentemente, Avila e colaboradores (2016) utilizaram as sequências peptídicas de $(Ac\text{-}FLIVI)_2\text{-}K\text{-}K_4\text{-}CO\text{-}NH_2$ e $(Ac\text{-}FLIVIGSII)_2\text{-}K\text{-}K_4\text{-}CO\text{-}NH_2$ na confecção de BAPCs contendo pDNA (DNA plasmidial) aderidos à superfície catiônica das nanocápsulas a fim de testar a sua viabilidade na transfecção da célula HeLa. Tal estudo demonstrou a capacidade das BAPCs de atuar no transporte de plasmídeos de diferentes tamanhos para o interior das células em cultura, com uma elevada eficiência de transfecção e mínima citotoxicidade. Além disso, testes *in vivo* evidenciaram o potencial do sistema no desenvolvimento de vacinas de DNA capazes de ativar respostas imunes responsáveis pelo controle de tumores induzidos pelo papilomavírus humano 16 (HPV-16), indicando mais uma das potencialidades de adaptação e uso das nanocápsulas peptídicas anfifílicas ramificadas.

3 OBJETIVOS

3.1 GERAL

Avaliar a viabilidade de nanocápsulas formadas por diferentes proporções dos peptídeos h_5 e h_9 para sua aplicação como sistema de nanocarreamento.

3.2 OBJETIVOS ESPECÍFICOS:

- Utilizar a técnica de F-moc para a síntese em fase sólida dos peptídeos (h_5)-K-K_4 e (h_9)-K-K_4;
- Utilizar os peptídeos (h_5)-K-K_4 e (h_9)-K-K_4 nas proporções de 1:0, 0.2:0.8, 0.8:0.2 e 0:1 no intuito de avaliar a viabilidade de formação de nanocpápsulas comparando os resultados aos das BAPCs formadas 0.5:0.5 de ambos os peptídeos previamente caracterizadas;
- Avaliar a resistência térmica das BAPCs na faixa de 4 °C - 95 °C por meio da análise de ruptura das BAPCs seguida do quenching do corante Eosina Y registrado pela técnica de espectroscopia de fluorescência;
- Analisar a intensidade de fuorescência do corante encapsulado nas BAPCs formadas a 4 °C, 25 °C e 37 °C no intuito de valiar a melhor temperatura de encapsulamento;
- Avaliar a eficiência de encapsulamento das BAPCs formadas por diferentes proporções peptídicas através do quenching de Eosina Y utilizando espectroscopia de fluorescência;
- Promover a caracterização das BAPCs formadas por meio de Dicroísmo circular, a fim de identificar os diferentes tipos de estruturas secundárias presentes;
- Utilizar espalhamento de luz dinâmico a fim de avaliar o tamanho da nanocápsulas formadas nas diferentes proporções de (h_5)-K-K_4 e (h_9)-K-K_4.
- Avaliar o potencial oxido-redutor das membranas constituintes das BAPCs por meio de técnica de voltametria cíclica;
- Avaliar e eficiência de transfecção e efeitos de citotoxicidade durante a entrega de pDNA-BAPCs para células da linhagem HEK-293 em cultura.

4 REFERÊNCIAS BIBLIOGRÁFICAS

ABHAY, S. C. et al. Dendrimer-mediated transdermal delivery: enhanced bioavailability of indomethacin. **J. Control Release**. v. 90, p. 335-343, 2003.

ADAMS, M. L.; KWON, G. S. Relative aggregation state and hemolytic activity of amphotericin B encapsulated by poly (ethylene oxide)-block–poly (Nhexyl-l-aspartamide)-acyl conjugate micelles: effects of acyl chain length. **J. Control Release**. v. 87, p. 23-32, 2003.

ALENCAR, M. S. M; BOCHNER, R.; DIAS, M. F. F. Nanotecnologia em Ciências da Saúde no Brasil: um olhar informétrico sobre os grupos de pesquisa. **Rev. Liinc**. v. 9, p. 47-65, 2013.

ALLEN, T. M.; CHONN, A. Large unilamellar liposomes with low uptake into the reticuloendothelial system. **FEBS Lett.** v. 223, p. 42-46, 1987.

ALLEN, T. M.; CULLIS, P. R. Drug delivery systems: entering the mainstream. **Science**. v. 303, p. 1818-1822, 2004.

AMBLARD. M.; FEHRENTZ. J. A.; MARTINEZ, J.; SUBRA, G.; "Methods and protocols of modern solid phase peptide synthesis". **Molecular Biotechnology**. v. 33, p. 239-254. 2006.

ANDRADE, C. A. S. et al. Antitumor Activity of Cratylia mollis Lectin Encapsulated into lipossomes. **Int. J. Pharm.** v. 278, p. 435-445, 2004.

ANDERSON, M.; OMRI, A. The Effect of Different Lipid Components on the In Vitro Stability and Release Kinetics of Liposome Formulations. **Drug Deliv.** v. 11, p. 33-39, 2004.

ANDREO-FILHO, N. et al. Quantitative determination of phosphatidylcholine by high performance liquid chromatography using silica column. **Rev. Bras. Cienc. Farm**. v. 20, p.107-115, 1999.

AVILA, L. A. Gene delivery and immunomodulatory effects of plasmid DNA associated with Branched Amphiphilic Peptide Capsules. **J. Control. Release.** v. 241, p. 15 -24, 2016.

AZEVÊDO, E. S. Terapia Gênica. **Rev. Bioética.** v. 5, p. 1-11, 2009.

BAE, Y. et al. Multifunctional polymeric micelles with folate-mediated cancer cell targeting and pH-triggered drug releasing properties for active intracellular drug delivery. **Mol. Biosyst.** v. 1, p. 242-250, 2005.

BAREFIELD, E. K.; CARRIER, A. M.; VANDERVEER, D. G. X-Ray structure of mer-trichloro [N - (3 – aminopropyl) – 1, 3 – diaminopropine] – cobalt (III). **Inorg. Chim. Acta.** v. 42, p. 271 – 275, 1980.

BAUM, C. et al. Side effects of retroviral gene transfer into hematopoietic stem cells. **Blood.** v. 101, p. 2099–2113, 2003.

BASEL, M. T. et al. Protease-sensitive, polymer-caged liposomes: a method for making highly targeted liposomes using triggered release. **ACS Nano**. v. 5, p. 2162-2175, 2011.

BEREZOV, A. et al. Disabling ErbB Receptors with Rationally Designed Exocyclic Mimetics of Antibodies: Structure−Function Analysis. **J. Med. Chem.** v. 44 p. 2565–2574, 2001.

BILTONEN, R. L.; LICHTENBERG, D. The use of differential scanning calorimetry as a tool to characterize liposome preparations. **Chem. Phys. Lipids.** v. 64 p. 129–142, 1993.

BITOUNIS, D.; FANCIULLINO, R.; ILIADIS, A. Optimizing Druggability through Liposomal Formulations: New Approaches to an Old Concept. **ISRN Pharmaceutics.** v. 2012, p.1-11, 2012.

BOAS, U.; HEEGAARD, P. M. Dendrimers in drug research. **Chem. Soc**. v. 33, p. 43-63, 2004.

BOISSEAU, P.; LOUBATON, B. Nanomédecine et nanotechnologies pour la medicine. **C. R. Phys.** v. 12, p. 620–636, 2011.

CADIOLI, L. P.; SALLA, L. D. Nanotecnologia: um estudo sobre seu histórico, definição e principais aplicações desta inovadora tecnologia. **Rev. Ciênc. Exatas Tecnol**. v. 1, p. 98-105, 2006.

CAMPOS, T. A. Complexo de inclusão ácido fumarprotocetrárico: 2-hidroxipropil-βciclodextrina; preparação, caracterização e encapsulação em lipossomas. 2012. 83 p. dissertação (Mestrado em Saúde Humana e Meio Ambiente) - Centro Acadêmico de Vitória, Universidade Federal de Pernambuco (UFPE), Vitória de Santo Antão, 2012.

CENTRO DE GESTÃO E ESTUDOS ESTRATÉGICOS (CGEE). Parceiras Estratégicas. n 18. Brasília, 2004.

CORTESI, R. et al. Non-phospholipid vesicles as carriers for peptides and proteins: Production, characterization and stability studies. **Int. J. Pharm.** v. 339, p. 52– 60, 2007.

CHAUHAN, A. S. et al. Solubility enhancement of indomethacin with poly (amidoamine) dendrimers and targeting to inflammatory regions of arthritic rats. **J. Drug Target**. v.12, p. 575-583, 2004.

CHAN, W. C.; WHITE, P. D. **Fmoc Solid Phase Peptide Synthesis**: A Practical Approach. Editora Oxford University Press, 2000, 288 p.

CHOUCAIR, A.; EISENBERG, A. Interfacial solubilization of model amphiphilic molecules in block copolymer micelles. **J. Am. Chem. Soc**. v. 125, p. 11993-12000, 2003.

DAVIDSEN, J. et al. Secreted phospholipase A2 as a new enzymatic trigger mechanism for localized liposomal drug release and absortion in diseased tissue. **Biochim. Biophys. Acta.** v. 1609, p. 95 - 101, 2003.

DEMICHELI, C.; FRÉZARDI, F.; SCHETTINI, D. A. Lipossomas: propriedades físico-químicas e farmacológicas, aplicações na Quimioterapia à base de antimônio. **Quim. Nova**. v. 28, p. 511-518, 2005.

DISCHER, D. E.; EISENBERG, A. Polymer vesicles. **Science.** v. 297, p. 967–973, 2002.

DISCHER, D. E.; AHMED, F. Polymersomes. **Annu. Rev. Biomed. Eng.** v. 8 p. 323–341, 2006.

DUNCAN, R. Nanomedicine gets clinical. **Mater Today**. v. 8, p. 16-17, 2005.

DURÁN, N.; DE AZEVEDO, M. M. M. O que é nanobiotecnologia? Atualidades e perspectivas. Monografia (Laboratório de **Química** do Estado Sólido). Instituto de Química, UNICAMP, São Paulo, 2002.

DURAN, N.; DE MORAIS, P. C.; MATTOSO, L. H. C. **Nanotecnologia:** Introdução, preparação e caracterização de nanomateriais e exemplos de aplicação. São Paulo: Artliber, 2006, 208 p.

DRUMMOND, C. J.; FONG, C. Surfactant self-assembly objects as novel drug delivery vehicles. **Curr. Opin. Colloid Interface Sci.** v. 4 p. 449-456, 1999.

EDWARDS, K. A.; BAEUMNER, A. J. Liposomes in analyses. **Talanta**. v. 68, p.1432-1441, 2006.

ELSABAHY, M.; NAZARALI, A.; FOLDVARI, M. Non-viral nucleic acid delivery: key challenges and future directions. **Curr. Drug Deliv**. v. 8, p. 235−244, 2011.

ESF, Scientific Forward Look on Nanomedicine. European Science Foundation Policy Briefing, February 23, 2005. Disponível em: http://www.esf.org/fileadmin/Public_documents/Publications/Nanomedicine_01.pdf. Acesso em: Agosto/ 2016.

EWERT, K. et al. Lipoplex structures and their distinct cellular pathways. **Adv. Genet.** v. 53 p. 119-155, 2005.

FAHMY, T. M. Targeted for drug delivery. **Mater Today**. v. 8, p. 18-26, 2005.

FAROKHZAD, O. C.; LANGER, R. Impact of Nanotechnology on Drug Delivery. **ACS Nano**. v. 3, p. 16-20, 2009.

FASMAN, G. D., Editor Handbook of Biochemistry and Molecular Biology. Ed. 3, v. 1, p. 183-203, CRC Press: Cleveland, OH, 1976.

FDA. **Guidance for Industry.** Considering Whether an FDA-Regulated Product Involves the Application of Nanotechnology, 2014.
Disponível em: http://www.fda.gov/RegulatoryInformation/Guidances/ucm257698.htm.

FENDLER, J. H. **Memb. Mim. Chem**. New York: Wiley-Interscience, 1982.

FENDLER, J. H. Reactivity Control in membrane mimetic systems. **Pure Appl. Chem**. v. 54, p. 1809-1817, 1982.

FEYNMAN, R. P. There's plenty of room at the bottom. **Eng. Sci**. v. 23, p. 22–36, 1960.

FETTERLY, G. J.; STRAUBINGER, R. M. Pharmacokinetics of paclitaxel-containing liposomes in rats. **AAPS Pharm. Sci**. v. 5, E32. 2003.

FIELDS, G. B, NOBLE R. L. Solid phase peptide synthesis utilizing 9-fluorenylmethoxycarbonyl amino acids. **Int. J. Pept. Protein Res.** v. 35, p. 161–214, 1990.

GABIZON, A. A., SHMEEDA, H., ZALIPSKY, S. Pros and cons of the liposome platform in cancer drug targeting. **J. Liposome Res.** v. 16, p. 175-183, 2006.

GEBHARDT, K. E. et al. Role of secondary structure changes on the morphology of polypeptide-based block copolymer vesicles. **J. Colloid Interface Sci.**. v. 317, p. 70-76, 2008.

GIRIGOSWAMI, A.; DAS, S.; DE, S. Flororescence and dinamic light scattering of niosomes-membrane mimetic systems. **Spectrochim. Acta, Part A**. v. 64, p. 859-866, 2006.

GOMES, C. R. et al. Aplicações da nanotecnologia na indústria de alimentos: Uma Revisão. **Rev. Bras. Hig. San. Animal**. v.9, p.1-8, 2015.

GROVE, A. et al. Design of a functional calcium channel protein: Inferences about an ion channel-forming motif derived from the primary structure of voltage-gated calcium channels. **Protein Sci.** v.2, p. 1918-1930, 1993.

GUDLUR, S. et al. Peptide Nanovesicles Formed by the Self-Assembly of Branched Amphiphilic Peptides. **PLOS ONE**. v. 7, p. 53-74, 2012.

HANDJANI-VILA, R. M. et al. Dispersions of lamellar phases of non-ionic lipids in cosmetic products. **Int. J. Cosmet. Sci**. v.1, p. 303-314, 1979.

HAMMAN, J. H.; ENSLIN, G. M.; KOTZE, A. F. Oral delivery of peptide drugs: barriers and developments. **Bio. Drugs**. v.19, p. 165-177, 2005.

HART, S. L. Lipid carriers for gene therapy. **Curr. Drug Deliv**. v.2, p. 423-428, 2005.

HAWKER, C. J.; FRECHET, J. M. J. Preparation of polymers with controlled molecular architecture. A new convergent approach to dendritic macromolecules. **J. Am. Chem. Soc.** v. 112, p. 7638-7647, 1990.

HAWKER, C. J.; WOOLEY, K. L.; FRECHET, J. M. J. Unimolecular micelles and Globular amphiphiles: dendritic macromolecules as novel recyclable solubilization agents. **J. Chem. Soc. Perkin Trans**. v.1, p 1287-1297, 1993.

HAWKER, C. J.; WILLIAMS, C. R.; BAKER, J. R. Current dendrimer applicatuions in cancer diagnosis and therapy. **Curr. Top. Med. Chem**. v.8, p. 1165-1179, 2008.

HILL, R.M. **Aplications Of Surfactant Mixtures**: Mixed Surfactant Systems. Ed. 46 New York: Marcel Dekker, 1993.

HOLOWKA, E. P.; POCHAN, D. J.; DEMING. T. J. Charged polypeptide vesicles with controllable diameter, **J. Am. Chem. Soc**. v. 127, p. 12423-12428, 2005.

HSIAO, M. S. et al. Crystalization-driven selfassembly of block copolymers with a short crystallizable core-forming segment: Controlling micelle morphology through the influence of molar mass and solvent selectivity. **Macromolecules**. v. 47, p. 2361-2372, 2014.

ISO. International Organization for Standardization/Technical Specification,Nanotechnologies Vocabulary-Part 1: Core terms, 2010 (ISO/TS 80004-1:2010).

IWAMOTO, T. et al. Chemical synthesis and characterization of peptides and oligomeric proteins designed to form transmembrane ion channels. **Int. J. Pept. Protein Res**. v. 43, p. 597-607, 1994.

JEONG, W.; LIM, Y. Macrocyclic Peptides Self-Assemble into Robust Vesicles with Molecular Recognition Capabilities. **Bioconjugate Chem**. v. 25, p. 1996−2003, 2014.

JEVPRASESPHANT, R. et al. The influence of surface modification on the cytotoxicity of PAMAM dendrimers. **Int. J. Pharm**. v. 252, p. 263-266, 2003.

JIAO, D. et al. Supramolecular Peptide Amphiphile Vesicles through Host–Guest Complexation Angew. **Chem. Int**. v. 51, p. 9633 –9637, 2012.

JOST, F.; LEITER, H.; SCHWUGER, M. J. Synergisms in Binary Surfactant Mixtures. **Colloid. Polym. Sci.** v. 266, p. 554-561, 1988.

KAFRI, T. et al. Cellular immune response to adenoviral vector infected cells does not require de novo viral gene expression: Implications for gene therapy. **Proceedings of the National Academy of Sciences.** v. 95, p. 11377–11382, 1998.

KATAOKA, K.; HARADA, A.; NAGASAKI, Y. Block copolymer micelles for drug delivery: design, characterization and biological significance. **Adv. Drug Deliv. Rev.** v. 47, p. 113-131, 2001.

KAZI, K. M. et al. Niosome: A future of targeted drug delivery systems. **J. Adv. Pharm. Technol. Res.** v. 1, p. 374-380, 2010.

KEMPS, J. M. A.; CROMMELIN, D. J. A. Chemische stabiliteit van fosfolipiden in farmaceutische preparaten. I. Hydrolyse van fosfolipiden in waterig milieu. **J. Pharm. Weekbl**. v. 123, p. 355–363, 1988.

KIM, J. S. et al. Mechanism of ribonuclease cytotoxicity. **J. Biol. Chem**. v. 270, p. 31097–31102, 1995.

KIM, J. K. et al. Natural and synthetic biomaterials for controlled drug delivery. **Arch. Pharm. Res**. v. 37, p. 60-68, 2014.

KINGSLEY, J. D.; DOU, H.; MOREHEAD, J. Nanotechnology: a focus on nanoparticles as a drug delivery system. **J. Neuroim. Pharm.** v. 1, p. 340-50, 2006.

KOO, O. M.; RUBINSTEIN, I.; ONYUKSEL, H. Role of nanotechnology in targeted drug delivery and imaging: a concise review. **Nanomedicine: NBM.** v.1, p. 193-212, 2005.

LASIC, D. D. et al. Papahadjopoulos, D. Sterically stabilized liposomes: a hypothesis on the molecular origin of the extended circulation times. **Biochim. Biophys. Acta**. v. 1070, p. 187-192, 1991.

LETCHFORD, K.; Burt, H. A review of the formation and classification of amphiphilic block copolymer nanoparticulate structures: micelles, nanospheres, nanocapsules and polymersomes. **Eur. J. Pharm. Biopharm.** v. 65, p. 259-269, 2007.

LEVINE, D. H. et al. Polymersomes: A new multi-functional tool for cancer diagnosis and therapy. **Methods.** v. 46, p. 25-32, 2008.

LI, Y.; KWON, G. S. Methotrexate esters of poly(ethylene oxide)-block-poly(2hydroxyethyl-L-aspartamide). Part I: Effects of the level of methotrexate conjugation on the stability of micelles and on drug release. **Pharm. Res**. v.17, p. 607-611, 2000.

LIMA, F. C. Investigação de Complexos Mistos Polímeros-Surfactantes em Misturas de Dodecilsulfato de Sódio e Decilfosfato de Sódio com Polióxido de Etileno. Tese de Doutorado em Química, UFSC, Florianópolis, 1998.

MARCONI, D. M. O. Efeitos de Micelas Aniônicas Funcionais e Inertes e de Pré-Agregados Micelares sobre as Reações de Hidrólise do Anidrido Benzóico e de Alcanoatos de 2,4-Dinitrofenilina. Tese de Doutorado, UFSC, Florianópolis, 1995.

MARIANECCI, C. et al. Niosomes from 80s to present: The state of the art. Adv. **Colloid Interface Sci**. v. 205, p. 187-206, 2013.

MANIASSO, N. Ambientes Micelares em Química Analítica. **Quím. Nova**. v. 24 p. 87-93, 2001.

MASSINI, K. C.; JESUS, K. R. E.; ASSI, O. B. G. Indicadores de risco do desenvolvimento das nanotecnologias: uma ferramenta de apoio à decisão. In: VII Workshop de Nanotecnologia Aplicada ao Agronegócio. Anais Eletrônicos. Embrapa Gado de Leite, Juiz de Fora/MG, 2014.

MENG, F.; ZHONG, Z.; FEIJEN, J. Stimuli-responsive polymersomes for programmed drug delivery. **Biomacromolecules.** v. 10, p. 197–209, 2009.

MEZEI, M.; GULASEKHARAM, V. Liposomes: a selective drug delivery system for the topical route of administration I. Lotion dosage form. **Life Sciences**. v. 26, p. 1473-1477, 1980.

MI, Y.; LIU, Y.; FENG, S. S. Formulation of docetaxel by folic acid-conjugated d-α-tocopheryl polyethylene glycol succinate 2000 (Vitamin E TPGS 2k) micelles for targeted and synergistic chemotherapy. **Biomaterials**. v. 32 p. 4058-4066, 2011.

MIEDERER, M.; SCHEINBERG, D. A.; MCDEVITT, M. R. Realizing the potential of the Actinium-225 radionuclide generator in targeted alpha particle therapy applications. **Adv. Drug. Deliv. Rev**. v. 60, p. 1371-1382, 2008.

MIJAJLOVIC, M. et al. Microfluidic hydrodynamic focusing based synthesis of POPC liposomes for model biological system. **Colloids Surf., B.** v.104, p. 276–28, 2013.

MISHRA, D. et al. Evaluation of uptake and generation of immune response by murine dendritic cells pulsed with hepatitis B surface antigen-loaded elastic liposomes. **Vaccine**. v. 25, p. 6939-6940, 2007.

MINISTÉRIO DA CIÊNCIA E TECNOLOGIA , 2015. Portaria n. 3, de 6 de maio de 2015 (CAT Nanotecnologia). Disponível em: http://www.mctic.gov.br/mctic/opencms/tecnologia/tecnologias_convergentes/paginas/nanotecnologia/NANOTECNOLOGIA.html.

MO, X. et al. Design of 11-residue peptides with unusual biophysical properties: Induced secondary structure in the absence of water. **Biophys. J**. v. 94, p. 1807-1817, 2008.

MOGHIMI, S. M.; SZEBENI, J. Stealth liposomes and long circulating nanoparticles: critical issues in pharmacokinetics, opsonization and protein-binding properties. **Prog. Lipid Res**. v. 42, p. 463-478, 2003.

MOSES, M. A.; BREM, H.; LANGER, R. Advancing the field of drug delivery: taking aim at cancer. **Cancer Cell**. v. 4, p. 337-341, 2003.

MOGHIMI, S. M.; SZEBENI, J. Stealth liposomes and long circulating nanoparticles: critical issues in pharmacokinetics, opsonization and protein-binding properties. **Prog. Lipid Res**. v. 42 p. 463-478, 2003.

MU, L; SPRANDO, R. L. Application of Nanotechnology in Cosmetics. **Pharm. Res**. v. 27, p. 1746–1749, 2010.

NAAHIDI, S. et al. Biocompatibility of engineered nanoparticles for drug delivery. **J. Controlled Release**. v. 166, p. 182-194, 2012.

NASSERI, B. Effect of cholesterol and temperature on the elastic properties of niosomal membranes. **Int. J. Pharm**. v. 300, p. 95-101, 2005.

NEEDHAM, D.; ZHELEV, D. V. **Vesicles.** The Mechanochemistry of Lipid Vesicles Examined by Micropipette Manipulation Techniques in Vesicles. v. 62, ch. 9, New York: Marcel Dekker, p. 373-444, 2000.

NIGAVEKAR, S. S. et al. 3H dendrimer nanoparticle organ/tumor distribution. **Pharm. Res**. v. 21, p. 476-483, 2004.

NING, S. et al. Carboxymethyl dextran-coated liposomes: Toward a robust drug delivery platform. **Soft Matter**. v. 7, p. 9394-9401, 2011.

NIKALJE, A. P. Nanotechnology and its Applications in Medicine. **Med. Chem.** v. 5, p. 81-89, 2015.

PABST, G. et al. Liposomes, Lipid Bilayers and Model Membranes: From Basic Research to Application. Ed. 1, Boca Raton, FL: CRC Press, 478 p., 2014.

PARDAKTHY, A.; VARSHOSAZ, J.; ROUHOLAMINI, A. In vitro of polyoxyethylene alkyl ether niosomes for delivery of insulin. **Int. J. Pharm.** v. 328, p. 130-141, 2007.

PARDRIDGE, W. M. Gene targeting in vivo with pegylated immunoliposomes. **Meth. Enzymol**. v. 373, p. 507-528, 2003.

PARVEEN, S.; MISRA, R.; SAHOO, S. K. Nanoparticles: a boon to drug delivery, therapeutics, diagnostics and imaging. **Nanomedicine**. v. 8, p. 147-166, 2012.

PASCHOALINO, M. P. Os nanomateriais e a questão ambiental. **Quím. Nova**. v. 33, p. 421-430, 2010.

PAWAR, R.; BEN-ARI, A.; DOMB, A. J. Protein and peptide parenteral controlled delivery. **Expert Opin. Biol. Ther**. v. 4, p. 1203-1212, 2004.

PERCEC, V. et al. Self-assembly of janus dendrimers into uniform dendrimersomes and other complex architectures. **Science**. v. 328, p. 1009-1014, 2010.

PIMENTEL, L. F. et al. Nanotecnologia Farmacêutica Aplicada ao Tratamento de Malária. **Rev. bras. ciênc. farm.** v. 43, p. 503-514, 2007.

POLLOCK, S. et al. Uptake and trafficking of liposomes to the endoplasmic reticulum. **FASEB J**. v. 24, p. 1866-1878, 2010.

RAMANATHAN, M. et al. Amphiphile nanoarchitectonics: from basic physical chemistry to advanced applications. **Phys. Chem. Chem. Phys.** v. 15, p.10580-10611, 2013.

RAMOS, B. G. Z.; CRECZYNSKI-PASA, T. B. O desenvolvimento da nanotecnologia: cenário mundial e nacional de investimentos. **Rev. Bras. Farm**. v.89, p. 95-101, 2008.

RIOS-DORIA, J. et al. A Versatile Polymer Micelle Drug Delivery System for Encapsulation and In Vivo Stabilization of Hydrophobic Anticancer Drugs. **J. Drug Deliv**. v. 2012, p. 1-8, 2012.

ROMANO, G. et al. Latest development in gene transfer technology: achievements, perspectives, and controversies over therapeutic applications. **Stem Cells**. v. 18, p. 19-39, 2000.

ROSEN, B. M. et al. Dendron-mediated self-assembly, disassembly, and self-organization of complex systems. **Chem. Rev**. v.109, p. 6275-6540, 2009.

SABÍNA, J. et al. Insertion of semifluorinated diblocks on DMPC and DPPC liposomes: Influence on the gel and liquid states of the bilayer. J. **Colloid Interface Sci**. v. 348, p. 388-392, 2010.

SAMAD, A.; SULTANA, Y.; AQIL, M. Liposomal drug delivery systems: an update review. **Curr. Drug Deliv**. v. 4, p. 297-305, 2007.

SANTOS, C. M. B. Efeito da Variação do Processo de Síntese nas Propriedades Estruturais de Nanopartículas de $CoFe_2O_4$.. Dissertação de Mestrado, Universidade de Brasília, 2008.

SANTOSO, S. Self-assembly of surfactant-like peptides with variable glycine tails to form nanotubes and nanovesicles. **Nano Lett**. v. 2, p. 687-691, 2002.

SCHAFFAZICK, R. Caracterização e estabilidade físico-química de sistemas poliméricos nanoparticulados para administração de fármacos. **Quím. Nova**, v. 26, p. 726-737, 2003.

SCHLAAD, H.; ANTONETTI, M. Block copolymers with amino acid sequences: Molecular chimeras of polypeptides and synthetic polymers. **Eur. Phys**. **J**. v.10, p. 17-23, 2003.

SETHI, V.; ONYUKSEL, H.; RUBINSTEIN, I. Liposomal vasoactive intestinal peptide. **Methods Enzymol**. v. 391, p. 377-395, 2005.

SESSA, G.; WEISSMANN, G. Phospholipid spherules (liposomes) as a model for biological membranes. **J. Lipid Res.** v. 9, p. 310-318, 1968.

SHARMA**,** U. S.; BALASUBRAMANIAN, S. V.; STRAUBINGER, R. M. Pharmaceutical and physical properties of paclitaxel (Taxol) complexes with cyclodextrins. **Journal of Pharmaceutical Sciences**. v. 84, p. 1223-1230, 1995.

SHAW, D. J. Introduction to colloid and surface chemistry. Ed. 4. Oxford: Butterworth Heinemann, 1992.

SHEN, H.; ZHANG, L.; EISENBERG, A. Multiple pH-Induced Morphological Changes in Aggregates of Polystyrene-block-poly(4-vinylpyridine) in DMF/H2O Mixtures. **J. Amer. Chem. Soc**. v. 121, p. 2728-2740, 1999.

SHEN, X. et al. Adhesion and structure properties of protein nanomaterials containing hydrophobic and charged amino acids. **J. Nanosci Nanotechnol.** v. 6, p. 837-844, 2006.

SHI, J. et al. Nanotechnology in drug delivery and tissue engineering: from discovery to applications. **Nano Lett**. v. 10, p. 3223-3230, 2010.

SILVA, G. A. Introduction to nanotechnology and its applications to medicine. **Surg. Neurol**. v. 61, p. 216-220, 2004.

SINHA, V. R. Poly-epsiloncaprolactone microspheres and nanospheres: an overview, **Int. J. Pharm.** v. 278, p. 1-23, 2004.

SOUSA, E. C. Avaliação da atividade in vitro de Nanoemulsões e nanocápsulas de Fluconazol contra Candida spp. Diseertação de Mestrado em Ciências Biológicas, Universidade Federal de Outro Preto, Minas Gerais, 2007.

SOFOU, S. Enhanced retention of the α-particle emitting daughters of Actinium-225 by liposome carriers. **Bioconjug. Chem**. v. 18, p. 2061–2067, 2007.

SUH, W. H. et al. Nanotechnology, nanotoxicology and neuroscience. **Prog. Neurobiol.** v. 87, p. 133–170, 2009.

SUKTHANKAR, P. et al. Branched Oligopeptides Form Nano-Capsules with Lipid Vesicle Characteristics. **Langmuir. v.** 29 p. 14648−14654, 2013.

SUKTHANKAR, P. et al. Thermally Induced Conformational Transitions in Branched Amphiphilic Peptide Capsules. **Langmuir**. v. 31, p. 2946-2955, 2015.

SVENSON, S. Dendrimers as versatile platform in drug delivery applications. **Eur. J. Pharm. Biopharm.** v. 7, p. 445-462, 2009.

TAKEUCHI, H. et al. Evaluation of circulation profiles of liposomes coated with hydrophilic polymers having different molecular weights in rats. **J. Control. Release**. v.75, 83-91, 2001.

TANISAKA**,** H. et al. Near-infrared fluorescent labeled peptosome for application to cancer imaging. **Bioconjugate Chem**. v. 19, p. 109-117, 2008.

TANIGUCHI, N. On the basic concept of nanotechnology. **Proc. ICPB.** Tokyo, 1974.

THOMAS, C. E. et al. Preexisting antiadenoviral immunity is not a barrier to efficient and stable transduction of the brain, mediated by novel high-capacity adenovirus vectors. **Hum. Gene Ther.** v. 12, 839–846, 2001.

TORCHILIN, V. P. et al. Amphiphilic poly-Nvinylpyrrolidones: synthesis, properties and liposome surface modification. **Biomaterials**. v. 22, p. 3035-3044, 2001.

TORCHILIN, V. P. et al. Cell transfection in vitro and in vivo with nontoxic TAT peptide-liposome-DNA complexes. **Proc Natl Acad Sci USA** v. 10, p. 1972–1977, 2003.

TORCHILIN, V. P. Recent advances with liposomes as pharmaceutical carriers. **Nature Rev.** v. 4, p. 145-160, 2005.

TOMALIA, D. A. et al. A New Class of Polymers: Starbust-Dendritic Macromolecules. **Polym. J.** v. 17, p. 117-132, 1985.

TOMALIA, D. A. et al. Dendritic macromolecules: synthesis of starburst dendrimers. **Macromolecules**. v. 19, p. 2466-2468, 1986.

TOMALIA, D. A. Dendrimer molecules, **Sci. Am.** v. 272, p. 62-66, 1995.

TORCHILIN, V. P. Multifunctional nanocarriers. **Adv. Drug Deliv. Rev.** Amsterdan, v. 58, p. 1532–1555, 2006.

TORCHILIN, V. P. Recent Advances With Liposomes as Pharmaceutical Carriers. **Nature Rev**. v. 4, p. 145-160, 2005.

TRIPATHI, P. K. et al. Dendrimer grafts for delivery of 5-fluorouracil. **Pharmazie**. v. 57, p. 261-264, 2002.

TSONCHEV, S. et al. On the structure and stability of self-assembled zwitterionic peptide amphiphiles: A Theoretical study. **Nano Lett.** v. 4, p. 427-431, 2004.

UCHEGBU, I. F.; VYAS, S. P. Non-ionic surfactant based vesicles (niosomes) in drug delivery. **Int. J. Pharm.** v. 172, p. 33-70, 1998.

VAN HELL, A. J. et al. Self-Assembly of Recombinant Amphiphilic Oligopeptides into Vesicles. **Biomacromolecules**. v. 8, p. 2753-2761, 2007.

VAN HELL, A. J. M. M; FRETZ, D. J. A. Crommelin, W.E. Hennink, E. Mastrobattista, Peptide nanocarriers for intracellular delivery of photosensitizers. **J. Control. Release**. v. 141, p. 347-353, 2010.

VANDERMEULEN, G. W.; KLOK, H. A. Peptide/protein hybrid materials: enhanced control of structure and improved performance through conjugation of biological and synthetic polymers. **Macromol. Biosci**. v. 4, p. 383-398, 2004.

VAN ZANTEN, J. et al. A nonviral carrier for targeted gene delivery to tumor cells. **Cancer Gene Ther.** v. 11, p. 156 - 64, 2004.

VAUTHEY, S. et al. Molecular self-assembly of surfactant-like peptides to form nanotubes and nanovesicles. **Proc. Natl. Acad. Sci**. v. 99, p. 5355-5360, 2002.

VANLERBERGHE, G.; HANDJANI-VILA, R. M.; RIBIER, A. Les niosomes, une nouvelle famille de vesicules a base d'amphiphiles non ioniques. In Physicochimie des compose´s amphiphiles. **Coll. Nat. CNRS. Editions du CNRS**. Paris. p. 303–311, 1978.

VASHIST, A. et al. Recent advances in hydrogel based drug delivery systems for the human body. : **J. Mater. Chem. B.** v. 2, p147-166, 2014.

VASIR, J. K.; LABHASETWAR, V. Targeted drug delivery in cancer therapy. **Technol Cancer Res Treat.** v. 4, p. 363-374, 2005.

VELICHKO, Y. S.; STUPP, S. I.; DE LA CRUZ, M. O. Molecular simulation study of peptide amphiphile self-assembly. **J. Phys. Chem. B**. v. 112, p. 2326-2334, 2008.

VEMURI, S.; RHODES, C. T. Preparation and characterization of liposomes as therapeutic delivery systems: a review. **Pharm Acta Helv**. v. 70, p. 95-111, 1995.

VOGTLE, F. et al. Functional dendrimers. **Prog. Polym. Sci.** v. 25, p. 987-1041, 2000.

VONARBOURG, A. et al. Parameters influencing the stealthiness of colloidal drug delivery systems. **Biomaterials**. v. 27, p. 4356-4373, 2006.

WANG, L. et al. Self-assembled polypeptide-blockpoly(vinylpyrrolidone) as prospective drug-delivery systems. **Colloids Surf., B**. v. 74, p. 284-292, 2009.

WATNASIRICHAIKUL, S. et al. Preparation of biodegradable insulin nanocapsules from biocompatible microemulsions. **Pharm. Res.** v. 17, p. 684-689, 2000.

WU, G. Y.; WU, C. H. Receptor-mediated gene delivery and expression in vivo. **J. Biol. Chem.** v. 263, p. 14621 - 14624, 1988.

XU, W.; LING, P.; ZHANG, T. Polymeric Micelles, a Promising Drug Delivery System to Enchace Bioavailability of Poorly Water-Soluble Drugs. **J. Drug Deliv**. v. 2013, p. 1-15, 2013.

YASAM, V. R. et al. A review on novel vesicular drug delivery: proniosomes. **J. Drug Deliv**. v. 21, p. 243-249, 2014.

YOUNG, S. Future direction of Nanomedicine in Gastrointestinal Cancer. **Korean J. Gastroenterol**. v. 49, p. 271-279, 2007.

ZHANG, Y. et al. Organ-specific gene expression in the rhesus monkey eye following intravenous non-viral gene transfer. **Mol. Vis.** v. 9, p. 465-472, 2003.

ZHAO, X. et al. Molecular self-assembly and applications of designer peptide amphiphiles. **Chem. Soc. Ver.** v. 39, p. 3480-3498, 2010.

ZHIVOTOVSKY, B. et al. Injected cytochrome c induces apoptosis. **Nature.** v. 391, p. 449–450, 1998.

ZHOU, T. et al. Nanostructure induced DNA condensation. **Nanoscale.** v. 5, p. 8288 - 8306, 2013.

5 ARTIGO I

Artigo Publicado na revista “Archives of Biochemistry and Biophysics”
(Fevereiro de 2016)

Barros, S. M., Whitaker, S. K., Sukthankar, P. R., Gudlur, S., Warner, M. Beltrão, E. I. C., Tomich, J.M. A Review of Solute Encapsulating Nanoparticles used as Delivery Systems with Emphasis on Branched Amphipathic Peptide Capsules. *Arch Biochem Biophys.* (2016) 596: 22-42.

Archives of Biochemistry and Biophysics 596 (2016) 22–42

Contents lists available at ScienceDirect

Archives of Biochemistry and Biophysics

journal homepage: www.elsevier.com/locate/yabbi

Review article

A review of solute encapsulating nanoparticles used as delivery systems with emphasis on branched amphipathic peptide capsules

Sheila M. Barros [a, b], Susan K. Whitaker [a], Pinakin Sukthankar [a, 1], L. Adriana Avila [a, 2], Sushanth Gudlur [a, 3], Matt Warner [a], Eduardo I.C. Beltrão [b], John M. Tomich [a, *]

[a] Department of Biochemistry and Molecular Biophysics, Kansas State University, Manhattan, KS 66506, USA
[b] Department of Biochemistry, Federal University of Pernambuco-UFPE, Recife, Pernambuco, 50670-901, Brazil

ARTICLE INFO

Article history:
Received 5 November 2015
Received in revised form
24 February 2016
Accepted 26 February 2016
Available online 27 February 2016

Keywords:
BAPCs
Nanoparticle
Drug delivery
Self-assembly
Peptide bilayer

ABSTRACT

Various strategies are being developed to improve delivery and increase the biological half-lives of pharmacological agents. To address these issues, drug delivery technologies rely on different nano-sized molecules including: lipid vesicles, viral capsids and nano-particles. Peptides are a constituent of many of these nanomaterials and overcome some limitations associated with lipid-based or viral delivery systems, such as tune-ability, stability, specificity, inflammation, and antigenicity. This review focuses on the evolution of bio-based drug delivery nanomaterials that self-assemble forming vesicles/capsules. While lipid vesicles are preeminent among the structures; peptide-based constructs are emerging, in particular peptide bilayer delimited capsules.

The novel biomaterial—Branched Amphiphilic Peptide Capsules (BAPCs) display many desirable properties. These nano-spheres are comprised of two branched peptides—bis(FLIVI)-K-KKKK and bis(FLIVIGSII)-K-KKKK, designed to mimic diacyl-phosphoglycerides in molecular architecture. They undergo supramolecular self-assembly and form solvent-filled, bilayer delineated capsules with sizes ranging from 20 nm to 2 μm depending on annealing temperatures and time. They are able to encapsulate different fluorescent dyes, therapeutic drugs, radionuclides and even small proteins. While sharing many properties with lipid vesicles, the BAPCs are much more robust. They have been analyzed for stability, size, cellular uptake and localization, intra-cellular retention and, bio-distribution both in culture and in vivo.

Contents

* Corresponding author. Department of Biochemistry and Molecular Biophysics, 141 Chalmers Hall, Kansas State University, Manhattan, KS, 66506, USA.
E-mail address: jtomich@ksu.edu (J.M. Tomich).
[1] Current address: Department of Molecular Biosciences, University of Kansas, Lawrence KS 66045, USA.
[2] Current address: Department of Chemistry and Biochemistry, Auburn University Auburn AL 36849, USA.
[3] Current address: Center for Biomimetic Sensor Science (CBSS) Nanyang Technological University, 637553 Singapore.

http://dx.doi.org/10.1016/j.abb.2016.02.027
0003-9861/

1. Introduction

A goal of pharmaceutical research is to deliver drugs at appropriate dosages to target cells or tissues in a safe and reproducible manner [1]. While tremendous progress has been made in defining fundamental biological processes and discovering compounds that interact with these molecules, translation of these findings into advanced therapies has lagged behind. Limitations in delivering therapeutic moieties to selective tissues with minimal off-target damage are often cited for this lapse [1,2]. Novel molecular pharmacological agents with proven biological activities but limited aqueous solubilities or short circulating half-lives in vivo will face substantive barriers. These delivery impediments limit or reduce therapeutic activity and disfavor potential pharmaceutically interesting compounds from entering clinical drug trials [1]. Conventional modes of drug administration such as pills, eye drops, intravenous solutions, ointments, inhalers etc., fall short in meeting these expectations. The oral route for example is one of the most commonly employed and preferred modes for drug administration due to its minimally invasive nature. However the adequate delivery of peptide and protein drug candidates fuelled by the recent advances in recombinant biotechnology [2], are ineffective via this route [3,4]. Overcoming numerous barriers including—the acid environment of the human stomach, proteolytic degradation, limited intestinal uptake and first pass effects of the liver is essential. All of these factors reduce, alter and block absorption of almost all biomacromolecular therapeutics [5,6].

Self-assembling nano-carriers (Fig. 1) show promise as delivery vehicles that overcome many of the poor absorption issues that plague certain classes of drugs. Both hydrophobic and hydrophilic small molecules, proteins, and nucleic acids can be bound to or encapsulated within the compartments of these nanomaterials and delivered in vitro or in vivo. The self-assembling carriers can be classified into a number of categories depending on whether they are solid or hollow and the materials that comprise them. They can be further categorized depending on whether they contain natural or synthetic polymers. Polymeric vesicles offer advantages over their natural counterparts (Liposomes) in terms of stability, storage and tune-ability. Drug delivery through polymeric vesicles increases the stability of the drug, extends the circulating time in the bloodstream and can be designed for controlled release. Most polymersomes and peptide amphiphiles have low “critical assembly concentrations” (CAC), a value similar to the critical micelle concentration (CMC), used to describe the minimum concentration needed to form lipid vesicles. Their CAC's fall in the range of 10^{-6} – 10^{-7} M, which is 1000 times lower than most surfactants (10^{-3} – 10^{-4} M) [7,8]. This allows for the retention of payloads for longer periods as well as improved delivery to distal areas of the body. A review of the literature reveals a plethora of compounds encapsulated and successfully delivered in vitro and in vivo using polymeric vesicles. These include various anti-cancer drugs like Doxorubicin and Paclitaxel, proteins like myoglobin, hemoglobin and albumin, fluorescent molecules, plasmids and siRNA. The review by Levine et al. (2008) [9] summarizes the literature on polymersome research related to cancer diagnosis and therapeutics, giving a more detailed account of the types of polymersomes and cargo that have been developed to that point.

Polymeric vesicles are also useful as diagnostic tools and in optical imaging when they encapsulate fluorescent agents. One example is the encapsulation of a porphyrin-based near infrared (NIR) fluorophore that is able to generate a signal even through a 1 cm solid tumor [10]. When such nanovesicles are injected into an animal, their biodistribution can be monitored using non-invasive NIR optical methods eliminating the need to sacrifice the animal.

The surface of these nanovesicles can be functionalized with various ligand molecules specific for up-regulated surface receptors on diseased cells. Such site-specific delivery reduces potential systemic side-effects observed using traditional delivery routes. Some of the ligand molecules attempted include various antibodies, transactivator of transcription (TAT) peptide and anti-HER-2/neu *peptide* mimetic (AHNP) peptides.

Nano-vectors have been shown to improve the pharmacological characteristics of these drug moieties. The utilization of nanotechnology for drug delivery has been shown to enhance the delivery of poorly soluble drugs, facilitate drug targeting in a cell/tissue-specific manner and enabled the co-delivery of two or more drugs as well the intracellular delivery of larger macromolecular drugs. By enhancing the efficacy of these drugs, new candidate drugs are advancing in clinical trials with improved safety and effectiveness [11]. The application of nanotechnology to drug delivery is expected to alter the landscape of pharmaceutical and biotechnology industries in the foreseeable future [11–14]. As of 2013, almost 250 nanotechnology based medicines had been approved or were in various stages of clinical investigation [15–17].

Nanoparticulates are colloidal macromolecular nanocarrier systems ranging from 10 to 200 nm and deemed as potentially

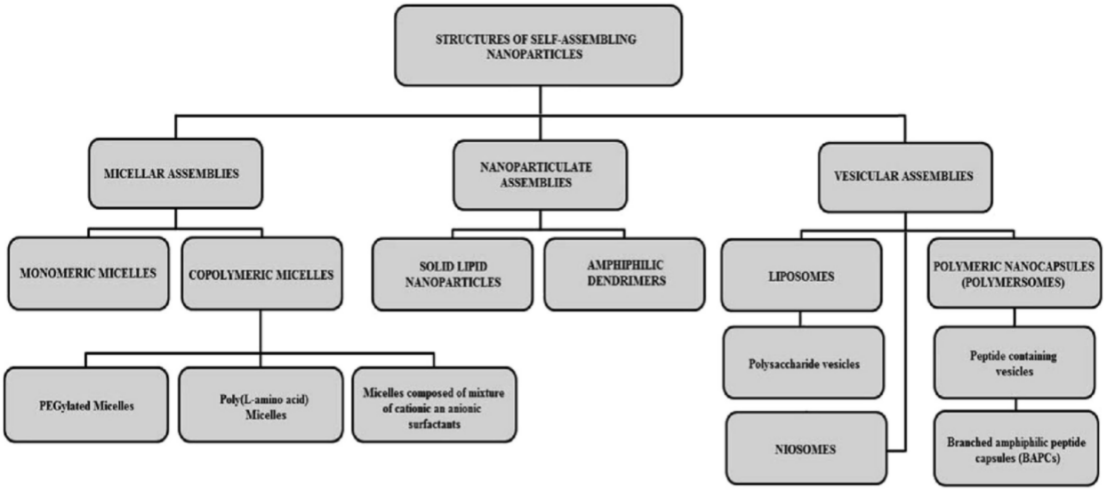

Fig. 1. Classification of nanocarrier systems for drug delivery.

attractive candidates for the entrapment and encapsulation of hydrophobic drugs. Solid nanoparticulates can either be defined as nanocapsules - where the active drug molecule is encapsulated within the carrier; or matrix based nanospheres - where the drug molecules are adsorbed and dispersed throughout the nanomaterial [18]. Nanoparticulates can be engineered using 'top down' or 'bottom up' methods [19]. In the former, a larger material is broken down into smaller particles whereas the bottom up approach involves the thermodynamically regulated, multi-step synthesis of the nanomaterial in a controlled reaction [20].

A competent nano-carrier functions safely, selectively, reliably delivering a therapeutic at the required dosage to the target site in the appropriate time frame [3,13,20,21]. Ideal nano-carriers possess several desirable attributes: they should reduce the concentrations of the active compound needed since the drugs are no longer systemically distributed [22] and the pharmacokinetics of biodistribution are enhanced due to improved tissues and organ targeting [12,23–25]. This preferential delivery along with the particle's ability to release drugs in a sustained or stimuli triggered manner will reduce off-target effects and decrease cytotoxicity. Utilization of nano-carriers has the added advantage of improving the delivery of hydrophobic drugs in water; thus enhancing their delivery through parenteral administration. Nano-carrier based delivery systems have also been shown to improve the half-lives of a wide variety of hydrophobic moieties and peptide drugs [26–28]. Moreover, nanotechnology based delivery vehicles composed of biocompatible molecules [29–32] are projected as safer alternatives to existing vehicles that have been known to cause peripheral neuropathy and hypersensitivity [33,34].

The search for nano-delivery systems involves numerous design elements. The large repertoire of available nano-carriers, apart the ones that are in development, present nano-systems with a variety of structural, functional and physiochemical characteristics that translate into case specific advantages and/or limitations. These include (i) biocompatibility of constituent material(s); (ii) simple and robust assembly processes; (iii) functionalization/pre-functionalization capability; (iv) intracellular stability and biodegradability; (v) long circulating half-life; (vi) a size compatible with facile cellular uptake, charge density, surface hydrophilicity and flexibility; and (vii) negligible immunogenicity.

It has been indicated that the complexity involved in nanoparticle fabrication and functionalization causes batch to batch variations leading to quality and purity concerns [3]. The development of targeted nano-carriers via a single step synthesis mediated by the self-assembly of pre-functionalized biomaterials would serve to alleviate these concerns by simplifying the optimization and the scalable manufacture of these systems [35–38].

Despite recent advancements in nano-medicine, several challenges remain – 1) over-coming physicochemical and biological hurdles such as low stability, low permeability, short half-life, enzymatic susceptibility, targeting and 2) immunogenicity [5]. Although a majority of these nano-therapeutic products have improved the pharmaceutical efficacy of clinically approved drugs, nanotechnology as a whole has not yet generated entirely new therapies [11].

2. Structures of self-assembling nanoparticles

The phenomenon of bio-molecular self-assembly is a common in nature. Assembled multi-protein complexes are required for a number of cellular functions. Diacylglycerol-phospholipid assembly is responsible for the structure of the various cell membranes. In the context of lipids and peptides, the self-assembling molecules are amphiphilic and are comprised of both hydrophobic and hydrophilic domains. These domains can be spatially separated either along the length of the molecule or along a defined face of the folded molecule [39]. The hydrophilic segments can either be uncharged (polar) or charged (cationic, anionic or zwitterionic) [40]. While such segments are spatially segregated in lipids, in amphipathic peptides the primary sequences contain alternating or random segments of hydrophobic and hydrophilic residues. Upon folding into either helices or β-sheets, the final functional structures have continuous faces of hydrophobic or hydrophilic residues that allow them to interact with solvent, a membrane, a ligand or an adjacent molecule.

Self-assembly in bio-macromolecules is usually facilitated by weak non-covalent interactions that can be any one or a mixture of hydrogen bonding, Van der Waal forces, ionic, and electrostatic interactions. When such amphiphilic molecules are introduced into an aqueous environment, the hydrophobic segments anneal to

exclude water thereby providing the driving force for assembly aided by inter- and intra-molecular associations. The hydrophilic segments of the molecule remain exposed to the aqueous solvent. Much of our understanding of self-assembly of amphiphiles comes from studies with lipids. Attempts to mimic lipid amphiphiles have led to the design and development of many different types of molecules that retain the amphiphilic character with relatively short acyl-chains [41,42].

Lipid and peptide amphiphiles assemble into a number of nano- and micro-sized structures such as micelles, vesicles or molecular gels [43] composed of rods and tubules [44], fibrils and fibers [45] with ordered structures. Micelles adopt spherical, worm like or disk shaped structures [46–51]. Vesicles when composed entirely of lipids are called liposomes, but other non-lipid vesicle types exist: niosomes, proniosomes, polyhedral niosomes, polymersomes and vesicles formed by the self-assembly of peptide amphiphiles (peptosomes) [52]. Finally, structures that do not fall into either of these common categories can be as diverse as, bipyramids, lamellar, hexagonal phase, cubic phase, icosahedral, cage like, high axial ratio microstructures (HARM) [53–55] and myelin fibrils [40]. The energetics, geometric constraints and strengths of the intra- and inter-interacting forces of the individual molecules determine the final architecture of the assembly. Other factors influencing the final assembly are pH, temperature, ionic strength of the solvent, as well as the concentration of the monomer. Using the packing parameter of the monomer one can predict the favored structure of the assembly [56]. The packing parameter depends on the area of the head group a_0, molal volume of the hydrocarbon chain or chains v, and the extended chain length l_0 of the monomer:

$$\text{Packing number} = \frac{v}{a_0 l}$$

While the head group of the amphiphiles plays a critical role in predicting the overall shape and size of the assemblies, the tail region directs the formation of spherical micelles, rod like micelles and spherical bilayer vesicles [43]. While there are numerous review articles focused on the different morphologies adopted by self-assembling molecules, this review is concerned with studies on spherical aggregates, namely micelles and vesicles.

2.1. Micellar assemblies

2.1.1. Monomeric micelles

Micelles are the simplest amphiphilic assembly. They are useful in encapsulating hydrophobic molecules within their hydrophobic core (Fig. 2).

Detergent micelles comprised of sulfated acyl chains (i.e. sodium dodecyl sulfate, SDS) adopt this structure. At concentrations below their CMC, the amphiphiles exist as monomers but as the monomer concentration exceeds the CMC, they begin to assemble into stable spherical structures. These structures are in a dynamic equilibrium with the monomers present in solution. The CMC is affected by further increases in concentration of the amphiphile that can lead to a change in the overall shape (discoidal, rod like or liquid crystalline phase), thus allowing one to tune the overall shape and size of the final assembly. Lipid micelles range from 10 to 100 nm in diameter and exhibit a core-shell architecture, in which the interior, being hydrophobic, entraps lipophilic drugs [57]. The CMC and structural features exhibited by micelles are a function of the nature of their hydrophilic and hydrophobic block constituents. Yu and Eisenberg [58] generated a variety of micellar conformers such as, spheres, rods, vesicles, tubules and lamellae depending on solvent conditions and the relative size of hydrophobic and hydrophilic segments. These different structures when tested for their ability to deliver drugs displayed varied pharmacokinetic properties. [59–63].

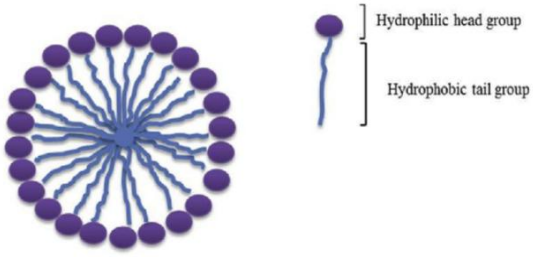

Fig. 2. Illustration of a micelle.

2.1.2. Copolymeric micelles

Copolymeric micelles are relatively new constructs that incorporate biodegradable polymers prepared from block copolymers. Block copolymers are linear repeating units of hydrophobic and hydrophilic residues covalently linked to impart amphilicity to the molecule. $K_{60}L_{20}$ is one such example of a diblock copolymer where a polypeptide comprised of sixty lysine residues is covalently linked to a polypeptide composed of twenty leucine residues. The block of leucine residues form the hydrophobic segment of the block copolymer while the positively charged lysine residues form the more hydrophilic segment [64]. Triblock copolymers are similar to diblock copolymers but differ in having an extra hydrophobic or hydrophilic segment that can be fused to either of the existing segments. In general, a polymeric micelle consists of two parts: a outer corona composed of the soluble hydrophilic segments (Fig. 3). While simple spherical micelles with a core particle and corona are common, more complex multi-lamellar structures have been recently reported that resemble onion-like micelles [65], shell cross-linked micelles [66], star shaped Janus micelles that allow for two different types of chemical interactions in the same molecule [67–69] schizophrenic diblock copolymer micelles [70], multi-compartmental hamburger micelles [71].

2.1.2.1. PEGylated micelles. Numerous copolymers have been used to produce micelles, but biocompatibility and biodegradability issues have limited their use in therapeutic applications [72]. Usually, the preferred choice for the hydrophilic block has been polyethylene glycol (PEG). In most micellar assemblies, the molecular weight of PEG tends to exceed that of the hydrophobic core-forming block [73]. This outer hydrophilic corona region tends to

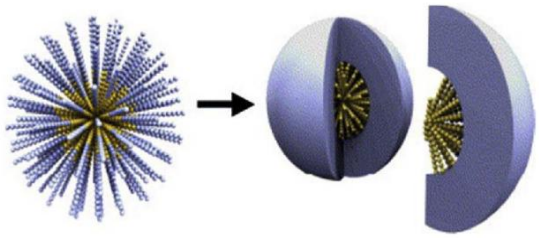

Fig. 3. Polymeric micelle. Self-assembly and polymerization of a block copolymers yielda shell cross-linked knedel polymer assemblies, where the cross-linked outer shell can be decorated with biologically relevant ligands. [Reprinted from *Adv Drug Deliv. Rev*, 56(11), Tu and Tirrell, Bottom-up design of biomimetic assemblies, 1537–1563 (2004) [42] with permission from Elsevier].

become hydrated resulting in a splayed appearance, giving rise to various structures, such as polymer brushes [74]. These conformations imbue the micelles with new properties that suppress binding of serum proteins and phagocytic attack in blood thereby decreasing clearance by the reticuloendothelial system (RES) [75]. PEGylated co-polymer micelles also have lower CAC's than traditional surfactants resulting in reduced cytotoxicity [76]. The highly hydrated corona and the hydrophobic core generate a dielectric gradient that aids in the solubilization of a range of non-polar compounds of varied hydrophobicities [77]. Micellar delivery systems, like many other ones, positively affect the biodistribution and pharmacokinetics of drugs by means of increased circulating half-lives and increased tumor accumulation [78].

2.1.2.2. Poly(L-amino acid) micelles. Poly(L-amino acid) micelles are formed from poly(L-Histidine)-PEG block co-polymers combined with poly(L-lactic acid)-PEG (PLLA-PEG). These micelles have been investigated as pH sensitive drug carriers for cancer therapy [79–81]. Cancerous cells - due to a higher rate of metabolism - tends to have intracellular pH values < 7.2 [82–84]. The imidazole side-chain of histidine has a pKa in this range; which leads to an increase in histidine hydrophobicity, destabilization of the micelle and subsequent drug release. The pH sensitivity of Poly(L-amino acid) micelles can be modulated by varying the %wt. of the poly(L-lactic acid)-PEG composition. Moreover, Poly(L-histidine) (PLHS) appears to have fusogenic activity with endosomes facilitating cytosolic drug release in cancer cells. More complex systems that incorporate phenylalanine ([poly(His-co-Phe)]-PEG) and 1,2-distearoyl-sn-glycero-3-phosphoethanolamine-polyethylene glycol-2000(DSPE-PEG) have recently been formulated to decrease the pH sensitivity of the pure poly L-histidine and also act as pH sensitive nanocarriers for cytosolic drug delivery [85]. Drugs have been conjugated to these poly(amino acid) copolymers via chemical modifications of the drugs, but not without concerns relating to drug decoupling at the target site [86–88]. Also, immunogenicity is a potential concern with these systems upon the increase in the number and diversity of amino acids used [71].

2.1.2.3. Micelles composed of mixtures of cationic and anionic surfactants. The preparation of micelles using two surfactants of opposite net charge is well established [89–91]. Charge repulsion of the head groups decreases the free energy of assembly [92]. The size and net charge of the detergent pair determines the CMC as well as the size of the resulting micelles [93]. In a single report the mixing of certain oppositely charged surfactants can lead to the spontaneous formation of single walled vesicles [94]. The size, charge and permeability of such vesicles was controlled by adjusting the molar ratios of the two surfactants. One example of such a charge balancing mixture is cetyl trimethylammonium tosylate (CTAT) and sodium dodecylbenzene sulfonate (SDBS).

2.2. Nanoparticulate assemblies

2.2.1. Solid lipid nanoparticles

Solid Lipid Nanoparticles (SLNs) are members of a class of nanoscale carriers consisting of a central solid hydrophobic core comprised of physiological lipids emulsified with an aqueous surfactant [95]. Hydrophobic drugs are dissolved in the solid hydrophobic core [96]. These nanoparticles due to their narrow size range (100–200 nm) evade the RES and cross the blood-brain barrier [97]. The biodegradable properties of these lipids minimize their cytotoxicity. SLNs also demonstrate stable drug entrapment, especially in case of very hydrophobic drugs and provide controlled release lasting several weeks. SLN can be conjugated to hydrophilic polymers and/or surfactants to minimize their hepatic uptake and improve bioavailability [58]. SLNs can be stabilized with stearic acid - PEG 2000, however cytotoxic effects have been observed upon the release of free stearic acid [98]. By choosing lipids with varying chain lengths and degrees of unsaturation the loading capacity of SLNs can be controlled. Overall, SLNs appear to be safe delivery systems for hydrophobic drugs especially to the brain and production is scalable with excellent reproducibility [99,100].

2.2.2. Amphiphilic dendrimers

Dendrimers are 1–10 nm sized hyper-branched synthetic polymers comprised of well-defined branched oligomers attached to a central core [101–103]. Dendrimers are synthesized using convergent or divergent approaches [103]. The former approach capitalizes on the symmetric nature of the dendrimer with synthesis commencing at the periphery and terminating at the core; while the divergent approaches builds out from the core [104]. Dendrimers display low poly-dispersity despite their large molecular mass. The branching of the dendrimers generates semi-globular/globular structures that are easily functionalized [103]. Glycol-, peptide- and silicon-capped dendrimers have been synthesized using carbohydrates, peptides and silicon [39,105]. Drugs can associate with dendrimers through physical entrapment within the void spaces or by attachment of the pro-drug to functional groups positioned on the dendrimer surface [94].

Amphiphilic dendrimers (Janus dendrimers) are capable of self-assembling into stable bilayer vesicles, referred to as dendrimersomes [106]. A Janus dendrimer is formed by covalently linking two distinct dendritic building blocks. They can be made amphiphilic by attaching a non-polar block (e.g. alkoxy gallate ether to a polar block such as aliphatic arborol) [107]. A review by Rosen et al. (2009) [108] details the self-assembly and disassembly

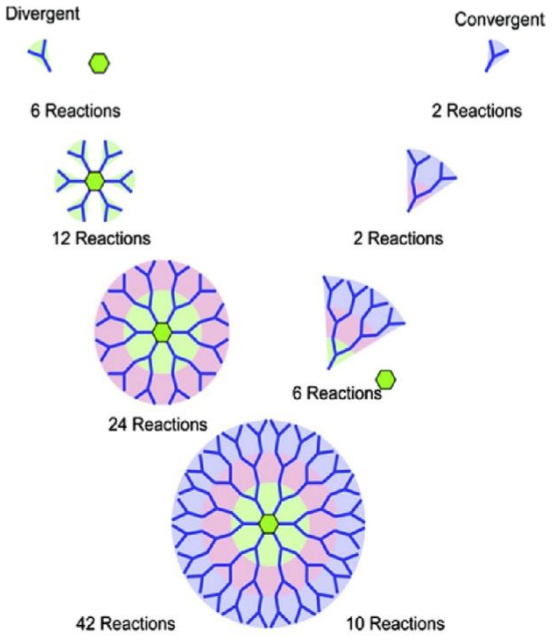

Fig. 4. Convergent and divergent synthesis of dendrimers and dendrons. Reprinted (adapted) with permission from Rosen et al. (2009) [108], Chem Rev., **109**(11), 6275–6540. Copyright 2009 American Chemical Society.

of dendrons. Fig. 4, is an illustration reproduced from the above review.

Dendrimers have been studied for the delivery of fluorouracil [109] and indomethacin [110]. Dendrimer size has been exponentially correlated with the duration of extravasation across the endothelium, with larger dendrimers indicating faster extravasations [111]. The positive charges on the polyamine and/or polyamide linkages used in some dendrimers pose a potential risk for cellular toxicity and immune activation. Partial derivatization of the dendrimer surface with PEG and/or fatty acids is known to mitigate these concerns by shielding the positive charges on the surface [112,113].

2.3. Vesicular assemblies

In contrast to the different micellar constructs discussed above where drugs are trapped within the micellar matrix, the ability of vesicles to encapsulate solutes offers increased versatility. Their hollow interiors permit encapsulation of higher concentrations of cargo, thus making them potentially better drug delivering vehicles. Vesicles are colloidal aggregates that are most often spherical. In biology, lipid vesicles are bilayer-delimited chambers that entrap solvent during the self-assembly process. The solvent is water containing dissolved solutes. In terms of drug delivery, solutes including peptides, proteins, genetic material, or bioactive compounds like anticancer drugs can be encapsulated. It can also trap non-polar or hydrophobic substances within their membrane, thereby increasing their utility. Such versatility has made them the most attractive choice for use in biology. Apart from its biological/medical uses, vesicles can be used as micro-chemical reactors and have found application in the cosmetic and food industries [114]. Lipid based vesicles are the most extensively studied drug carriers used today. Until recently, lipids were the only choice for generating artificial vesicles. However with the introduction of many new self-assembling molecules, one can choose from a variety of molecules. Figure 1, classifies the various polymeric vesicles described to date. It is difficult to precisely classify all of the various polymeric vesicles due to the issue of multi-functionality. This is particularly true with the introduction of hybrid polymers, where two or more different materials are used to make an amphiphile such as combining the synthetic polymer polyethylene oxide (PEO) to either a polypeptide or a diacylglycerol phospholipid. These hybrid polymers can improve solubility, increase circulating half-lives in the bloodstream and allow for the surface functionalizing with desired targeting ligands. Such a molecule could be classified as a block.

Copolymer, lipid vesicle or peptide vesicle depending on the proportions of the individual components and/or which component is driving the assembly [103]. Employing natural biopolymer vesicles as drug carriers over synthetic and semi-synthetic polymer vesicles improves their biocompatible and biodegradable. Lipids, polysaccharides and peptides are all capable of self-assembling into vesicles and other nano- and micro-sized structures [115].

2.3.1. Liposomes

Liposomes or lipid vesicles are possibly the oldest and most widely studied drug delivery systems and have been in use since the 1960s [116,117]. These artificially produced vesicles range from 30 nm to several micrometers in size and consist of an aqueous core surrounded by uni- or multi-lamellar membranes formed from the supramolecular-assembly of primarily phospholipids (Fig. 5) and cholesterol. Numerous studies have promoted the use of these structures [118–120].

Liposomes can be prepared from a variety of diacyl phospholipids including: 1,2-Dimyristoyl-*sn*-glycero-3-phosphocholine

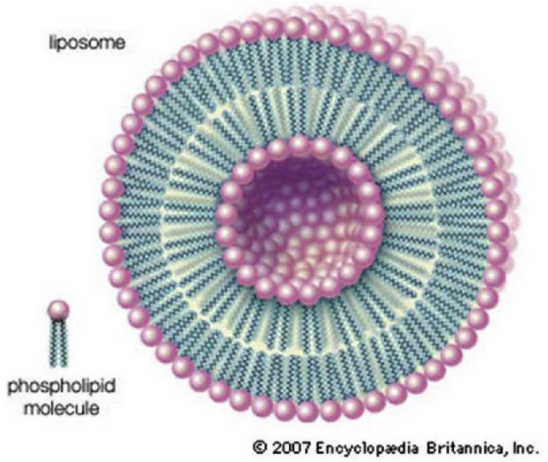

Fig. 5. Illustration of a Liposome. By courtesy of Encyclopaedia Britannica, Inc., copyright 2007; used with permission. [http://www.britannica.com/EBchecked/media/92244/Phospholipids-can-be-used-to-form-artificial-structures-called-liposomes].

(DMPC), 1,2 Dipalmitoyl-sn-glycero-3-choline (DPPC), and 1-palmitoyl-2-oleoyl-sn-glycero-3-phosphocholine (POPC), palmitoyl-2-oleoylphosphatidylethanolamine (POPE) among others. As an example we show POPC:POPE vesicles generated in our laboratory as well as their resizing after extrusion (Fig.6). Most of our knowledge on vesicle assembly, dynamics and physical properties come from studies on these assemblies. Since then, many different and diverse vesicles have been designed and developed. Unlike polypeptides and polysaccharides, lipids are not polymers. Liposomes have found uses in many biological, pharmaceutical and cosmetic applications. They are employed in studies related to cell physiology, as model cell membranes and drug delivery vehicles.

Their utility lies in their ability to fuse with cellular membranes [121] and lipid bilayers membranes or enter cells through clathrin-mediated endocytosis [122,123]. The properties of liposomes have been modulated to produce variation in size, lipid composition, surface charge and other characteristics [77]. The aqueous core of the liposomes is known to encapsulate large payloads of hydrophilic and moderately hydrophobic drugs; and their ability to naturally associate with tumors and the EPR effect has led to the development of numerous FDA approved drugs based on the liposome platform [72,100,124].

Numerous studies have been conducted to surface modify classical liposomes in an effort to increase their targeting capabilities and circulating half-lives. These include the introduction of linear dextrans [125], gangliosides containing sialic acid [126], lipid derivatives of hydrophilic polymers such as polyvinyl alcohol [127], polyethylene glycol [128,129] and poly-N-vinylpyrrolidones [130]. These modifications stabilize and protect them from uptake by the mononuclear phagocytic system (MPS). Targeted therapy has also been demonstrated using liposomes conjugated to monoclonal antibodies via a PEG linker [131], and protease-sensitive polymer-caged liposomes have been developed to enable selective targeting and drug release at the cancerous site by exploiting the natural tendency of affected cells to produce cancer associated proteases to destabilize the liposome [132].

Liposomes also appear to be the preferred carriers for purposes of radionuclide based targeting for cancer therapy. A variety of liposomes such as multi-vesicular liposomes (MUVEL) - small

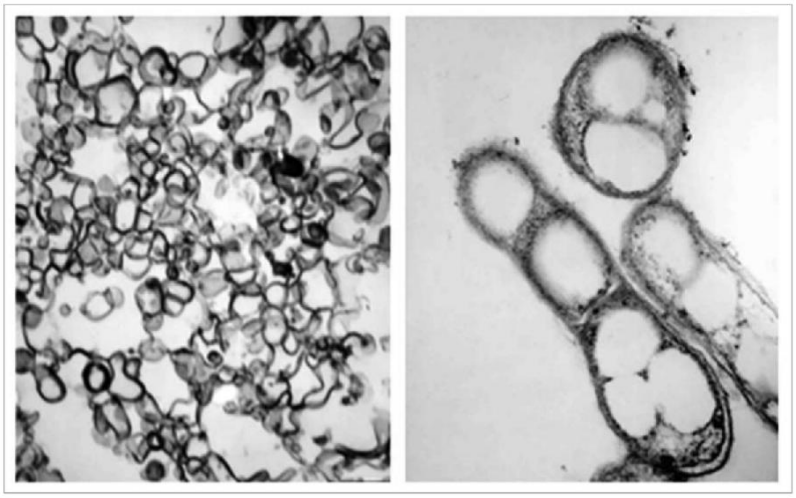

Fig. 6. Electron microscopy pictures of POPC:POPE (6:4) liposomes made using extrusion. Seabra, M.B. (2006) Studies of a Channel-Forming Peptide Inserted into Liposomes formed by POPC:POPS and POPC:POPE, (M.S. Thesis Kansas State University).

vesicles containing radionuclides trapped into large liposomes, polymer coated long circulating liposomes - with low bilayer permeability and low lipid exchange, sterically stabilized liposomes (SSL) - with high load capacity and tumor affinity, etc. have been developed exclusively for this purpose [75,133–135]. The therapeutic efficacy of targeted radiotherapy is due to the tumor's absorption of alpha (α) or beta (β) radiation emitted by the radionuclide. β-emitters such as ^{90}Y, ^{32}P, ^{89}Sr, ^{186}Re, ^{153}Sm, ^{177}Lu, and ^{131}I are by far the most widely utilized radionuclides as therapeutics and alleviation of bone pain [136]. β-electrons have low linear energy transfer (LET) values and long path-lengths. They can pass through tissue, and interact with atoms via energy loss causing ionization, generating free radicals thus causing DNA damage by inducing single strand breaks. On the other hand α-particles have high LET values and shorter path lengths, and are used to generate more localized cellular effects with high chromosomal damage during mitosis and irreparable double strand DNA breaks. Short half-life α-particles emitters such as ^{225}Ac, ^{211}At and ^{213}Bi are commonly employed for targeted alpha particle therapy (TAT) [137,138]. Naturally varying considerations exist in the selection of liposomal carriers based on whether they are employed for beta- or alpha-radiation therapy. For instance studies relating to the effect of surface charge of the liposomes on the radionuclide delivery demonstrated that the use of neutral lipids such as DMPC-Cholesterol in liposomal preparation substantially increased the effective maximum absorbed dosage of beta emitters such as ^{32}P, ^{67}Cu, ^{90}Y and ^{131}I at the tumor site as opposed to cationic DC-cholesterol lipids. On the other hand a study performed on cholesterol stabilized PEGylated liposomes with ^{225}Ac and ^{213}Bi showed high retention of the radionuclide and daughter isotopes only where larger cationic liposomes were involved [139].

Generally speaking, due to the low LET values exhibited by beta electrons, considerations of liposomal rupture due to beta-emissions are not as critical as in the case of alpha emitters where the high LET values of alpha particles coupled with the high energy recoil generated during the formation of daughter nuclides can damage and rupture the liposomal membrane. Moreover, the greater availability of beta-emitters for radiotherapy enables a greater choice in the selection of radionuclides as opposed to those employed in alpha-particle therapy. The ^{225}Ac used in most alpha particle therapies has a chemistry that is not well understood; and that precludes the effective utilization of these emitters in chelate complexes and from integration in larger compounds for the purposes of liposomal encapsulation. Time is yet another factor to be considered in case of radiotherapy. Unlike conventional drugs, radioactive moieties can rapidly decay over time, thus losing therapeutic potency. This is especially true in cases of radionuclides such as ^{213}Bi ($t_{1/2}$ = 45.7 min), where the long times taken for liposomal preparation come at the expense of decreasing therapeutic dosage.

Despite their versatility, biocompatibility, relative non-toxicity and wide application platform, liposome preparation is lengthy and tedious, and preparation steps have to be very carefully monitored to ensure reproducibility in size and entrapment efficiency [128]. Moreover, liposomes have been demonstrated to alter the pharmacokinetic properties of the drugs and are prone to systemic leakage [140]. All of these parameters must be factored in while selecting liposomes as candidates for therapeutic delivery.

2.3.1.1. Polysaccharide vesicles. This class of vesicles is less common. Dextran, chitin, chitosan and their derivatives have been investigated for their use as drug carriers. Most of the vesicles in this category are modified polysaccharides adducted with either small (trimethyl-) [141,142] or larger (3-pentadecylphenol-) [143,144] hydrophobic groups to render them amphipathic. Chitosan derived polymer vesicles are the most studied in this category. Due to their membrane-penetrating ability, these vesicles, palmitoyl glycol chitosan vesicles, are a good choice for intranasal, or oral administration of gut-labile molecules [145,146].

2.3.2. Niosomes

Niosomes or Non-ionic surfactant vesicles (NSVs) are nanoscopic lamellar structures that self-assemble into closed bilayers upon hydrating a preparation of non-ionic surfactants such as alkyl or dialkyl polyglycerol ethers; cholesterol and a charge-inducing agent [147]. They were first reported in the 1970s by researchers

in the cosmetic industry [148,149]. Niosomes were developed and patented by L'Oreal in the 1970s and 1980s and introduced in 1987 by Lancôme [150,151]. Examples of non-ionic surfactants used to generate niosomes include, C_{16} monoalkyl glycerol ether, sorbitan esters, and others.

Niosomes are capable of entrapping hydrophobic and hydrophilic solutes [152]. They can be unilamellar or multilamellar depending on the method of preparation. In many ways Niosomes are liposome analogs and are prepared much like liposomes through non-spontaneous processes involving the input of energy in the form of heat, ultrasound, physical agitation, application of pressure or a combination thereof [153]. Consequently, just like liposomes, most NSV preparation methods involve some hydration of the non-ionic surfactant at an elevated temperature followed by an optional size reduction to obtain the colloidal suspension [154]. Negatively charged molecules such as dicetyl phosphate (DCP) and phosphatidic acid, or positively charged molecules such as cetylpyridinium chloride and stearylamine (SA) can be added (2.5–5 mol%) to prevent aggregation and stabilize the niosomal bilayer [152,153].

There are some fundamental distinctions. While liposomes are made up of neutral or charged double chained phospholipids; niosomes are made up of uncharged single chain surfactants. And since non-ionic surfactants are more stable to enzymatic attack and resistant to air-oxidation than phospholipids, preparing quality niosomes is quite simple [148]. Liposome preparations are expensive owing to their need for special storage and handling due to their predisposition to breakdown when exposed to air.

When water-soluble carrier biomolecules such as sorbitol, sucrose stearate, maltodextrin, etc. are coated with a thin film of dry non-ionic surfactant, the resulting preparation is termed 'proniosomes' [155]. These proniosomes when hydrated generate niosomes. Since proniosomes are obtained as a dry powder; they can be formulated to make beads, capsules or tablets with convenient unit dosing and demonstrate reduced aggregation, fusion, leakage and increased drug entrapment efficiency [150,156].

Niosomes, due to the presence of lipophilic and hydrophilic domains can incorporate drugs with a wide range of solubilities, and indicate potential applications for the delivery of numerous pharmacological agents [150]. Niosome preparations have been investigated for the purposes of drug, gene and vaccine delivery through parenteral, oral, ocular, pulmonary and transdermal routes. The breadth of these studies precludes them from comment in this thesis. Marianecci et al. [154] provides an excellent and comprehensive review on the numerous potential applications of niosomes. Another interesting property of niosomes is their ability to deliver drugs via topical application. Dermal/transdermal drug delivery is a less invasive route for the localized delivery of high concentrations of drugs, by passing the limitations associated with systemic circulation and/or gastrointestinal degradation. The *stratum corneum* of the epidermis works as a barrier for permeation and consequently severely restricts the administration of most drugs through transdermal routes [156]. Niosomes loaded with drugs demonstrate enhanced permeation characteristics and niosomes formulations demonstrated greater skin permeation of enoxacin and higher stability of tretinoin when compared to their respective liposomal counterparts [157,158]. Acid sensitive niosomes generated with Span 60, cholesterol and cholesteryl hemisuccinate (CHEMS) were proposed for the topical delivery of ibuprofen and demonstrated a significant increase in drug penetration through skin [159]. Despite the numerous advantages niosomes have over liposomes, niosomal preparation is generally exhaustive, utilizes numerous moieties, involves the application of non-spontaneous energy consuming processes and takes considerable time.

2.3.3. Polymeric nanocapsules (polymersomes)

Block copolymers are synthetically linked segments of hydrophobic and hydrophilic polymeric units to generate the amphipathic molecule. The segments of block copolymers can be entirely synthetic, semi-synthetic or composed of biopolymers like polypeptides. Like phospholipids, these amphiphiles self-assemble into various ordered structures [58,160,161]. Vesicles formed from block copolymers are commonly referred to as polymersomes and are among the best characterized of the polymeric vesicles. By controlling the formula weight of the blocks, polymersomes with different properties are generated, including ones that vary in-elasticity, permeability and mechanical stability. By their very nature, polymeric building blocks allow for greater chemical diversity than lipids [162]. Due to their higher molecular weights, polymersomes are inherently thicker, tougher and more stable than conventional liposomes. It has been shown that polymersome membranes sustain dilatational strains up to 40–50% when compared with ~5% or less for lipid membranes [163]. A coarse grain molecular dynamics simulation supports the experimental observation that while lipid membranes require only about ~5% strain rate for rupture, while it takes 20% or more to rupture copolymer membranes [164]. Also polymersomes (Fig. 7) can be designed to be responsive to environmental factors such as pH, temperature, redox potential, magnetic field, light and ultrasound [162]. There are a number of comprehensive reviews on this topic [165,166]. Numerous variants of the block polymers have been tested in vitro for their ability to encapsulate and deliver cargo.

2.3.3.1. Peptide containing vesicles. Peptides derivatives linked to synthetic molecules form many different nanostructures: tubes, fibers, rods, micelles, vesicles, doughnuts, bilayers and others [167–173].

Vesicular structures, composed entirely of pure peptides, are relatively rare. Block copolymer monomers composed entirely of polypeptides (i.e. Ac-V_mK_n-NH_2, Ac-G_mD_n-OH, Ac-V_6D-OH, or Ac-KA_6-OH) have been reported to form vesicles [140,174,175]. Upon surveying the published works describing peptides that form vesicles, few were found compared to the many synthetic polymers capable of self-assembling into vesicles. The field of peptide vesicles is still in its infancy but growing at a rapid pace. Vauthey et al. (2002) [172] were the first to show that a simple 7–8 residue amphiphilic peptide is capable of self-assembling into nanotubes and nanovesicles. They called these peptides, "Surfactant-Like Peptide". Santoso et al. (2002) [174], designed similar peptides as the ones by Vauthey et al. (2002) [172] with glycine and aspartic acid capable of self-assembling into nanotubes and nanovesicles.

Peptide amphiphiles capable of self-assembling into nanovesicles can be a simple polypeptide sequence, or a more complex molecule, characterized by the addition of an alkyl chain or with a hydrophobic amino acid segment joined to a hydrophilic sequence (Fig. 8). The associating and stabilizing forces that direct lipid vesicle formation also apply to other polymeric vesicles comprised of long acyl chains attached to peptide amphiphiles. Some examples of designer peptide amphiphiles that form nano structures include G_nD_2, A_6D, V_6D, V_6D_2, A_6K, I_3K, A_6K_2, GAVILRR, $A_2V_2L_3WE_{(2\ or\ 7)}$ and similar peptides. In addition, amphiphilic block macrocyclic-copolypeptides have been used to generate bioactive nanovesicles that incorporate the arginine rich human immunodeficiency virus type-1 Rev protein to target the assembled vesicles. The macrocyclic protein sequence also includes tryptophan residues that add stability potentially through Pi-Pi stacking interactions [176]. The Sherman group employed a host-guest approach to drive self assembly using the macrocycle Cucurbit[8]

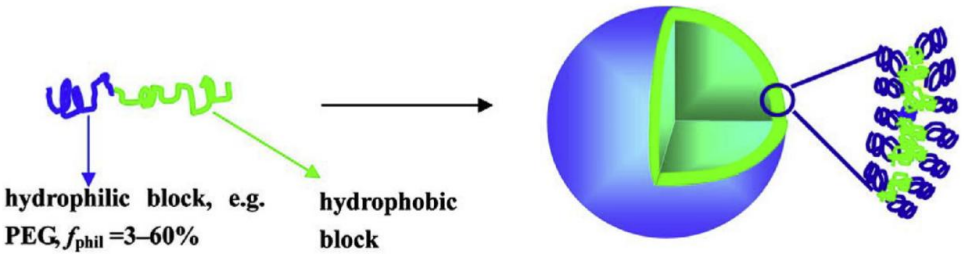

Fig. 7. Polymersomes derived from asymmetric block copolymers. Reprinted (adapted) with permission from Meng et al. (2009) *Biomacromolecules*, **10**(2), 197–209. Copyright 2009 American Chemical Society [156].

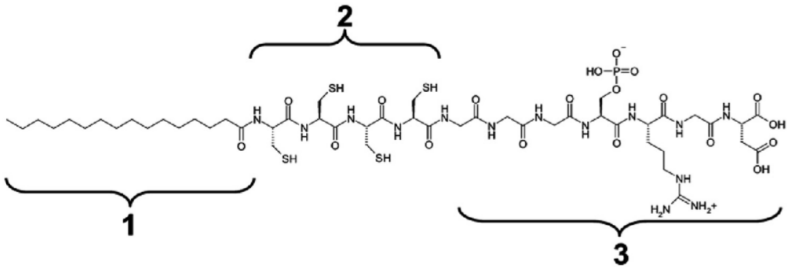

Fig. 8. Peptide amphiphile structure. The basic structural components of peptide nanoparticle components: (1) a hydrophobic tail, (2) lower, rigid part, including 4 cysteine residues (3) upper, flexible part, including 3 glycines, a phosphoserine group and an integrin-binding motif, RGD. "Reprinted (adapted) with permission from Tsonchev et al. (2004) [173].

uril (CB[8]). The ternary host complex formed by CB[8] bound two guest pyrene ligands yielding a tight binding constant with a CAC of 12 μM. This assembly generated larger vesicles ~150–250 nm in diameter [177]. Subsequently the same group was able to load the vesicles with basic fibroblast growth factor, retain it and subsequently release it for uptake by fibroblasts [178]. A third group was able to prepare bilayer-delimited vesicles in the 60 nm size range using a simple peptide Ac-Ala-Ala-Val-Val-Leu-Leu-Leu-Trp-Glu_2-COOH under acidic conditions [179]. The SA2 peptide has a CAC of around 50 μM and was able to entrap calcein [180]. These vesicles not only carry the advantage of being more biocompatible and biodegradable than other synthetic and semi-synthetic polymer vesicles and they where shown to be more stable than lipid and polysaccharide vesicles [179]. Recently another group studied the same SA2 assemblies using biophysical and computational tools to produce a visual model of the vesicles [181].

Reviews by Zhao et al. (2010) [175] and Zhang, S (2002) [182] summarize the various peptide amphiphiles that form nano structures and discuss a more exhaustive list of the various peptide amphiphiles. Some studies reported the use of oligo valines to promote inter-digitation, the mixing of oppositely charged peptides to reduce the critical aggregation concentration (CACs), and hydrophobic sequences containing complimenting small and large amino acids [183]. The hydrophobic chain length plays a critical role in the final assembly. Typically, the size of the hydrophobic tail in such peptide amphiphiles is about 3–9 hydrophobic residues. The length of the hydrophobic tail can determine the thickness of the outer layer of such nano structures but with longer chain lengths comes the issue of solubility and conversely, shorter chain lengths decrease the propensity of aggregation. Hence a balance of chain length is required for the desired property. This is achieved by increasing or decreasing the length of the hydrophilic segments of the molecule.

2.3.3.1.1. Branched amphiphilic peptide capsules (BAPCs). These structures represent a novel class of nanocarriers. First described by Gudlur et al. [184] in 2012, they are self-assembling structures where a water filled cavity is surrounded by an amphiphilic branched peptide bilayer. They are stable, biocompatible nanocarriers that are structurally similar to liposomes and polymersomes. The properties, applications and biophysical characterization of these carrier systems will be discussed at length in section 4.

3. Peptide vesicles stabilized by beta-sheet secondary structures

Most self-assembling peptide based polymeric vesicles either lack a defined secondary structure or adopt helical conformations in their assembled structures. Recently, however, vesicular [185–187] and micellar [160,188,189] assemblies stabilized by β-sheets have been reported. Gebhardt et al. studying poly(-butadiene) -poly(L-lysine) co-block polymers elucidated the effects of secondary structure on the morphology of vesicles [187]. In the case of poly(butadiene)$_{107}$-poly(L-lysine)$_{27}$ coblock polymers, the transition from α-helix to β-sheet takes place at a pH above the pKa (>10.5) of the lysine side chains. This transition resulted in a slight increase in the hydrodynamic radii of the vesicles and the overall assembly remained intact as determined by dynamic light scattering (DLS) and static light scattering (SLS). The formation of parallel β-sheets between the corona chains at the vesicular interface served to release interfacial curvature by creating a flatter interface. A molecular dynamics simulation study on the self-assembly of peptide amphiphiles [190] showed an interplay between hydrophobic interaction between the alkyl chains and hydrogen bonding between the peptide blocks, resulting in assemblies that were spherical β-sheets, micelles with β-sheets in the corona, and long cylindrical fibers (Fig. 9).

4. Studies on branched amphiphilic peptide capsules

4.1. Origin of the BAPC sequences

The concept of building diacyl phospholipid orthologs made up of just amino acids is not particularly new, however identifying a functional self-assembling sequence(s) is. The sequences used for the self-assembling branched amphipathic peptide vesicles evolved from earlier studies on several adhesive peptides. Previously, several peptide constructs were identified that produced nanofibrils with mechanical adhesive properties due to entanglement [191,192]. The hydrophobic core sequence used in the adhesives occurs in nature as an internal fragment of the human dihydropyridine sensitive L-type calcium channel segment, CaIVS3 (DPWNVFDFLIVIGSIIDVILSE). The underlined segment is a portion of one of the transmembrane helices that contribute to the central water-filled pore of this channel [193,194]. Lyophilization of the synthesized CaIVS3 peptide resulted in insoluble clumps resistant to mechanical disruption suggested that strong cohesive forces were driving this association. An α to β transition for the 9-residue sequence was observed that could be controlled predictably by adding charged amino acid segments to both ends of the underlined sequence (h_9) (Table 1) and by varying the pH [191,192]. An assay was used that measured the strength (MPa) required to shear (pulled at 180°) two glued cherry wood strips treated with a 4% w/v solution of the peptide dissolved in water and then adjusted to the indicated pH values before hot pressing the samples (Fig. 10). The sequences with the flanking tri-lysine or tri-diaminopropionic acid (DAP) segments performed best at pH 12.0, conditions in which the amino groups of the Lys and DAP residues are mostly deprotonated thereby increasing the hydrophobicity of the peptides. The DAP amino acid is a shortened lysine analog with just one methyl group on its side chain as compare to the four methyl groups in lysine. There were no statistical differences between the two different cationic residues or increasing the number of h_9 hydrophobic segments.

Table 2 summarizes the shear strength and hydrophobicity for a number of FLIVIGSII derived sequences. The two longer sequences simply incorporated the naturally occurring C- or N-terminal hydrophobic residues present in the CaIVS3 sequence. The shorter sequences represent truncated versions of the h_9 sequence and in some cases include single amino acid substitutions. Several known amyloid peptides as well as a twitter-ionic sequence were tested as controls.

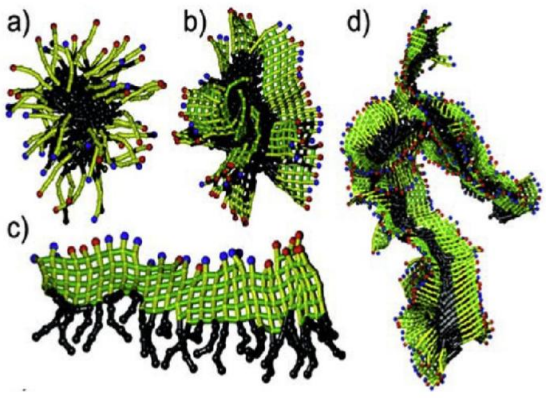

Fig. 9. Snapshots from molecular simulations of peptide amphiphiles. "(a) The spherical micelle, (b) the micelle with β-sheets on the outside forming the corona, (c) the β-sheets, and (d) the fiber aggregate". [Reprinted (adapted) with permission from Velichko et al. (2008) [190], *J. Phys Chem B.*, 112(8), 2326–34. Copyright 2008 American Chemical Society.].

Table 1
Adhesive peptide sequences [191]. Abbreviations: X = diaminopropionic acid.

Peptide	Sequence	MW (Daltons)
Eh_9E	EEEFLIVIGSIIEEE	1748.9
Kh_9E	KKKFLIVIGSIIEEE	1746.1
Eh_9K	EEEFLIVIGSIIKKK	1746.1
Kh_9K	KKKFLIVIGSIIKKK	1743.3
$(Kh_9)_2K$	KKKFLIVIGSIIKKKFLIVIGSIIKKK	3084.1
$(Kh_9)_3K$	KKKFLIVIGSIIKKKFLIVIGSIIKKKFLIVIGSIIKKK	4428.8
Xh_9X	XXXVLIVIGSIIXXX	1490.8

There are three h_5 sequences (*alpha*, *mezzo* and *omega*) derived by frame shifting a five-residue window within the h_9 sequence. In addition, four unrelated β-forming sequences were tested. The first three $A\beta_{16\text{-}21}$, $A\beta_{30\text{-}35}$, and $IAPP_{22\text{-}28}$ were reported nucleation sites for amyloid fiber formation and have sequences that closely resemble that of $K_3h_{5\alpha}K_3$. The last sequence, KAE_{16}-IV, contains both basic and acidic residues and should not display any pH dependence.

With the exception of KAE_{16}-IV, all of the sequences showed adhesive properties when dry pressed at 130 °C. The shorter $h_{5\alpha}$ containing sequence required the most force to shear the union holding the strips together. It was determined that this shorter sequence had the lowest free energy for the packed assembly and was the most hydrophobic. While reducing the size of the hydrophobic core sequence increased strength, reducing the number of flanking lysines from three to two had a negative effect on adhesive strength. All of the CaIVS3 derived sequences acted as adhesives even when the dry press temperature was reduced, although with decreased strength. However the amyloid derived sequences displayed no adhesive properties if heating was omitted during pressing. Several of the sequences showing strengths above 3 MPa were tested for their wet strength after emersion for 48 h (Table 3).

Structural analyses were conducted on both soluble peptides (CD) and dry pressed peptide (FTIR) processed at pH 12.0. All of the dry pressed peptides showed β-structure. Only $K_3h_{5\alpha}K_3$ and $K_3h_9K_3$ showed β-structure in water. $K_3h_{5\Omega}K_3$ and $K_3h_{5M}K_3$ showed β-structure only in ethylene glycol. No structure was observed for the amyloid forming peptides with either solvent.

In parallel, transmission electron microscopy was used to visualize the assemblies being generated at pH values of 12.0, 2.0 and 7.0 (Fig 11). The images taken at pH 12.0 show entangled nanofibers. Regarding the adhesive properties the peptides, they only bonded with rough surfaces. When the peptides were used to glue smooth glass slides together shear strengths of just ~1.5 MPa were required to separate the two pieces. If the slides were siliconized the peptides showed no effect in joining the glass slides.

Table 4 compares the different properties of the nano-fiber forming sequences. It is clear that the hydrophobic core sequences of FLIVIGSII and FLIVI have unique structural properties, in particular their ability to associate and assemble as a β-structure in water and their wet adhesive strength. Even though the K_3FLIVIK_3 sequence appeared unstructured in water at pH 2.0 and 7.0, transmission electron microscopy images were taken these sequences that were applied as solutions to the TEM grids and allowed to dry (Fig. 11).

The images show two distinct structures–at pH 7.0 the peptides associate to form a soot-like fractal while at pH 2.0 they resemble lipid micelles. Upon viewing the pH 2.0 structures and recalling that linear lipid detergents or soap amphipaths make similar micellar structures and that branched lipid amphipaths such as

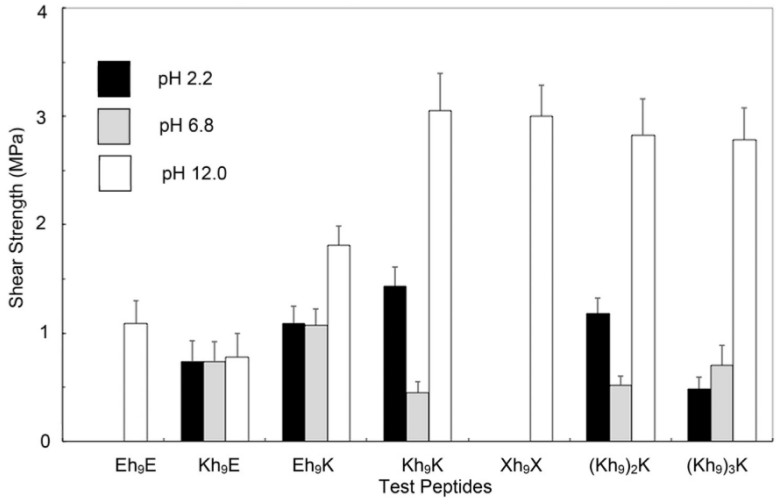

Fig. 10. Shear strength of peptide adhesives measured in Mega Pascals (MPa) with different tri-residue segments flanking the h_9 sequence. E, K and X represent the tripeptides $(Glu)_3$, $(Lys)_3$ and $(diaminopropionic\ acid)_3$, respectively. Peptide solutions– 4% (360 μL) were spread onto marked 8.0 cm by 2.0 cm areas on one side of two separate strips of wood. The coated strips sat for 15 min at RT, before being pressed together for 5 min at 130 °C and 1.4 MPa cm^{-1}.using a Hot Press Model 3890 Auto M (Carver Inc., Wabash, IN). The glued strips were then conditioned for 3 days at 50% relative humidity and 23 °C before being cut into test sized pieces. Reproduced from Shen et al. [191].

Table 2
Correlation of shear strength and hydrophobicity for a number of peptides showing adhesive properties [192]. Samples were prepared as described in Fig. 10.

Peptides	Sequences	Shear strength (MPa)	G_{avg} (kcal/mol)
$K_3h_9K_3$	KKKFLIVIGSIIKKK	3.0 ± 0.1	−0.46
$K_3h_{11}K_3$	KKKVFFLIVIGSIIKKK	2.9 ± 0.2	−0.48
$K_3h_{12}K_3$	KKKFLIVIGSIIVILKKK	2.2 ± 0.1	−0.50
$K_3h_7K_3$	KKKFLIVIGSKKK	2.6 ± 0.2	−0.42
$K_3h_{5\alpha}K_3$	KKKFLIVIKKK	3.3 ± 0.2	−0.62
$K_3h_{5M}K_3$	KKKIVIGSKKK	3.4 ± 0.2	−0.37
$K_3h_{5\Omega}K_3$	KKKIGSIIKKK	3.2 ± 0.2	−0.31
$K_2h_{5\alpha}K_2$	KKFLIVIKK	2.8 ± 0.1	−0.53
$K_2h_{5\Omega}K_2$	KKIGSIIKK	2.4 ± 0.2	−0.31
$K_3h_{5ML}K_2$	KKKIVLGSKKK	3.4 ± 0.2	−0.36
$K_3h_{5MA}K_2$	KKKIVAGSKKK	2.7 ± 0.1	−0.35
$A\beta_{16\text{-}21}$	KKKLVFFAKKK	3.4 ± 0.3	−0.50
$A\beta_{30\text{-}35}$	KKKAIIGLMKKK	3.4 ± 0.1	−0.39
$IAPP_{22\text{-}28}$	KKKIGGAILKKK	2.9 ± 0.4	−0.30
KAE_{16}-IV	$(KA)_4(EA)_4$-$CONH_2$	1.4 ± 0.1	+0.62

Table 3
Comparison between dry and wet strength for select peptide adhesives [176].All samples were used at 4% w/v and hot-pressed at 130 °C. Glue samples were soaked in water for 48 h before wet strength test. Adapted from Mo et al., 2008 [192].

Peptide sequence	Dry strength (MPa)	Wet strength (MPa)
$K_3h_{5\alpha}K_3$	3.3 ± 0.2	1.13 ± 0.3
$K_3h_{5\Omega}K_3$	3.2 ± 0.2	0.66 ± 0.2
$K_3h_{5M}K_3$	3.4 ± 0.2	0.0
$K_3h_9K_3$	3.0 ± 0.2	0.67 ± 0.1

diacylglycerol-phospholipids assemble into liposomes, the idea of altering the sequence from a linear to a branched one with all of the charges or one side was born.

4.2. Shared properties between BAPCS and lipid vesicles

To generate an all peptide bilayer delimited vesicle, the original design included 5 lysines at the C-terminus with the N-terminal lysine used to generate the branch point. The two hydrophobic segments were added simultaneously using standard Fmoc chemistries. It was decided from the beginning to include a mixture of two different sized peptides such that the shorter sequence would compensate for any strain due to curvature. These vesicles were formed from the two 15- and 23-residue branched amphiphilic peptides: bis(FLIVI)-K-K_4 and bis(FLIVIGSII)-K-K_4 commonly referred to as bis(h_5)-K-K_4 and bis(h_9)-K-K_4, respectively (Fig. 12). In 2012, Gudlur et al., first described the formation of these structures at 25 °C (RT) (Fig. 13) [184].

The linear (h_9)-K-K_4 sequence (Fig. 12) did not form any detectable structures. Henceforth these structures will be referred to as branched amphiphilic peptide capsules (BAPCs) to avoid confusion with lipid vesicles.

In Fig. 13, 50–150 nm spherical structures are present after a 2 h incubation period. The BAPCs in this image appear to be fusing. The resolution of these images was insufficient to identify whether or not the capsules were surrounded by a bilayer. Subsequently methyl mercury was added to the bis(FLIVI)-K-K_4 and bis(-FLIVIGSII)-K-K_4 peptides in which the thiol containing amino acid cysteine was added to the C-terminal lysine of both peptide sequences [195]. In this representative image (Fig. 14) of capsules formed at 25 °C, the bilayers are distinct due to the emission of a specific energy x-ray associated with mercury bombarded by electrons. The BAPCs remain water filled and a number of capsules appear to be fusing. Note that unlike many liposome preparations all of the BAPC structures are unilamellar.

Based on computer simulations these peptides behave much like phospholipids. As observed with membrane lipids, the hydrophobic regions of these peptide molecules are poorly soluble in water and in an analogous manner shield themselves by associating to form bilayers in aqueous solutions that appear to be 4 nm in thickness (Fig. 15). The aromatic side chains of phenylalanine residues and other aliphatic residues are buried in the interior of the newly formed membrane.

In addition to the aromatic and non-polar residues interacting

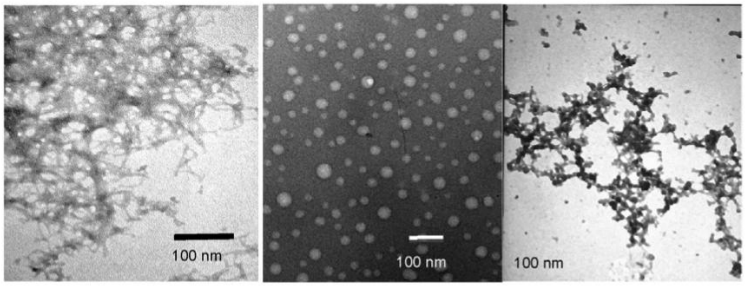

Fig. 11. TEM images of $K_3FLIVIK_3$ that were dried from peptide solutions prepared at different pH values. The left panel is peptide suspended at pH 12.0 and imaged at 70,000× magnification. The center panel is peptide incubated at pH 2.0 and imaged at 34,000×. The right panel is peptide dissolved at pH 7.0 and imaged at 70,000×.

Table 4
Comparison of structural and adhesive properties of test sequences. All sequences were tested in parallel for adhesive strength under different dry press conditions. Assembly properties were measured by analytic ultracentrifugation.

FLIVIGSII, FLIVI	IVIGS, IGSII	IFGAIL, KLVFF, AIIGL
Random structure at pH 2 and 7	Random structure at pH 2 and 7	Random structure at pH 2 and 7
β-structure at pH 12 in water	β-structure at pH 12 in ethylene glycol	No structure at pH 12 in any solvent
β-structure when dried from water	β-structure when dried from water	β-structure only when dry pressed
Assembles in water pH > 9	No assembly at pH 12	No assembly at pH 12
Adhesive after dry press, RT	Adhesive after dry press, 130 °C	Adhesive after dry press, 130 °c
Measurable wet adhesive strength	No wet adhesive strength	No wet adhesive strength
Forms entangled nano-fibrils	Forms entangled nano-fibrils	Forms entangled proto-fibrils

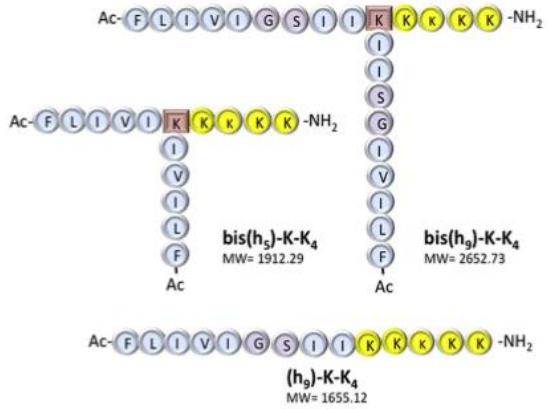

Fig. 12. Graphic representation of the branched and linear amphipathic sequences initially tested. The color coding is added to signify those residues that are cationic (yellow), non-polar (blue) and hydrophilic (violet) along with the branch point (pink).

with each other through hydrophobic interactions; CD and FT-IR indicated significant parallel β-like structure, indicative of hydrogen bonding networks. The positively charged lysines reside in the two aqueous phases, on both the inner and outer sides of the bilayer (Fig. 15). Additionally, this model seems to show a networks of hydrogen bonds between adjacent β-structures that help the organized structure stabilize at very low sub-micromolar concentrations - as judged by dilution studies determined by both CD and ITC—conditions where nearly all phospholipid assemblies would be fully dissociated. We have yet to determine the critical assembly concentrations (CAC) of BAPCs.

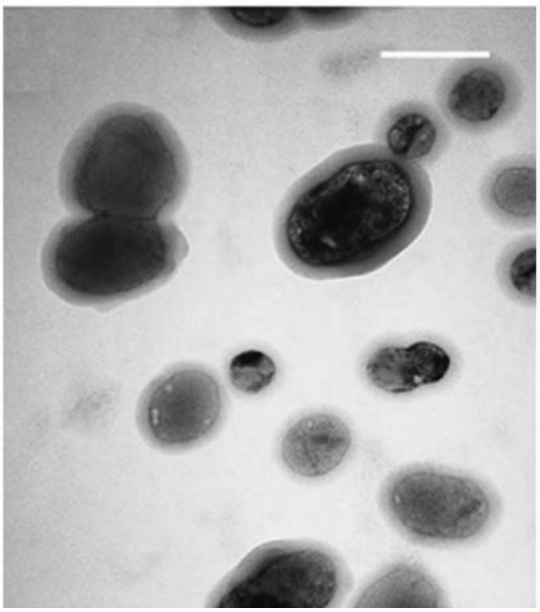

Fig. 13. Transmission electron microscopy (TEM) obtained from the synthesis of nanocapsules solution (1.5 mM). The image shows the process of fusing the nanocapsules, resulting in larger and more elongated structures (scale bar: 200 nm). Reproduced from Gudlur et al. (2012) [184].

4.2.1. BAPC assembly

Nanocapsules formation follows nearly the same steps used for the preparation of diacylglycerol phospholipid vesicles (Fig. 16).

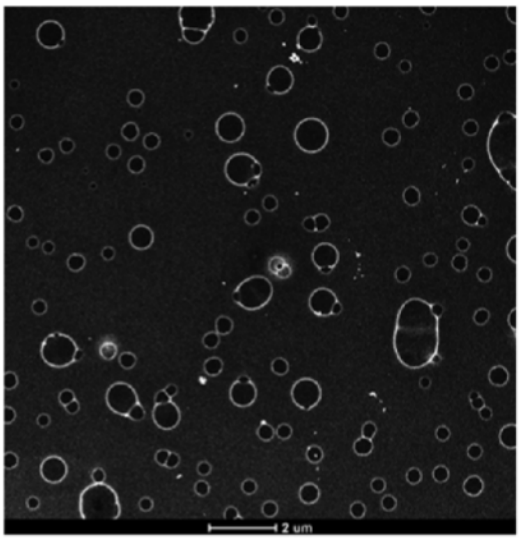

Fig. 14. Scanning transmission electron microscopy (STEM) of Cys containing peptides labeled with Me—Hg 24 h after mixing. Capsules were prepared with the peptides at 0.1 mM with 30% of them containing the Me—Hg. The images were captured using the inverted dark-field mode. Reproduced from Sukthankar et al. [195].

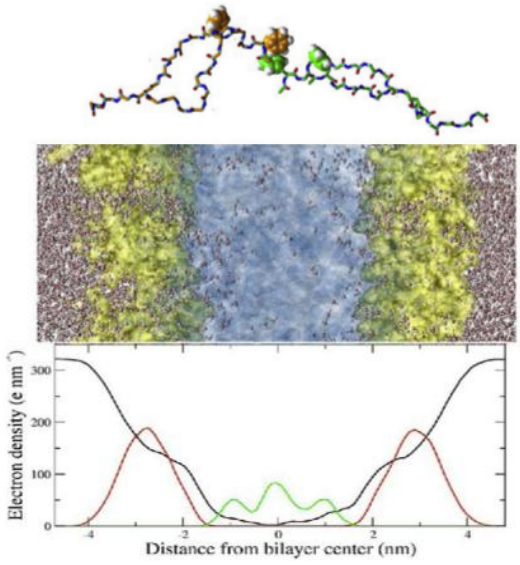

Fig. 15. Atomistic model of the BAPC peptide bilayer. In the center, the peptides are shown in a transparent surface, with Lys colored in yellow and other residues in blue and water in ball-and-stick mode. The top panel illustrates extensive π-π stacking interactions among Phe residues. The bottom panel shows the average electron density profiles of water (black line), Lys (red) and Phe residues (green line) calculated from last 40 ns of the 100 ns simulation.

Initially the two peptides, bis(FLIVI)-K-K_4 and bis(FLIVIGSII)-K-K_4, are dissolved individually in neat 2,2,2-trifluoroethanol (TFE). In this solvent the peptides adopt a helical structure. As helices they are monomeric, thereby ensuring complete mixing of the two sequences when combined. This solvent also ensures that they remain helical upon drying, based on FT-IR studies.

The individual dissolved peptide concentrations are determined using the molar absorptivity (ε) of phenylalanyl residues in the sequence (195 M^{-1} cm^{-1} at 257.5 nm) [184]. The two peptides are then mixed in equimolar ratios to generate desired concentrations and then dried in vacuo. All of the initial experiments limited the ratio to 1:1 to ensure an adequate concentration of the shorter peptide to accommodate the curvature of assembled capsules.

Distilled deionized water or aqueous solution containing solutes for encapsulation are added drop-wise to the dried peptides at the desired temperature. Different secondary structures and capsule sizes are seen when assembly occurs at different temperatures. This will be discussed later.

4.2.2. Fusion and sizing

Sukthankar et al. [195] followed the assembly process over 2 h (Fig. 17) and showed that within 5 min of hydrating the mercury-labeled peptides, nano-fibrils appeared which gradually began to group together forming the nanocapsules with a 20 nm average size by 30 min. At 60 min the small BAPCs appeared to coalese and by 2 h have fused into larger capsules. By 48 h, micron sized capsules are present. [184] While these STEM images provide a static view into the underlying assembly events, a solution study was designed to demonstrate the dynamic nature of fusion process (Fig. 18A & B) [195].

The dilution of the self-quenching fluorescent dye Eosin Y was recorded during fusion the process. Two populations of BAPCs, harvested and washed 30 min post hydration, containing either 2.2 mM dye (5 parts) or just water (95 parts), were mixed. At the earliest time points the dye containing BAPCs would be expected to fuse with the water filled ones thereby diluting the dye. This dilution was recorded as an increase in fluorescence. With each 5 min scan the intensity of the dye increased without any dye appearing in the 30 kDa cut-off filtrates, thus demonstrating fusion and the fact that the BAPCs are water filled. Lowering the BAPCs

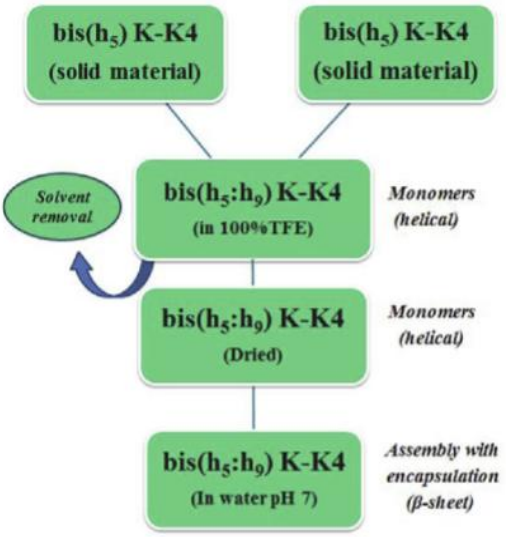

Fig. 16. Assembly protocol for peptides nanocapsules.

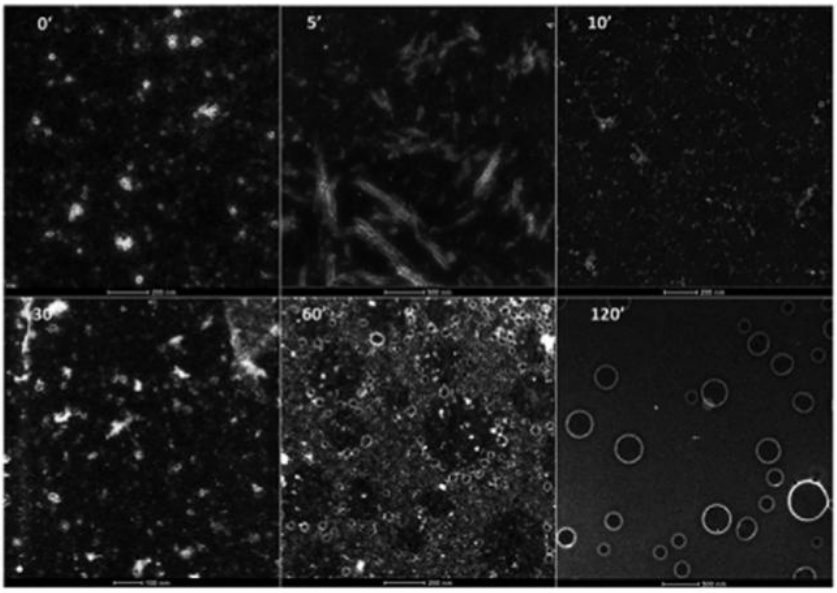

Fig. 17. BAPC fusion time course. Peptides(0.1 mM) bis(FLIVI)-K-K_4 and bis(FLIVIGSII)-K-K_4 containing 30% bis(FLIVI)-K-K_4-Cys-Hg-Me and bis(FLIVIGSII)-K-K_4-Cys-Hg-Me were hydrated with samples removed at the indicated times and dried. The STEM images are displayed in inverted dark field. The scale bar at the bottom of the micrographs are 200 nm, 500 nm, 200 nm, 100 nm, 200 nm and 500 nm, for the intervals of 0, 5, 10, 30, 60, and 120 min, respectively. Reproduced from Sukthankar et al. [195].

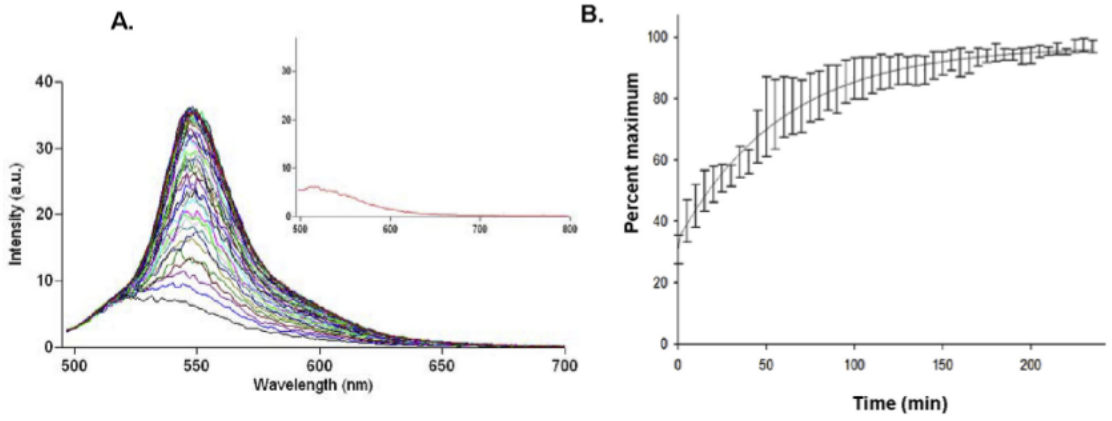

Fig. 18. BAPC Fusion Study. Panel A. Salt washed eosin Y trapped BAPCs were mixed with water filled BAPCs at 25 °C. Fluorescence scans were taken at 5 min intervals for 235 min. The inset shows spectrum of sample stored at 4 °C for 6.5 h. The units shown are identical to those in A. Panel B. Measured maximum eosin fluorescence intensity as a function of time during the fusion reaction. The t = 0 represents quenched value of salt washed eosin encapsulate in the capsules (2.2 mM). The data was fitted to a second order exponential with the error bars representing the SEM with n = 3. Reproduced from Sukthankar et al. [195].

temperature to 4 °C at t = 35 min (inset to Fig. 18A) shows that the fusion process can be stopped. Returning the 4 °C sample to RT did not restore fusion. This phenomenon is addressed later in Section 4.3.2.

Since the BAPCs fuse like liposomes, resizing of larger BAPCs was tested using polycarbonate filters using methods commonly employed to prepare small phospholipid vesicles (SUVs). Starting with a 24 h, 25 °C sample (200–500 nm diameter BAPCs) the BAPCs were extruded through a 100 nm pore filter, yielding a mixed population, 20–60 nm diameter capsules. Few if any 100 nm capsules were seen suggesting this size is disfavored over smaller ones. Those BAPCs were then extruded a second time through a 30 nm filter resulting in a relatively homogeneous population with sizes ranging from 20 to 30 nm. The 30 nm membrane is the smallest commercially available and attempting to go even smaller does not appear feasible since the BAPCs assemble as 20–30 nm structures. Once resized to 20–30 nm, the BAPCs should be cooled to 4 °C at RT to prevent their re fusion.

The inset to Fig. 18A showed that lowing the temperature to 4 °C after incubating at 25 °C for 35 min resulted in an altered BAPC that

was no longer able to fuse. Even increasing the temperature stepwise to 80 °C failed to restart fusion. In addition, the cooled BAPCs were no longer susceptible to disassembly in 50% TFE/water containing solutions. Based on these results the effect of temperature on BAPC properties were initiated. The results from these experiments indicate that there is a temperature dependence for assembly.

4.3. Distinctive properties of BAPCs

4.3.1. Temperature effects on BAPC formation

BAPC assembly was monitored at multiple temperatures with their final secondary structures determined [196]. To briefly summarize, BAPCs formed at 4 °C and 37 °C yield uniform BAPCs that are 20–30 nm in diameter, do not fuse yet are disassembled in 50% TFE. The 4 °C BAPCs are predominantly unstructured while the 37 °C display beta-like structure. The BAPCs formed at 25 °C were the only ones that displayed the fusogenic property and disassembled in 50% TFE. They displayed secondary structure that appear to be a mixture of random coil and beta-like structure. Over time as the BAPCs grew in size they became more beta-like in structure. It was hypothesized that the mixture of random and beta structure is higher energy and meta-stable and that fusion leads to a lower free energy state. Assembly at 25 °C for 30 min followed by 1 h of cooling at 4 °C and then rewarming to temperatures >25 °C makes the BAPCs even more stable and resistant to disassembly in 50% TFE. Their structures changed during the experiment from a combination of random and beta at 25 °C to mostly random at 4 °C and then back to mixed upon rewarming. It was postulated that during the thermal cycling entanglement of the hydrophobic segments occurred during the transition from random coil back to the mixed conformer. This unusual BAPC is referred to as being in a "locked" conformation. This particular BAPC has proven to be useful in delivering DNA to cells (not discussed in this review).

4.3.2. BAPC stability

The thermal stability of the nanocapsules was also evaluated by Gudlur et al. [184], using Differential Scanning Calorimetry (DSC) for temperatures ranging from 20 to 95 °C. This experiment was confirmed over the same temperature range using BAPCs containing the quenched dye Eosin Y (2.1 mM). No fluorescence intensity increase was observed over the full temperature range indicating that the BAPCs did not rupture and release contents. The lack of a phase transition over this temperature range indicates maintenance of the bilayer's structural and functional integrity. This observation is important because phospholipid membranes comprised of acyl chains of 18 carbons or less with no double bonds generally exhibit phase transition temperatures between 35 and 55 °C [197]. At these temperatures, lipid vesicles tend to become permeable. This propertyis a disadvantage due to the release of internal contents when exposed to elevated temperatures. In addition to thermal stability the BAPCs are resistant to proteases, chaotropes, dodecylsulfate and dilution [184].

4.3.3. Cellular uptake

As showed by Sukthankar et al. [198] nanocapsules are formed with an average diameter of 20–30 nm with an internal volume of 4000 nm^3 allowing them to be considered as possible candidates for the encapsulation of a large number of different molecules including proteins. For this purpose BAPCs were used to encapsulate TAMRA-labeled TRNase A (RNase A, 13.7 kDa) and TAMRA-labeled cytochrome c (Tcytc, ~12 kDa). These apoptogenic proteins were chosen since their release from the BAPCs would trigger a measurable cytotoxic effect. For the positive delivery control the amphipathic peptide called Pep-1 was employed. This peptide reagent is known to induce cellular uptake of proteins and peptides [199,200].

Both cytochrome c and RNase A were successfully encapsulated in the BAPCs and efficiently delivered into HeLa cells (Fig. 19). In the images obtained we observed a slightly lower signal when comparing the transport of Tcytc using BAPCs with the control Pep-1.

Both cytochrome c and RNase A are known for their apoptotic effects [201,202]. This BAPC experiments do not record any obvious signs of apoptosis whereas the transport mediated by Pep-1 exhibited the expected effect of cellular cytotoxicity. This was the first experiment that indicated that the cell's degradative machinery did not act on the BAPCs. This study (Fig. 20) also showed that the BAPCs are retained intact in HeLa cells for long periods of time. The images generated with confocal microscopy revealed that even after 14 days, the BAPCs labeled with Rhodamine B persisted inside the HeLa cells and interestingly are transferred without any apparent degradation to the daughter cells formed during mitotic divisions.

4.3.4. In vivo studies-encapsulated alpha-emitting radionuclides

The remarkable stability of BAPCs makes them singularly useful in several applications and ill suited for others. Given their temperature stability and flexibility (based on resizing results) BAPCs were used to encapsulate an alpha-particle emitting radioisotope. Molecular nuclear medicine plays important roles in the diagnosis and treatment of cancer. Depending on the radioisotope's properties, the compounds can be used for diagnostic and/or therapeutic purposes. Targeted alpha-particles have a significant advantage in targeted radiotherapy because of their high potency, specificity as well as their ability to kill non-proliferating cells and without the need for oxygenation [203]. Current targeted alpha radioimmunotherapy takes advantage of the specificity of antibody-conjugated radionuclides to deliver biocidal radiation to cancer cells [204]. Alpha-emitting radionuclides such as Actinium-225 and Bismuth-213 are commonly used for this purpose. This method does have some disadvantages in that the high energy of the ejected alpha particle can collide with and destroy the covalent bond between the chelator molecule and the antibody. Also the energy released during the recoil of the daughter nuclide is sufficient to dislodge the radionuclide from the chelator itself. This release of free radionuclides can cause off-target accumulation and potential damage [205].

For the BAPC encapsulation studies ^{225}Actinium was tried. This radionuclide has a T½ = 9.92 days while releasing 4 α-particles as it decays to ^{209}Bismuth [203]. Alpha particles are emitted with a velocity of 5% the speed of light. The average energy of the 4 ejected helium nuclei is 6.93 MeV [203]. The average mass of the daughter nuclei must have equal and opposite momenta which accounting for the mass difference calculates to an average energy of 0.13 MeV. As shown in Fig. 21 the BAPCs are able to retain 95% of the radionuclides (parent and daughters) for 7 days. As previously mentioned theoretical calculations by Sofou et al. [134,135] suggest negligible (<0.001%) daughter retention for the last isotope of ^{225}AC for 100 nm diameter liposomes and 50% retention for liposomes with a diameter larger than 650 nm. Even giant liposomes (1 μm diameter), have retention values < 65% and in fact, the measured last daughter retention for the 650 nm liposomes was found to be substantially lower (11%) than predicted [134,135].

Given the demonstrated robust properties of our peptide capsule design, we have started investigating the delivery of the alpha particle emitting Actinium to cells. To date [198], (in vitro) we have been able to load the BAPCs with ^{225}Ac that have stably retained ≥95% of their activity over 7 days, and shown that cultured

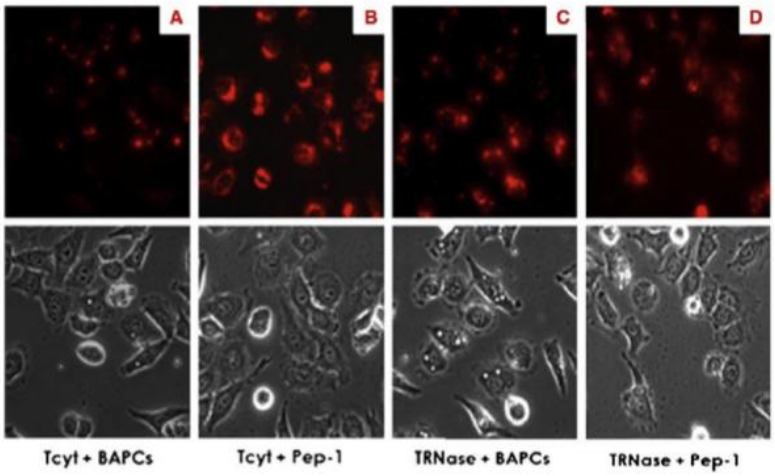

Fig. 19. Fluorescence Microscopy images of BAPCs delivering TAMRA labeled protein to HeLa Cells. A) HeLa cells uptake of BAPCs carrying Tcytc; B) Control with Tcytc with Pep-1; C) BAPCs uptake containing TRNase; D) Control TRNase A with Pep-1. Reproduced from Sukthankar et al. [198].

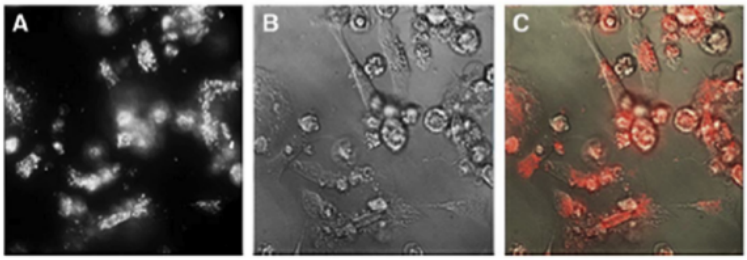

Fig. 20. Time function of the BAPCs integrity. Images obtained with confocal microscopy of BAPC uptake by HeLa cells after 2 weeks showing: A) Excitation of Rhodamine in Dark field image; B) DIC image; C) Merge images exhibiting the Rhodamine inside of the BAPCs. Reproduced from Sukthankar et al. [198].

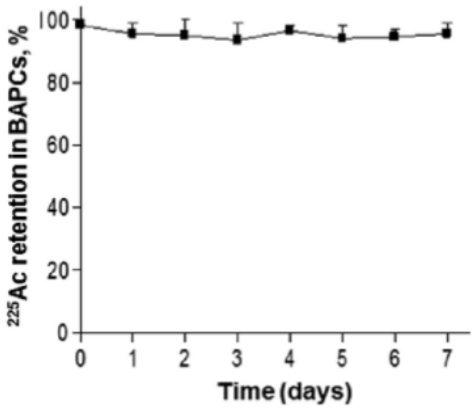

Fig. 21. Retention of BAPCs encapsulated with ^{225}Ac. Encapsulation and retention of ^{225}Ac within BAPCs over 7 days. Reproduced from Sukthankar et al. [198].

cells readily take-up non-lethal concentrations of encapsulated ^{225}Ac. *In vivo* (Fig. 22), free ^{225}Ac completely cleared from the blood while ^{225}Ac-loaded capsules continued to circulate due to their small size.

Free ^{225}Ac accumulated significantly more in the liver ($P = 0.03$) and in the bone ($P = 0.02$) than the ^{225}Ac- BAPCs which points to the tight incorporation of ^{225}Ac inside the BAPCs. At 1 h when both ^{225}Ac-BAPCs and free ^{225}Ac were still exiting the peritoneal cavity there was no significant difference in organ uptake between ^{225}Ac-BAPCs and free ^{225}Ac except for the bone where free ^{225}Ac tends to accumulate. The only organ where there was more ^{213}Bi present compared to ^{225}Ac were kidneys which serve as the "sink" for ^{213}Bi which has been released from any organ in the body.^{213}Bi daughter was present together with ^{225}Ac indicating the possible retention of the daughter by the BAPCs as well. Together, these preliminary results point to the ability of BAPCs to incorporate and retain ^{225}Ac and its daughter ^{213}Bi. Being able to selectively deliver this isotope to a location just outside the nucleus using targeting molecule adducted BAPCs should improve therapeutic efficacy while reducing off-target damage and lowering the whole body dose of radiation needed to kill targeted cells.

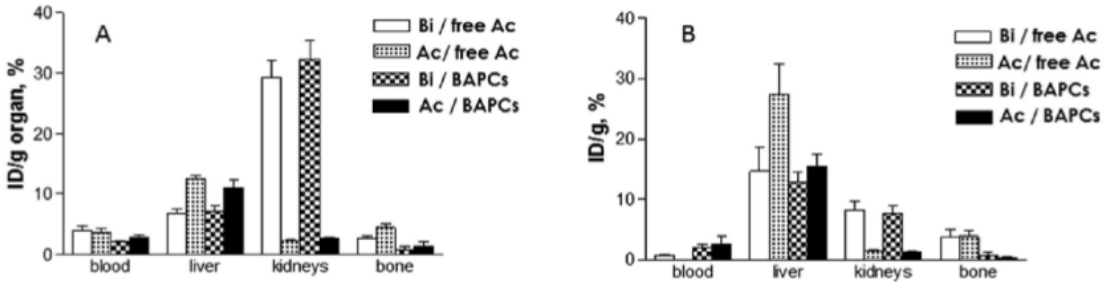

Fig. 22. Biodistribution of free and BAPC-encapsulated, ^{225}Ac and its daughter ^{213}Bi, in CD1 mice. A) 1 h time point; B) 24 h time point. Reproduced from Sukthankar et al. [198].

5. Summary

There are three fundamental factors that go into the development of a competent nano-encapsulating system, viz - characteristics of the diseased state, choice of therapeutics and the nature of the delivery vehicle. The choice of the therapeutic and the nature of its action need to be carefully considered during the selection of a delivery platform. The drug's site and mechanism of action define what carrier system will achieve optimal delivery. For example; drugs that require intracellular sites of action require intracellular delivery for bioactivity and therefore necessitate a delivery vehicle that enables homogenous tissue penetration.

Fundamental research into the nature of diseased state biomarkers and associated ligands, play vital roles in the design of functionalized delivery vehicles. Even in cases where targeting is not employed, an understanding into the characteristics of the diseased site, tissue accumulation and cellular uptake can help us engineer more efficient non-specific drug delivery systems by modulating the biophysical properties of nano-carriers [206,207]. BAPCs by their very nature represent a new and exciting class of novel encapsulating nano-system for drug delivery, not only because of their versatility, tune-ability, extraordinary stability, biocompatibility or target-ability; but also because of the unique structural potentialities of its branched parent sequences that result in the formation of a pure peptide bilayer delimited nano-vesicle similar to liposomes in its organizational architecture. Indeed it could be said that the branched peptide sequences that constitute BAPCs are in themselves a unique class of biomaterial with great potential in a variety of chemical, physical and biological applications. An exhaustive investigation of these nano-materials is currently in progress.

Acknowledgments

We thank Professor Jianhan Chen for carrying out the computer simulation that generated Fig. 16. This is publication **16-158-J** from the Kansas Agricultural Experiment Station. Partial support for this project was provided by PHS-NIH grant # GM074096 and a Terry Johnson Cancer Center Innovation Award (to J.M.T), Scholarship award (to S. B.) from the Coordenação de Aperfeiçoamento de Pessoal de Nível Superior (CAPES) Process number: PDSE - 99999.007690/2014-02, Affilation: CAPES Foundation, Ministry of Education, Brasilia–DF 70.040-020, Brazil and the Terry Johnson Cancer Center at Kansas State University for summer support (for P.S. and S.G.).

References

[1] J. Shi, A.R. Votruba, O.C. Farokhzad, R. Langer, Nanotechnology in drug delivery and tissue engineering: from discovery to applications, ACS Nano Lett. 10 (2010) 3223–3230.
[2] J.K. Kim, H.J. Kim, J.Y. Chung, J.H. Lee, S.B. Young, Y.H. Kim, Natural and synthetic biomaterials for controlled drug delivery, Arch. Pharm. Res. 37 (2014) 60–68.
[3] J.H. Hamman, G.M. Enslin, A.F. Kotze, Oral delivery of peptide drugs: barriers and developments, Bio. Drugs. 19 (2005) 165–177.
[4] R. Pawar, A. Ben-Ari, A.J. Domb, Protein and peptide parenteral controlled delivery, Expert Opin. Biol. Ther. 4 (2004) 1203–1212.
[5] S.K. Sahoo, S. Parveen, J.J. Panda, The present and future of nanotechnology in human health care, Nanomed. NBM. 3 (2007) 20–31.
[6] D.J. Brayden, Controlled release technologies for drug delivery, Drug Discov. Today. 8 (2003) 976–978.
[7] L. Wang, R. Zeng, C. Li, R. Qiao, Self-assembled polypeptide-block-poly(vinylpyrrolidone) as prospective drug-delivery systems, Coll. Surf. B Biointerfaces. 74 (1) (2009) 284–292.
[8] S.M. Moghimi, J. Szebeni, Stealth liposomes and long circulating nanoparticles: critical issues in pharmacokinetics, opsonization and protein-binding properties, Prog. Lipid. Res. 42 (2003) 463–478.
[9] D.H. Levine, P.P. Ghoroghchian, J. Freudenberg, G. Zhang, M.J. Therien, M.I. Greene, D.A. Hammer, R. Murali, Polymersomes: a new multi-functional tool for cancer diagnosis and therapy, Methods. 46 (1) (2008) 25–32.
[10] H. Tanisaka, S. Kizaka-Kondoh, A. Makino, S. Tanaka, M. Hiraoka, S. Kimura, Near-infrared fluorescent labeled peptosome for application to cancer imaging, Bioconjugate Chem. 19 (1) (2008) 109–117.
[11] M. Ferrari, Cancer nanotechnology: opportunities and challenges, Nat. Rev. Cancer 5 (2005) 161–171.
[12] D.A. LaVan, T. McGuire, R. Langer, Small-scale systems for in vivo drug delivery, Nat. Biotechnol. 21 (2003) 1184–1191.
[13] L. Zhang, F.X. Gu, J.M. Chan, A.Z. Wang, R.S. Langer, O.C. Farokhzad, Nanoparticles in medicine: therapeutic applications and developments, Clin. Pharmacol. Ther. 83 (2008) 761–769.
[14] R. Langer, New methods of drug delivery, Science. 249 (1990) 1527–1533.
[15] M.L. Etheridge, S.A. Campbell, A.G. Erdman, C.L. Haynes, S.M. Wolf, J. McCullough, The big picture on nanomedicine: the state of investigational and approved nanomedicine products, Nanomed. NBM. 9 (2013) 1–14.
[16] W.H. Gmeiner, S. Ghosh, Nanotechnology for cancer treatment, Nanotechnol. Rev. 3 (2) (2015) 111–122.
[17] K.M. Gharpure1, S.Y. Wu, C. Li, G. Lopez-Berestein, A.K. Sood, Nanotechnology: future of oncotherapy, Clin. Cancer Res. 21 (14) (2015) 3121–3130.
[18] B. Mishra, B.B. Patel, S. Tiwari, Colloidal nanocarriers: a review on formulation technology, types and applications toward targeted drug delivery, Nanomed. NBM. 6 (2010) 9–24.
[19] F. Alexis, J.W. Rhee, J.P. Richie, A.F. Radovic-Moreno, R. Langer, O.C. Farokhzad, New frontiers in nanotechnology for cancer treatment, Urol. Oncol. 26 (2008) 74–85.
[20] O. Kayser, A. Lemke, N. Hernandez-Trejo, The impact of nanobiotechnology on the development of new drug delivery systems, Curr. Pharm. Biotechnol. 6 (2005) 3–5.
[21] T. Kubik, K. Bogunia-Kubik, M. Sugisaka, Nanotechnology on duty in medical applications, Curr. Pharm. Biotechnol. 6 (2005) 17–33.
[22] H. Devalapally, D. Shenoy, S. Little, R. Langer, A. Mansoor, Poly(ethylene oxide)-modified poly(beta-amino ester) nanoparticles as a pH-sensitive system for tumor-targeted delivery of hydrophobic drugs: part 3. Therapeutic efficacy and safety studies in ovarian cancer xenograft model, Cancer Chemother. Pharmacol. 59 (4) (2006) 477–484.
[23] J.L. Au, S.H. Jang, J. Zheng, C.T. Chen, S. Song, L. Hu, M.G. Wientjes, Determinants of drug delivery and transport to solid tumors, J. Control Release. 74 (2001) 31–46.
[24] G.J. Fetterly, R.M. Straubinger, Pharmacokinetics of paclitaxel-containing liposomes in rats, AAPS PharmSci. 5 (2003) E32.
[25] D. Hoarau, P. Delmas, S. David, E. Roux, J.C. Leroux, Novel long-circulating lipid nanocapsules, Pharm. Res. 21 (2004) 1783–1789.
[26] O.M. Koo, I. Rubinstein, H. Onyuksel, Camptothecin in sterically stabilized

phospholipid micelles: a novel nanomedicine, Nanomedicine 1 (2005) 77–84.
[27] J. Kristl, B. Volk, M. Gasperlin, M. Sentjurc, P. Jurkovic, Effect of colloidal carriers on ascorbyl palmitate stability, Eur. J. Pharm. Sci. 19 (2003) 181–189.
[28] A. Arnedo, J.M. Irache, M. Merodio, M.S. Espuelas Millan, Albumin nanoparticles improved the stability, nuclear accumulation and anticytomegaloviral activity of a phosphodiester oligonucleotide, J. Control Release. 94 (2004) 217–227.
[29] J.A. Zhang, G. Anyarambhatla, L. Ma, S. Ugwu, T. Xuan, T. Sardone, I. Ahmad, Development and characterization of a novel Cremophor EL free liposome-based paclitaxel (LEP-ETU) formulation, Eur. J. Pharm. Biopharm. 59 (2005) 177–187.
[30] N.K. Ibrahim, N. Desai, S. Legha, P. Soon-Shiong, R.L. Theriault, E. Rivera, B. Esmaeli, S.E. Ring, A. Bedikian, G.N. Hortobagyi, J.A. Ellerhorst, Phase I and pharmacokinetic study of ABI-007, a Cremophor-free, protein-stabilized, nanoparticle formulation of paclitaxel, Clin. Cancer Res. 8 (2002) 1038–1044.
[31] T.Y. Kim, D.W. Kim, J.Y. Chung, S.G. Shin, S.C. Kim, D.S. Heo, N.K. Kim, Y.J. Bang, Phase I and pharmacokinetic study of Genexol-PM, a Cremophor-free, polymeric micelle-formulated paclitaxel, in patients with advanced malignancies, Clin. Cancer Res. 10 (2004) 3708–3716.
[32] A. Krishnadas, I. Rubinstein, H. Onyuksel, Sterically stabilized phospholipid mixed micelles: in vitro evaluation as a novel carrier for water-insoluble drugs, Pharmacol. Res. 20 (2003) 297–302.
[33] H. Gelderblom, J. Verweij, K. Nooter, A. Sparreboom, Cremophor EL: the drawbacks and advantages of vehicle selection for drug formulation, Eur. J. Cancer. 37 (2001) 1590–1598.
[34] A.J. ten Tije, J. Verweij, W.J. Loos, A. Sparreboom, Pharmacological effects of formulation vehicles : implications for cancer chemotherapy, Clin. Pharmacokinet. 42 (2003) 665–685.
[35] M.E. Davis, The first targeted delivery of siRNA in humans via a self-assembling, cyclodextrin polymer-based nanoparticle: from concept to clinic, Mol. Pharm. 6 (2009) 659–668.
[36] P. Decuzzi, R. Pasqualini, W. Arap, M. Ferrari, Intravascular delivery of particulate systems: does geometry really matter? Pharmacol. Res. 26 (2009) 235–243.
[37] Y.B. Patil, U.S. Toti, A. Khdair, L. Ma, J. Panyam, Single-step surface functionalization of polymeric nanoparticles for targeted drug delivery, Biomaterials. 30 (2009) 859–866.
[38] B.S. Kim, S.W. Park, P.T. Hammond, Hydrogen-bonding layer-by-layer-assembled biodegradable polymeric micelles as drug delivery vehicles from surfaces, ACS Nano. 2 (2008) 386–392.
[39] R.V. Rughani, J.P. Schneider, Molecular design of beta-hairpin peptides for material construction, MRS Bull. 33 (5) (2008) 530–535.
[40] H.S. Giddi, M.A. Arunagirinathan, J.R. Bellare, Self-assembled surfactant nano-structures important in drug delivery: a review, Indian J. Exp. Bio. 45 (2) (2007) 133–159.
[41] K. Rajagopal, J.P. Schneider, Self-assembling peptides and proteins for nanotechnological applications, Curr. Opin. Struct. Biol. 14 (4) (2004) 480–486.
[42] R.S. Tu, M. Tirrell, Bottom-up design of biomimetic assemblies, Adv. Drug Deliv. Rev. 56 (11) (2004) 1537–1563.
[43] V. Prasad, N. Kumar, P.R. Mishra, Amphiphilic gels as a potential carrier for topical drug delivery, Drug Deliv. 14 (2) (2007) 75–85.
[44] J.H. Fuhrhop, U. Bindig, U. Siggel, Micellar rods and vesicular tubules made of 14", 16"-diaminoporphyrins, J. Am. Chem. Soc. 115 (23) (1993) 11036–11037.
[45] J.D. Hartgerink, E. Beniash, S.I. Stupp, Peptide-amphiphile nanofibers: a versatile scaffold for the preparation of self-assembling materials, Proc. Natl. Acad. Sci. U. S. A. 99 (8) (2002) 5133–5138.
[46] G. Porte, Giant micelles in ideal solutions. Either rods or vesicles, J. Phys. Chem. 87 (18) (1983) 3541–3550.
[47] S. Chuanoi, Y. Anraku, M. Hori, A. Kishimura, K. Kataoka, Fabrication of polyion complex vesicles with enhanced salt and temperature resistance and their potential applications as enzymatic nanoreactors, Biomacromolecules. 15 (7) (2014) 2389–2397.
[48] M. Johnsson, K. Edwards, Liposomes, disks, and spherical micelles: aggregate structure in mixtures of gel phase phosphatidylcholines and poly(ethylene glycol)-phospholipids, Biophys. J. 85 (6) (2003) 3839–3847.
[49] S.J. Holder, N.A.J.M. Sommerdijk, New micellar morphologies from amphiphilic block copolymers: disks, toroids and bicontinuous micelles, Polym. Chem. 2 (2011) 1018–1028.
[50] A.G. Daful, J.B. Avalos, A.D. Mackie, Model shape transitions of micelles: spheres to cylinders and disks, Langmuir 28 (8) (2012) 3730–3743.
[51] H. Honggang Cui, T.K. Hodgdon, E.W. Kaler, L. Abezgauz, D. Danino, M. Lubovsky, Y. Talmond, D.J. Pochan, Elucidating the assembled structure of amphiphiles in solution via cryogenic transmission electron microscopy, Soft Matter 3 (2007) 945–955.
[52] A. Trent, R. Marullo, B. Lin, M. Black, M. Tirrell, Structural properties of soluble peptide amphiphile micelles, Soft Matter 7 (2011) 9572–9582.
[53] S. dos Santos, B. Medronho, T. dos Santos, F.E. Antunes, Amphiphilic molecules in drug delivery systems, in: J. Coelho (Ed.), Drug Delivery Systems: Advanced Technologies Potentially Applicable in Personalised Treatment, Advances in Predictive, Preventive and Personalised Medicine, Springer Science and Business Media, Dordrecht, Netherlands, 2013, pp. 35–85.
[54] C.J. Drummond, C. Fong, Surfactant self-assembly objects as novel drug delivery vehicles, Curr. Opin. Colloid Interface Sci. 4 (6) (1999) 449–456.
[55] A.S. Goldstein, A.N. Lukyanov, P.A. Carlson, P. Yager, M.H. Gelb, Formation of high-axial-ratio-microstructures from natural and synthetic sphingolipids, Chem. Phys. Lipids. 88 (1) (1997) 21–36.
[56] J. Israelachvili, Intermolecular and Surface Forces, third ed., Academic Press, New York, 2011.
[57] K. Letchford, H. Burt, A review of the formation and classification of amphiphilic block copolymer nanoparticulate structures: micelles, nanospheres, nanocapsules and polymersomes, Eur. J. Pharm. Biopharm. 65 (2007) 259–269.
[58] K. Yu, A. Eisenberg, Bilayer morphologies of self-assembled crew-cut aggregates of amphiphilic PS-b-PEO diblock copolymers in solution, Macromolecules 31 (11) (1998) 3509–3518.
[59] M.-S. Hsiao, S.F.M. Yusoff, M.A. Winnik, I. Manners, Crystallization-driven self-assembly of block copolymers with a short crystallizable core-forming segment: controlling micelle morphology through the influence of molar mass and solvent selectivity, Macromolecules 47 (7) (2014) 2361–2372.
[60] H. Shen, L. Zhang, A. Eisenberg, Multiple pH-Induced morphological changes in aggregates of polystyrene-block-poly(4-vinylpyridine) in DMF/H_2O mixtures, J. Am. Chem. Soc. 121 (1999) 2728–2740.
[61] A. Choucair, A. Eisenberg, Interfacial solubilization of model amphiphilic molecules in block copolymer micelles, J. Am. Chem. Soc. 125 (2003) 11993–12000.
[62] A. Choucair, A. Eisenberg, Control of amphiphilic block copolymer morphologies using solution conditions, Eur. Phys. J. E. Soft Matter 10 (2003) 37–44.
[63] J.-F. Le Meins, O. Sandre, S. Lecommandoux, Recent trends in the tuning of polymersomes' membrane properties, Eur. Phys. J. E. Soft Matter 34 (14) (2011) 1–17.
[64] E.P. Holowka, D.J. Pochan, T.J. Deming, Charged polypeptide vesicles with controllable diameter, J. Am. Chem. Soc. 127 (2005) 12423–12428.
[65] G. Cai, H. Zhang, P. Liu, L. Wang, H. Jiang, Triggered disassembly of hierarchically assembled onion-like micelles into the pristine core-shell micelles via a small change in pH, Acta Biomater. 7 (10) (2011) 3729–3737.
[66] E.S. Read, S.P. Armes, Recent advances in shell cross-linked micelles, Chem. Commun. (Camb). 29 (2007) 3021–3035.
[67] R. Erhardt, A. Böker, H. Zettl, H. Kaya, W. Pyckhout-Hintzen, G.V. Krausch, A. Abetz, H.E. Müller, Janus micelles, Macromolecules 34 (4) (2001) 1069–1075.
[68] R. Erhardt, M. Zhang, A. Böker, H. Zettl, C. Abetz, P. Frederik, G. Krausch, V. Abetz, A.X.E. Müller, Amphiphilic janus micelles with polystyrene and poly(methacrylic acid) hemispheres, J. Am. Chem. Soc. 125 (11) (2003) 3260–3267.
[69] I.K. Voets, A. de Keizer, P. de Waard, P.M. Frederik, P.H. Bomans, H. Schmalz, A. Walther, S.M. King, F.A.M. Leermakers, M.A.C. Stuart, Double-faced micelles from water-soluble polymers, Angew. Chem. Int. Ed. Engl. 45 (40) (2006) 6673–6676.
[70] V. Bütün, S. Liu, J.V.M. Weaver, X. Bories-Azeau, Y. Cai, S.P. Armes, A brief review of 'schizophrenic' block copolymers, React. Funct. Polym. 66 (1) (2006) 157–165.
[71] Z. Li, M.A. Hillmyer, T.P. Lodge, Control of structure in multicompartment micelles by blending μ-ABC star terpolymers with AB diblock copolymers, Macromolecules. 39 (2) (2006) 765–771.
[72] V.P. Torchilin, Recent advances with liposomes as pharmaceutical carriers, Nat. Rev. Drug Discov. 4 (2005) 145–160.
[73] G.S. Kwon, Polymeric micelles for delivery of poorly water-soluble compounds, Crit. Rev. Ther. Drug Carr. Syst. 20 (2003) 357–403.
[74] A. Vonarbourg, C. Passirani, P. Saulnier, J.P. Benoit, Parameters influencing the stealthiness of colloidal drug delivery systems, Biomaterials. 27 (2006) 4356–4373.
[75] G. Henriksen, B.W. Schoultz, T.E. Michaelsen, Ø.S. Bruland, R.H. Larsen, Sterically stabilized liposomes as a carrier for á-emitting radium and actinium radionuclides, Nucl. Med. Biol. 31 (2004) 441–449.
[76] M. Miederer, D.A. Scheinberg, M.R. McDevitt, Realizing the potential of the actinium-225 radionuclide generator in targeted alpha particle therapy applications, Adv. Drug Deliv. Rev. 60 (2008) 1371–1382.
[77] H. Takeuchi, H. Kojima, H. Yamamoto, Y. Kawashima, Evaluation of circulation profiles of liposomes coated with hydrophilic polymers having different molecular weights in rats, J. Control. Release 75 (2001) 83–91.
[78] D. Garrec, M. Ranger, J. Leroux, Micelles in anticancer drug delivery, Am. J. Drug Deliv. 2 (2004) 15–42.
[79] E.S. Lee, K. Na, Y.H. Bae, Polymeric micelle for tumor pH and folate-mediated targeting, J. Control Release. 91 (2003) 103–113.
[80] E.S. Lee, K. Na, Y.H. Bae, Doxorubicin loaded pH-sensitive polymeric micelles for reversal of resistant MCF-7 tumor, J. Control Release. 103 (2005) 405–418.
[81] Y. Matsumura, T. Hamaguchi, T. Ura, K. Muro, Y. Yamada, Y. Shimada, K. Shirao, T. Okusaka, H. Ueno, M. Ikeda, N. Watanabe, Phase I clinical trial and pharmacokinetic evaluation of NK911, a micelle-encapsulated doxorubicin, Br. J. Cancer 91 (2004) 1775–1781.
[82] A. Nagai, Y. Nagai, H. Qu, S. Zhang, Dynamic behaviors of lipid-like self-assembling peptide A6D and A6K nanotubes, J. Nanosci. Nanotechnol. 7 (2) (2007) 2246–2252.
[83] A.S. Ojugo, P.M. McSheehy, D.J. McIntyre, C. McCoy, M. Stubbs, M.O. Leach, I.R. Judson, J.R. Griffiths, Measurement of the extracellular pH of solid

tumours in mice by magnetic resonance spectroscopy: a comparison of exogenous (19)F and (31)P probes, NMR Biomed. 12 (1999) 495–504.
[84] K. Engin, D.B. Leeper, J.R. Cater, A.J. Thistlethwaite, L. Tupchong, J.D. McFarlane, Extracellular pH distribution in human tumours, Int. J. Hyperth. 11 (1995) 211–216.
[85] H. Wu, L. Zhu, V.P. Torchilin, pH-sensitive poly(histidine)-PEG/DSPE-PEG co-polymer micelles for cytosolic drug delivery, Biomaterials 34 (2013) 1213–1222.
[86] A. Lavasanifar, J. Samuel, G.S. Kwon, Poly(ethylene oxide)-block-poly(L-amino acid) micelles for drug delivery, Adv. Drug Deliv. Rev. 54 (2002) 169–190.
[87] Y. Li, G.S. Kwon, Methotrexate esters of poly(ethylene oxide)-block-poly(2-hydroxyethyl-L-aspartamide). Part I: effects of the level of methotrexate conjugation on the stability of micelles and on drug release, Pharm. Res. 17 (2000) 607–611.
[88] Y. Bae, N. Nishiyama, S. Fukushima, H. Koyama, M. Yasuhiro, K. Kataoka, Preparation and biological characterization of polymeric micelle drug carriers with intracellular pH-triggered drug release property: tumor permeability, controlled subcellular drug distribution, and enhanced in vivo antitumor efficacy, Bioconjug. Chem. 16 (2005) 122–130.
[89] A. Graciaa, M. Ben Ghoulam, G. Marion, J.J. Lachaise, Critical concentrations and compositions of mixed micelles of sodium dodecylbenzenesulfonate, tetradecyltrimethylammonium bromide, and polyoxyethylene octylphenols, J. Phys. Chem. 93 (1989) 4167–4173.
[90] Z.J. Yu, G.X. Zhao, Micellar compositions in mixed surfactant solutions, J. Colloid Interface Sci. 156 (2) (1993) 325–328.
[91] M. Ishikawa, K. Matsumura, K. Esumi, K. Meguro, Mixed micelle formation between anionic surfactant and α,ω-type cationic surfactant in aqueous solutions: sodium dodecyl sulfate and N,N'-1,12-dodecanediylbis(triethylammonium bromide) system, J. Colloid Interface Sci. 141 (1) (1991) 10–20.
[92] C. Tanford, The Hydrophobic Effect Formation of Micelles and Biological Membranes, Wiley-Interscience NY, NY, 1980.
[93] P. Jokela, B. Joensson, A. Khan, Phase equilibria of catanionic surfactant-water systems, J. Phys. Chem. 91 (1987) 3291–3298.
[94] E.W. Kaler, A.K. Murthy, B.E. Rodriguez, J.A. Zasadzinski, Spontaneous vesicle formation in aqueous mixtures of single-tailed surfactants, Science 245 (4924) (1989) 1371–1374.
[95] R.H. Müller, K. Mäder, S. Gohla, Solid lipid nanoparticles (SLN) for controlled drug delivery – a review of the state of the art, Eur. J. Pharm. Biopharm. 50 (2000) 161–177.
[96] I.P. Kaur, R. Bhandari, S. Bhandari, V. Kakkar, Potential of solid lipid nanoparticles in brain targeting, J. Control Release. 127 (2008) 97–109.
[97] P. Blasi, S. Giovagnoli, A. Schoubben, M. Ricci, C. Rossi, Solid lipid nanoparticles for targeted brain drug delivery, Adv. Drug Deliv. Rev. 59 (2007) 454–477.
[98] G.P. Zara, R. Cavalli, A. Bargoni, A. Fundaro, D. Vighetto, M.R. Gasco, Intravenous administration to rabbits of non-stealth and stealth doxorubicin-loaded solid lipid nanoparticles at increasing concentrations of stealth agent: pharmacokinetics and distribution of doxorubicin in brain and other tissues, J. Drug Target. 10 (2002) 327–335.
[99] A. Sinaga, T.A. Hatton, K.C. Tam, Poly(acrylic acid)-block-poly(L-valine): evaluation of beta-sheet formation and its stability using circular dichroism technique, Biomacromolecules 8 (9) (2007) 2801–2808.
[100] S.A. Wissing, O. Kayser, R.H. Muller, Solid lipid nanoparticles for parenteral drug delivery, Adv. Drug Deliv. Rev. 56 (2004) 1257–1272.
[101] A. Quintana, E. Raczka, L. Piehler, I. Lee, A. Myc, I. Majoros, A.K. Patri, T. Thomas, J. Mule, J.R. Baker Jr., Design and function of a dendrimer-based therapeutic nano-device targeted to tumor cells through the folate receptor, Pharm. Res. 19 (2002) 1310–1316.
[102] U. Boas, P.M. Heegaard, Dendrimers in drug research, Chem. Soc. Rev. 33 (2004) 43–63.
[103] R.M. Mainardes, L.P. Silva, Drug delivery systems: past, present, and future, Curr. Drug Targets. 5 (2004) 449–455.
[104] A. Carlmark, C. Hawker, A. Hult, M. Malkoch, New methodologies in the construction of dendritic molecules, Chem. Soc. Rev. 38 (2008) 352–362.
[105] M.J. Cloninger, Biological applications of dendrimers, Curr. Opin. Chem. Biol. 6 (2002) 742–748.
[106] V. Percec, D.A. Wilson, P. Leowanawat, C.J. Wilson, A.D. Hughes, M.S. Kaucher, D.A. Hammer, D.H. Levine, A.J. Kim, F.S. Bates, K.P. Davis, T.P. Lodge, M.L. Klein, R.H. DeVane, E. Aqad, B.M. Rosen, A.O. Argintaru, M.J. Sienkowska, K. Rissanen, S. Nummelin, J. Ropponen, Self-assembly of janus dendrimers into uniform dendrimersomes and other complex architectures, Science. 328 (5981) (2010) 1009–1014.
[107] J. Ropponen, S. Nummelin, K. Rissanen, Bisfunctionalized janus molecules, Org. Lett. 6 (15) (2004) 2495–2497.
[108] B.M. Rosen, C.J. Wilson, D.A. Wilson, M. Peterca, M.R. Imam, V. Percec, Dendron-mediated self-assembly, disassembly, and self-organization of complex systems, Chem. Rev. 109 (11) (2009) 6275–6540.
[109] P.K. Tripathi, A.J. Khopade, S. Nagaich, S. Shrivastava, S. Jain, N.K. Jain, Dendrimer grafts for delivery of 5-fluorouracil, Pharmazie. 57 (2002) 261–264.
[110] A.S. Chauhan, N.K. Jain, P.V. Diwan, A.J. Khopade, Solubility enhancement of indomethacin with poly(amidoamine) dendrimers and targeting to inflammatory regions of arthritic rats, J. Drug Target. 12 (2004) 575–583.
[111] M. El-Sayed, M.F. Kiani, M.D. Naimark, A.H. Hikal, H. Ghandehari, Extravasation of poly(amidoamine) (PAMAM) dendrimers across microvascular network endothelium, Pharm. Res. 18 (2001) 23–28.
[112] R. Jevprasesphant, J. Penny, R. Jalal, D. Attwood, N.B. McKeown, A. D'Emanuele, The influence of surface modification on the cytotoxicity of PAMAM dendrimers, Int. J. Pharm. 252 (2003) 263–266.
[113] S.S. Nigavekar, L.Y. Sung, M. Llanes, A. El-Jawahri, T.S. Lawrence, C.W. Becker, L. Balogh, M.K. Khan, 3H dendrimer nanoparticle organ/tumor distribution, Pharm. Res. 21 (2004) 476–483.
[114] F.E. Antunes, E.F. Marques, M.G. Miguel, B. Lindman, Polymer-vesicle association, Adv. Colloid Interface Sci. 147–148 (2009) 18–35.
[115] M.A. Moses, H. Brem, R. Langer, Advancing the field of drug delivery: taking aim at cancer, Cancer Cell 4 (2003) 337–341.
[116] A. Samad, Y. Sultana, M. Aqil, Liposomal drug delivery systems: an update review, Curr. Drug Deliv. 4 (2007) 297–305.
[117] S.L. Hart, Lipid carriers for gene therapy, Curr. Drug Deliv. 2 (2005) 423–428.
[118] M.A. Moses, H. Brem, R. Langer, Advancing the field of drug delivery: taking aim at cancer, Cancer Cell 4 (2003) 337–341.
[119] T.M. Allen, P.R. Cullis, Drug delivery systems: entering the mainstream, Science 303 (2004) 1818–1822.
[120] S. Ning, Q. Huang, X. Sun, C. Li, Y. Zhang, J. Li, Y.-N. Liu, Carboxymethyl dextran-coated liposomes: toward a robust drug delivery platform, Soft Matter 7 (2011) 9394–9401.
[121] H.R. Marsden, I. Tomatsua, A. Kros, Model systems for membrane fusion, Chem. Soc. Rev. 40 (2011) 1572–1585.
[122] K. Ewert, H.M. Evans, A. Ahmad, N.L. Slack, A.J. Lin, A. Martin-Herranz, C.R. Safinya, Lipoplex structures and their distinct cellular pathways, Adv. Genet. 53 (2005) 119–155.
[123] S. Pollock, R. Antrobus, R. Newton, B. Kampa, J. Rossa, S. Latham, N.B. Nichita, R.A. Dwek, N. Zitzmann, Uptake and trafficking of liposomes to the endoplasmic reticulum, FASEB J. 24 (6) (2010) 1866–1878.
[124] T.M. Allen, A. Chonn, Large unilamellar liposomes with low uptake into the reticuloendothelial system, FEBS Lett. 223 (1987) 42–46.
[125] S. Ning, Q. Huang, X. Sun, C. Li, Y. Zhang, J. Li, Y.-N. Liu, Carboxymethyl dextran-coated liposomes: toward a robust drug delivery platform, Soft Matter 7 (2011) 9394–9401.
[126] A. Chonn, P.R. Cullis, Ganglioside GM1 and hydrophilic polymers increase liposome circulation times by inhibiting the association of blood proteins, J. Liposome Res. 2 (3) (1992) 397–410.
[127] H. Takeuchi, H. Yamamoto, T. Toyoda, H. Toyobuku, T. Hino, Y. Kawashima, Physical stability of size controlled small unilameller liposomes coated with a modified polyvinyl alcohol, Int. J. Pharm. 164 (1998) 103–111.
[128] M.L. Immordino, F. Dosio, L. Cattel, Stealth liposomes: review of the basic science, rationale, and clinical applications, existing and potential, Int. J. Nanomed. 1 (3) (2006) 297–315.
[129] S.H. Jung, S. Jung, H. Seong, S.H. Cho, K.S. Jeong, B.C. Shin, Polyethylene glycol-complexed cationic liposome for enhanced cellular uptake and anticancer activity, Int. J. Pharm. 382 (1–2) (2009) 254–261.
[130] V.P. Torchilin, T.S. Levchenko, K.R. Whiteman, A.A. Yaroslavov, A.M. Tsatsakis, A.K. Rizos, E.V. Michailova, M.I. Shtilman, Amphiphilic poly-N-vinylpyrrolidones: synthesis, properties and liposome surface modification, Biomaterials 22 (2001) 3035–3044.
[131] D.B. Kirpotin, D.C. Drummond, Y. Shao, M.R. Shalaby, K. Hong, U.B. Nielsen, J.D. Marks, C.C. Benz, J.W. Park, Antibody targeting of long-circulating lipidic nanoparticles does not increase tumor localization but does increase internalization in animal models, Cancer Res. 66 (2006) 6732–6740.
[132] M.T. Basel, T.B. Shrestha, D.L. Troyer, S.H. Bossmann, Protease-sensitive, polymer-caged liposomes: a method for making highly targeted liposomes using triggered release, ACS Nano. 5 (3) (2011) 2162–2175.
[133] Y.S. Kim, M.W. Brechbiel, An overview of targeted alpha therapy, Tumour Biol. 33 (2012) 573–590.
[134] S. Sofou, J.L. Thomas, H.Y. Lin, M.R. McDevitt, D.A. Scheinberg, G. Sgouros, Engineered liposomes for potential alpha-particle therapy of metastatic cancer, J. Nucl. Med. 45 (2004) 253–260.
[135] S. Sofou, B.J. Kappel, J.S. Jaggi, M.R. McDevitt, D.A. Scheinberg, G. Sgouros, Enhanced retention of the alpha-particle-emitting daughters of actinium-225 by liposome carriers, Bioconjug. Chem. 18 (2007) 2061–2067.
[136] O. Sartor, Radioisotopic treatment of bone pain from metastatic prostate cancer, Curr. Oncol. Rep. 5 (2003) 258–262.
[137] M. Hamoudeh, M.A. Kamleh, R. Diab, H. Fessi, Radionuclides delivery systems for nuclear imaging and radiotherapy of cancer, Adv. Drug Deliv. Rev. 60 (2008) 1329–1346.
[138] O.M. Koo, I. Rubinstein, H. Onyuksel, Role of nanotechnology in targeted drug delivery and imaging: a concise review, Nanomed. NBM. 1 (2005) 193–212.
[139] A.A. Gabizon, H. Shmeeda, S. Zalipsky, Pros and cons of the liposome platform in cancer drug targeting, J. Liposome Res. 16 (2006) 175–183.
[140] T.M. Allen, L.G. Cleland, Serum-induced leakage of liposome contents, Biochem. Biophys. Acta Biomembr. 597 (1980) 418–426.
[141] V.K. Moyrya, N.N. Inamdar, Trimethyl chitosan and its applications in drug delivery, J. Mater. Sci. Mater. Med. 20 (5) (2009) 1057–1079.
[142] H.Y. Nam, S.M. Kwon, H. Chung, S.-Y. Lee, S.-H. Kwon, H. Jeon, Y. Kim, J.H. Park, J. Kim, S. Her, Y.-K. Oh, I.C. Kwon, K. Kim, S.Y. Jeong, Hydrophobically modified glycol chitosan nanoparticles-encapsulated camptothecin enhance the drug stability and tumor targeting in cancer therapy, J. Control Release 127 (3) (2008) 208–218.
[143] P.S. Pramod, R. Shah, S. Chaphekar, N. Balasubramanian, M. Jayakannan, Polysaccharide nano-vesicular multidrug carriers for synergistic killing of

cancer cells, Nanoscale 6 (2014) 11841–11855.
[144] P.S. Pramod, R. Shah, M. Jayakannan, Dual stimuli polysaccharide nanovesicles for conjugated and physically loaded doxorubicin delivery in breast cancer cells, Nanoscale 7 (2015) 6636–6652.
[145] V.K. Moyrya, N.N. Inamdar, Trimethyl chitosan and its applications in drug delivery, J. Mater. Sci. Mater. Med. 20 (5) (2009) 1057–1079.
[146] H.Y. Nam, S.M. Kwon, H. Chung, S.-Y. Lee, S.-H. Kwon, H. Jeon, Y. Kim, J.H. Park, J. Kim, S. Her, Y.-K. Oh, I.C. Kwon, K. Kim, S.Y. Jeong, Hydrophobically modified glycol chitosan nanoparticles-encapsulated camptothecin enhance the drug stability and tumor targeting in cancer therapy, J. Control Release 127 (3) (2008) 208–218.
[147] I.F. Uchegbu, S.P. Vyas, Non-ionic surfactant based vesicles (niosomes) in drug delivery, Int. J. Pharm. 172 (1998) 33–70.
[148] G. Vanlerberghe, R.M. Handjani-Vila, A. Ribier, Les niosomes, une nouvelle famille de vesicules a' base d'amphiphiles non ioniques, in: Physicochimie des compose's amphiphiles. Coll. Nat, CNRS. Editions du CNRS, Paris, 1978, pp. 303–311.
[149] R.M. Handjani-Vila, A. Ribier, B. Rondot, G. Vanlerberghie, Dispersions of lamellar phases of non-ionic lipids in cosmetic products, Int. J. Cosmet. Sci. 1 (5) (1979) 303–314.
[150] Handjani-Vila, R. M., Guy, V. (1975) Procédé de fabrication de dispersions aqueuses de spérules lipidiques et nouvelles compositions correspondantes, L'Oréal, French Patent 2315991–A1.
[151] Handjani-Vila, R. M., Ribier, A., Vanlerberghie, G, Zabotto, A., Griat, J. (1989) Cosmetic and pharmaceutical compositions containing niosomes and a water-soluble polyamide, and a process for preparing these compositions, L'Oréal, U. S. Patent No. 4830857.
[152] T. Yoshioka, B. Sternberg, A.T. Florence, Preparation and properties of vesicles (niosomes) of sorbitan monoesters (span 20, 40, 60 and 80) and a sorbitan triester (span 85), Int. J. Pharm. 105 (1) (1994) 1–6.
[153] K.M. Kazi, A.S. Mandal, N. Biswas, A. Guha, S. Chatterjee, M. Behera, K. Kuotsu, Niosome: a future of targeted drug delivery systems, J. Adv. Pharm. Technol. Res. 1 (2010) 374–380.
[154] C. Marianecci, L. Di Marzio, F. Rinaldi, C. Celia, D. Paolino, F. Alhaique, S. Esposito, M. Carafa, Niosomes from 80s to present: the state of the art, Adv. Colloid Interface Sci. 205 C (2013) 187–206.
[155] C. Hu, D.G. Rhodes, Proniosomes: a novel drug carrier preparation, Int. J. Pharm. 185 (1999) 23–35.
[156] V.R. Yasam, S.L. Jakki, J. Natarajan, G. Kuppusamy, A review on novel vesicular drug delivery: proniosomes, Drug Deliv. 21 (4) (2014) 243–249.
[157] J.Y. Fang, C.T. Hong, W.T. Chiu, Y.Y. Wang, Effect of liposomes and niosomes on skin permeation of enoxacin, Int. J. Pharm. 219 (2001) 61–72.
[158] M. Manconi, C. Sinico, D. Valenti, F. Lai, A.M. Fadda, Niosomes as carriers for tretinoin. III. A study into the in vitro cutaneous delivery of vesicle-incorporated tretinoin, Int. J. Pharm. 311 (2006) 11–19.
[159] M. Carafa, C. Marianecci, F. Rinaldi, E. Santucci, S. Tampucci, D. Monti, Span and tween neutral and pH-sensitive vesicles: characterization and in vitro skin permeation, J. Liposome Res. 19 (2009) 332–340.
[160] D.A. Hajduk, M.B. Kossuth, M.A. Hillmyer, F.S. Bates, Complex phase behavior in aqueous solutions of poly(ethylene oxide)-Poly(ethylethylene) block copolymers, J. Phys. Chem. B 102 (22) (1998) 4269–4276.
[161] H.E. Warriner, S.H. Idziak, N.L. Slack, P. Davidson, C.R. Safinya, Lamellar biogels: fluid-membrane-based hydrogels containing polymer lipids, Science 271 (5251) (1996) 969–973.
[162] F. Meng, Z. Zhong, J. Feijen, Stimuli-responsive polymersomes for programmed drug delivery, Biomacromolecules. 10 (2) (2009) 197–209.
[163] D. Needham, D.V. Zhelev, in: M. Rosoff (Ed.), The Mechanochemistry of Lipid Vesicles Examined by Micropipette Manipulation Techniques in Vesicles, Marcel Dekker, New York, 2000. Ch. 9.
[164] G. Srinivas, D.E. Discher, M.L. Klein, Self-assembly and properties of diblock copolymers by coarse-grain molecular dynamics, Nat. Mater. 3 (9) (2004) 638–644.
[165] H. Hu, M. Gopinadhan, C.O. Osuji, Directed self-assembly of block copolymers: a tutorial review of strategies for enabling nanotechnology with soft matter, Soft Matter 10 (2014) 3867–3889.
[166] Y. Mai, A. Eisenberg, Self-assembly of block copolymers, Chem. Soc. Rev. 41 (2012) 5969–5985.
[167] S. Santoso, W. Hwang, H. Hartman, S. Zhang, Self-assembly of surfactant-like peptides with variable glycine tails to form nanotubes and nanovesicles, Nano Lett. 2 (7) (2002) 687–691.
[168] G. Von Maltzahn, S. Vauthey, S. Santoso, S. Zhang, Positively charged surfactant-like peptides self-assemble into nanostructures, Langmuir 19 (10) (2003) 4332–4337.
[169] H. Xu, J. Wang, S. Han, J. Wang, D. Yu, H. Zhang, D. Xia, X. Zhao, T.A. Waigh, J.R. Lu, Hydrophobic-region-induced transitions in self-assembled peptide nanostructures, Langmuir. 25 (7) (2009) 4115–4123.
[170] S.J. Yang, S. Zhang, Self-assembling behavior of designer lipid-like peptides, Supramol. Chem. 18 (5) (2006) 389–396.
[171] X. Zhao, F. Pan, S. Perumal, H. Xu, J.R. Lu, J.R.P. Webster, Interfacial assembly of cationic peptide surfactants, Soft Matter. 5 (8) (2009) 1630–1638.
[172] S. Vauthey, S. Santoso, H. Gong, N. Watson, S. Zhang, Molecular self-assembly of surfactant-like peptides to form nanotubes and nanovesicles, Proc. Natl. Acad. Sci. U.S.A. 99 (2002) 5355–5360.
[173] S. Tsonchev, A. Troisi, G.C. Schatz, M.A. Ratner, On the structure and stability of self-assembled zwitterionic peptide amphiphiles: a Theoretical study, Nano Lett. 4 (3) (2004) 427–431.
[174] S. Santoso, W. Hwang, H. Hartman, S. Zhang, Self-assembly of surfactant-like peptides with variable glycine tails to form nanotubes and nanovesicles, Nano Lett. 2 (2002) 687–691.
[175] X. Zhao, F. Pan, H. Xu, M. Yaseen, H. Shan, C.A. Hauser, S. Zhang, J.R. Lu, Molecular self-assembly and applications of designer peptide amphiphiles, Chem. Soc. Rev. 39 (9) (2010) 3480–3498.
[176] W. Jeong, Y. Lim, Macrocyclic peptides self-assemble into robust vesicles with molecular recognition capabilities, Bioconjug. Chem. 25 (2014) 1996–2003.
[177] D. Jiao, J. Geng, X.J. Loh, D. Das, T.-C. Lee, O.A. Sherman, Supramolecular peptide amphiphile vesicles through host–guest complexation, Angew. Chem. Int. Ed. Engl. 51 (2012) 9633–9637.
[178] X.J. Loh, J. del Barrio, T.-C. Lee, O.A. Sherman, Supramolecular polymeric peptide amphiphile vesicles for the encapsulation of basic fibroblast growth factor, Chem. Commun. 50 (2014) 3033–3035.
[179] A.J. van Hell, C.J.C.A. Costa, F.M. Flesch, M. Sutter, W. Jiskoot, D.J.A. Crommelin, W.E. Hennink, E. Mastrobattista, Self-Assembly of Recombinant Amphiphilic Oligopeptides into Vesicles, Biomacromolecules. 8 (2007) 2753–2761.
[180] A.J. van Hell, M.M. Fretz, D.J.A. Crommelin, W.E. Hennink, E. Mastrobattista, Peptide nanocarriers for intracellular delivery of photosensitizers, J. Control Release. 141 (3) (2010) 347–353.
[181] M. Rad-Malekshahi, K.M. Visscher, J.P. Rodrigues, R. de Vries, W.E. Hennink, M. Baldus, A.M. Bonvin, E. Mastrobattista, M. Weingarth, The supramolecular organization of a peptide-based nanocarrier at high molecular detail, J. Am. Chem. Soc. 137 (2015) 7775–7784.
[182] S. Zhang, Emerging biological materials through molecular self-assembly, Biotechnol. Adv. 20 (5–6) (2002) 321–339.
[183] D.J. Adams, D. Atkins, A.I. Cooper, S. Furzeland, A. Trewin, I. Young, Vesicles from peptidic side-chain polymers synthesized by atom transfer radical polymerization, Biomacromolecules 9 (11) (2008) 2997–3003.
[184] S. Gudlur, P. Sukthankar, J. Gao, L.A. Avila, Y. Hiromasa, J. Chen, T. Iwamoto, J.M. Tomich, Peptide nanovesicles formed by the self-assembly of branched amphiphilic peptides, PLoS One 7 (2012) e45374.
[185] H. Iatrou, H. Frielinghaus, S. Hanski, N. Ferderigos, J. Ruokolainen, O. Ikkala, D. Richter, J. Mays, N. Hadjichristidis, Architecturally induced multiresponsive vesicles from well-defined polypeptides: formation of gene vehicles, Biomacromolecules 8 (7) (2007) 2173–2181.
[186] S. Kar, M.G. Drew, A. Pramanik, Formation of vesicles through solvent assisted self-assembly of hydrophobic pentapeptides: encapsulation and pH responsive release of dyes by the vesicles, Protein Pept. Lett. 18 (9) (2011) 886–897.
[187] K.E. Gebhardt, S. Ahn, G. Venkatachalam, D.A. Savin, Role of secondary structure changes on the morphology of polypeptide-based block copolymer vesicles, J. Colloid Interface Sci. 317 (1) (2008) 70–76.
[188] J. Sun, X. Chen, T. Lu, S. Liu, H. Tian, Z. Guo, X. Jing, Formation of reversible shell cross-linked micelles from the biodegradable amphiphilic diblock copolymer poly(L-cysteine)-block-poly(L-lactide), Langmuir. 24 (18) (2008) 10099–10106.
[189] R.E. Sallach, M. Wei, N. Biswas, V.P. Conticello, S. Lecommandoux, R.A. Dluhy, E.L. Chaikof, Micelle density regulated by a reversible switch of protein secondary structure, J. Am. Chem. Soc. 128 (36) (2006) 12014–12019.
[190] Y.S. Velichko, S.I. Stupp, M.O. de la Cruz, Molecular simulation study of peptide amphiphile self-assembly, J. Phys. Chem. B 112 (8) (2008) 2326–2334.
[191] X. Shen, X. Mo, R. Moore, S.J. Frazier, T. Iwamoto, J.M. Tomich, X.S. Sun, Adhesion and structure properties of protein nanomaterials containing hydrophobic and charged amino acids, J. Nanosci. Nanotechnol. 6 (3) (2006) 837–844.
[192] X. Mo, Y. Hiromasa, M. Warner, A.N. Al-Rawi, T. Iwamoto, T.S. Rahman, X. Sun, J.M. Tomich, Design of 11-residue peptides with unusual biophysical properties: induced secondary structure in the absence of water, Biophys. J. 945 (2008) 1807–1817.
[193] A. Grove, J.M. Tomich, T. Iwamoto, M. Montal, Design of a functional calcium channel protein: inferences about an ion channel-forming motif derived from the primary structure of voltage-gated calcium channels, Protein Sci. 2 (11) (1993) 1918–1930.
[194] T. Iwamoto, A. Grove, M.O. Montal, M. Montal, J.M. Tomich, Chemical synthesis and characterization of peptides and oligomeric proteins designed to form transmembrane ion channels, Int. J. Pept. Protein Res. 43 (6) (1994) 597–607.
[195] P. Sukthankar, S. Gudlur, L.A. Avila, S. Whitaker, B.B. Katz, Y. Hiromasa, J. Gao, P. Thapa, D. Moore, T. Iwamoto, J.M. Tomich, Branched oligopeptides form nano-capsules with lipid vesicle characteristics, Langmuir 29 (2013) 14648–14654.
[196] P. Sukthankar, S.K. Whitaker, M. Garcia, A. Herrera, M. Boatwright, O. Prakash, J.M. Tomich, Thermally induced conformational transitions in nascent branched amphiphilic peptide capsules, Langmuir 31 (10) (2015) 2946–2955.
[197] R.L. Biltonen, D. Lichtenberg, The use of differential scanning calorimetry as a tool to characterize liposome preparations, Chem. Phys. Lipids. 64 (1993) 129–142.
[198] P. Sukthankar, L.A. Avila, S.K. Whitaker, T. Iwamoto, A. Morgenstern, C. Apostolidis, K. Liu, R.P. Hanzlik, E. Dadachova, J.M. Tomich, Branched

amphiphilic peptide capsules: cellular uptake and retention of encapsulated solutes, Biochim. Biophys. Acta, Biomembr. 1838 (2014) 2296–2305.
[199] M.C. Morris, J. Depollier, J. Mery, F. Heitz, G. Divita, A peptide carrier for the delivery of biologically active proteins into mammalian cells, Nat. Biotechnol. 19 (2001) 1173–1176.
[200] S. Fawell, J. Seery, Y. Daikh, C. Moore, L.L. Chen, B. Pepinsky, J. Barsoum, Tat-mediated delivery of heterologous proteins into cells, Proc. Natl. Acad. Sci. U.S.A. 91 (1994) 664–668.
[201] B. Zhivotovsky, S. Orrenius, O.T. Brustugun, S.O. Doskeland, Injected cytochrome c induces apoptosis, Nature. 391 (1998) 449–450.
[202] J.S. Kim, J. Soucek, J. Matousek, R.T. Raines, Mechanism of ribonuclease cytotoxicity, J. Biol. Chem. 270 (1995) 31097–31102.
[203] J. Elgqvist, S. Frost, J.-P. Pouget, P. Albertsson, The potential and hurdles of targeted alpha therapy –, Clin. Trials Beyond. Front Oncol. 3 (2014) 1–9.
[204] O. Couturier, S. Supiot, M. Degraef-Mougin, A. Faivre-Chauvet, T. Carlier, J.F. Chatal, F. Davodeau, M. Cherel, Cancer radioimmunotherapy with alpha-emitting nuclides, Eur. J. Nucl. Med. Mol. Imaging 32 (2005) 601–614.
[205] M.R. McDevitt, R.D. Finn, G. Sgouros, D. Ma, D.A. Scheinberg, An 225Ac/213Bi generator system for therapeutic clinical applications: construction and operation, Appl. Radiat. Isot. 50 (1999) 895–904.
[206] A. Verma, O. Uzun, Y. Hu, Y. Hu, H.S. Han, N. Watson, S. Chen, D.J. Irvine, F. Stellacci, Surface-structure-regulated cell-membrane penetration by monolayer-protected nanoparticles, Nat. Mater 7 (2008) 588–595.
[207] S.E. Gratton, P.A. Ropp, P.D. Pohlhaus, J.C. Luft, V.J. Madden, M.E. Napier, J.M. DeSimone, The effect of particle design on cellular internalization pathways, Proc. Natl. Acad. Sci. U. S. A. 105 (2008) 11613–11618.

6 ARTIGO II

Artigo Publicado na revista “Langmuir”

(Junho de 2017)

Sheila de M. Barros, L. Adriana Avila, Susan K. Whitaker, Kayla E. Wilkinson, Pinakin Sukthankar, Eduardo I. C. Beltrão, and John M. Tomich. Branched Amphipathic Peptide Capsules: Different Ratios of the Two Constituent Peptides Direct Distinct Bilayer Structures, Sizes, and DNA Transfection Efficiency. *Langmuir*. (2017) 33: 7096−7104.

LANGMUIR

Article

pubs.acs.org/Langmuir

Branched Amphipathic Peptide Capsules: Different Ratios of the Two Constituent Peptides Direct Distinct Bilayer Structures, Sizes, and DNA Transfection Efficiency

Sheila de M. Barros,[†,‡] L. Adriana Avila,[§] Susan K. Whitaker,[†] Kayla E. Wilkinson,[†] Pinakin Sukthankar,[∥] Eduardo I. C. Beltrão,[‡] and John M. Tomich*[,†]

[†]Department of Biochemistry and Molecular Biophysics, Kansas State University, Manhattan, Kansas 66506, United States

[‡]Department of Biochemistry, Federal University of Pernambuco-UFPE, Recife, Pernambuco 50670-901, Brazil

[§]Department of Chemistry and Biochemistry, Auburn University, Auburn, Alabama 36849, United States

[∥]Department of Molecular Biosciences, University of Kansas, Lawrence, Kansas 66045, United States

Supporting Information

ABSTRACT: Branched amphipathic peptide capsules (BAPCs) are biologically derived, bilayer delimited, nanovesicles capable of being coated by or encapsulating a wide variety of solutes. The vesicles and their cargos are readily taken up by cells and become localized in the perinuclear region of cells. When BAPCs are mixed with DNA, the BAPCs act as cationic nucleation centers around which DNA winds. The BAPCs-DNA nanoparticles are capable of delivering plasmid DNA in vivo and in vitro yielding high transfection rates and minimal cytotoxicity. BAPCs share several biophysical properties with lipid vesicles. They are however considerably more stable—resisting disruption in the presence of chaotropes such as urea and guanidinium chloride, anionic detergents, proteases, and elevated temperature (~95 °C). To date, all of our published results have utilized BAPCs that are composed of equimolar concentrations of the two branched sequences (Ac-FLIVI)$_2$-K-K$_4$-CO-NH$_2$ and (Ac-FLIVIGSII)$_2$-K-K$_4$-CO-NH$_2$. The mixture of sizes was utilized to relieve potential curvature strain in the spherical capsule. In this article, different molar ratios of the two peptides were studied to test whether alternate ratios produced BAPCs with different biological and biophysical properties. Additionally, preparation (annealing) temperature was included as a second variable.

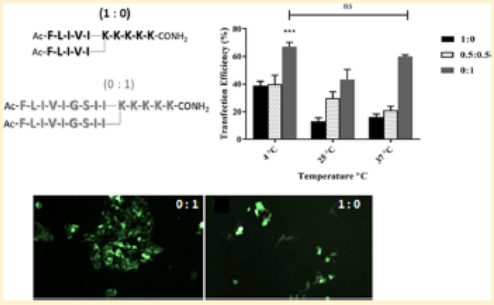

INTRODUCTION

Self-assembling polymeric vesicles have shown promise as gene and drug delivery systems. Vesicles prepared from different oligomers can be generated from a variety of self-assembling molecules[1−7] with amphiphilic block copolymers being among the most widely studied. The amphiphilic blocks can be synthetic, natural, or a mixture of both. When a peptide comprises one of the segments, the resulting assemblies are termed peptide vesicles or peptosomes. However, few peptide vesicles have been reported in the literature compared to the numerous synthetic polymers capable of self-assembling into vesicles. Vauthey et al.[8] described a short peptide termed surfactant-like peptide that assembled into nanotubes and nanovesicles. Matsuura et al.[9,10] reported an artificial C3-symmetric peptide conjugates, trigonal (FKFE)$_2$, capable of self-assembly into viral-sized peptide nanospheres in water. Van Hell et al.[11] showed the self-assembly of an amphiphilic oligopeptide SA2 into nanosized vesicles. More recently, aromatic dipeptides,[12,13] dipeptides containing a C-terminal glutamic acid residue,[14] and a tripeptide[15] have been reported to self-assemble into nanovesicles.

Our contribution in this area is branched amphipathic peptide capsules (BAPCs). They are formed through the spontaneous supramolecular assembly of the two peptides (Ac-FLIVI)$_2$-K-K$_4$-CO-NH$_2$ and (Ac-FLIVIGSII)$_2$-K-K$_4$-CO-NH$_2$ in water. We have introduced the term "capsule" in an effort to avoid confusion between our peptidic nanospheres and traditional lipid vesicles. A history detailing the origins of the BAPCs is described in a recent review.[16] Previous studies that included transmission electron microscopy (TEM) and computational simulations indicated that the hollow capsules are bound by a peptide bilayer.[17] The peptides are mixed as helical monomers in the absence of water, dried, and then hydrated to start the annealing process. BAPCs formation is observed after 30 min with nascent capsules assembling into

Received: March 16, 2017
Revised: June 14, 2017
Published: June 27, 2017

DOI: 10.1021/acs.langmuir.7b00912
Langmuir 2017, 33, 7096−7104

sizes ranging from 20 to 30 nm in diameter.[17] If the peptides are assembled at 25 °C, the nascent capsules undergo fusion and within a few hours form heterogeneous spherical structures that ranged in size (50−200 nm).[18] It was observed that BAPCs formed at 25 °C and then moved to 4 °C for as little as 1 h blocked fusion even when they were returned to elevated temperatures (up to 80 °C). BAPCs prepared at either 4 or 37 °C do not undergo fusion and retain the size of the nascent capsules. Sukthankar et al.[18] examined the temperature dependence on the secondary structure, size, and encapsulation efficiency of BAPCs. The peptides present in the BAPCs adopted different conformations: with 4 °C BAPCs showing mostly random structure, 25 °C BAPCs displaying a mixture of random and beta-structure, and the 37 °C ones being mostly in beta.

Peptide vesicles capable of delivering nucleic acids into cells are also relatively rare. To the best of our knowledge, only two research groups had reported the use of peptide vesicles for gene delivery. Li and co-workers[19] described cationic dipeptides (H-Phe-Phe-NH_2·HCl) that self-assemble into nanotubes and rearrange to form vesicles upon dilution. These vesicles were able to deliver small oligos into cells in culture. Our group demonstrated the ability of BAPCs to deliver plasmid DNA (pDNA) in vivo and in vitro.[20,21] In vitro, BAPCs associated with DNA were capable of delivering plasmid DNA with transfection rates ~55% and minimal cytotoxicity.[21] In vivo, BAPCs were capable of delivering a vaccine DNA encoding the E7 oncoprotein of HPV-16 (pgDE7) in mice. Mice immunized with pgDE7-BAPC nanocapsules complexes constrained tumor growth up to one month after transplantation of tumor cells without significant toxic effects.[21] TEM and AFM analysis showed that BAPCs can act as cationic nucleation centers around which DNA winds generating peptide−DNA complexes with a size ranging from 50 to 100 nm.[21]

All of these published studies utilized a 1:1 ratio of the two peptides (Ac-FLIVI)$_2$-K-K_4-CO-NH_2 and (Ac-FLIVIGSII)$_2$-K-K_4-CO-NH_2 (Figure 1). This ratio was chosen arbitrarily to allow enough of the smaller peptide to line the inner leaflet with the larger sequence making up the outer leaflet of the assembled bilayer to compensate for any strain due to curvature. In this report we prepared BAPCs where the ratio of the two peptides and the annealing temperatures were modified with an eye toward examining how these variables affected the physical properties and gene delivery efficacies (in vitro) of the capsules. BAPCs were prepared with the following (Ac-FLIVI)$_2$-K-K_4-CO-NH_2:(Ac-FLIVIGSII)$_2$-K-K_4-CO-NH_2 ratios −1:0, 0.8:0.2, 0.5:0.5, 0.2:0.8, and 0:1. Also, capsules were annealed at 4, 25, and 37 °C. BAPCs prepared at 4 °C showed the highest efficiency in encapsulating the fluorescent dye Eosin Y and those prepared using just (Ac-FLIVIGSII)$_2$-K-K_4-CO-NH_2 showed the maximal transfection rates. These results suggest that equimolar concentrations of BAPCs are not essential for encapsulating solutes and delivering complexed DNA into living cells.

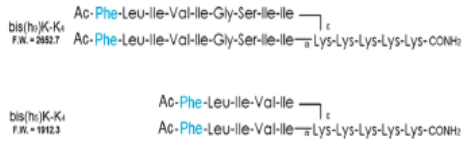

Figure 1. Branched amphipathic peptide capsule (BAPC) forming sequences. The peptides are described in the text as (Ac-FLIVI)$_2$-K-K_4-CO-NH_2 and (Ac-FLIVIGSII)$_2$-K-K_4-CO-NH_2, respectively.

MATERIALS AND METHODS

Peptide Synthesis. Peptides were synthesized by solid phase peptide chemistry on 4-(2,4-dimethoxyphenyl-Fmoc-aminomethyl)-phenoxyacetyl-norleucyl-cross-linked ethoxylate acrylate resin[22] (Peptides International Inc.; Louisville, KY) on a 0.1 mmol scale using Fmoc (*N*-(9-fluorenyl) methoxycarbonyl)/*tert*-butyl chemistry on an ABI Model 431 peptide synthesizer (Applied Biosystems; Foster City, CA) with modified cycles and resin with reduced substitutions. The Fmoc L-amino acids were obtained from Anaspec, Inc. (Fremont, CA). The branch point was introduced by incorporating $N^{\alpha,\varepsilon}$ di-Fmoc-L-lysine in the fifth position from the C-terminus. Deprotection of this moiety leads to the generation of two reactive amino sites, thereby generating the bifurcated peptide branch point. This enables the addition two predominantly hydrophobic N-terminal tail segments FLIVI and FLIVIGSII to the common hydrophilic oligo-lysine segment by the stepwise addition of Fmoc amino acids.[23] The N-termini of the peptides were acetylated on the resin using acetic anhydride/*N*,*N*-diisopropylethylamine/1-hydroxybenzotriazole just prior to cleavage. The peptides were cleaved from the resin using TFA/water (98:2, v/v) for 90 min at RT to generate C-terminal carboxamide. The peptide products were washed 3× with diethyl ether. At this point the two peptides were treated differently. The shorter peptide was redissolved in water prior to lyophilization. The water used throughout this study is first deionized then reverse osmosis treated and finally glass distilled. The larger peptide was dried directly from the ether. The larger peptide has a propensity to form beta-structure in water, leading to the formation of aggregates that persist after lyophilization. Drying directly from ether prevents this. The larger peptide was hydrated just before performing any analysis. The RP-HPLC purified peptides were dried in vacuo and characterized on a Bruker Ultraflex III matrix-assisted laser desorption ionization time-of-flight mass spectrometer (MALDI TOF/TOF) (Bruker Daltonics, Billerica, MA) using 2,5-dihydroxybenzoic acid matrix (Sigma-Aldrich Corp., St. Louis, MO). The dried peptides were stored at room temperature.

Capsule Formation and Encapsulation. The (Ac-FLIVI)$_2$-K-K_4-CO-NH_2 and (Ac-FLIVIGSII)$_2$-K-K_4-CO-NH_2 peptides were dissolved individually in neat 2,2,2-trifluoroethanol. In this solvent the peptides are helical and monomeric, thereby ensuring complete mixing when combined. Concentrations were determined for the stock TFE dissolved samples using the molar extinction coefficient (ε) of phenylalanine residues (two per sequence) at 257.5 nm (195 cm^{-1} M^{-1}).[24,25] The (Ac-FLIVI)$_2$-K-K_4-CO-NH_2 and (Ac-FLIVIGSII)$_2$-K-K_4-CO-NH_2 peptide solutions of known concentration were mixed to yield ratios of 1:0, 0.8:0.2, 0.5:0.5, 0.2:0.8, and 0:1 and then dried in vacuo. BAPCs (50 μM) samples were prepared by hydrating the dried monomeric mixture of the constituent peptides dried from 100% TFE with aqueous Eosin Y (2.13 mM) or Rhodamine 6G (2 mM and 0.1 mM) and then allowed to assemble for 60 min at 4, 25, or 37 °C. Fluorescence of Eosin Y strongly quenched at this concentration. Rhodamine 6G, which is also self-quenching, was used at two concentrations: one that was quenching (2.0 mM) and the other at a concentration that yielded maximum fluorescence (0.1 mM) (Supporting Information Figure S1). The dye-loaded BAPCs were then washed by centrifugation carried out at 14000*g* in Amicon ultra-0.5 mL 30 kDa molecular weight cutoff centrifugal cellulose filters (Millipore, Billerica, MA) using a Thermo Electron Legend 14 personal microcentrifuge (Thermo Fisher Scientific Inc., Waltham, MA) to remove nonencapsulated dye. Samples were then subjected to multiple centrifugation cycles starting with a 5 min preincubation with 200 mM Na-TFA salt. The TFA^- counterion successfully displaces negatively charged Eosin Y associated with the outer capsule surface.[18] For the second−sixth wash cycles, the dye encapsulated capsules were incubated with just water prior to centrifugation. At the conclusion of the sixth spin, the removable-filter unit was inverted and placed in a fresh tube and spun at 2000*g* for 5 min to recover the remaining

DOI: 10.1021/acs.langmuir.7b00912
Langmuir 2017, 33, 7096−7104

volume containing the washed capsules. This sample was then diluted to the desired concentration with water.

For studies examining encapsulation efficiency and temperature effects Eosin Y (Sigma-Aldrich Corp., St. Louis, MO) or Rhodamine 6G (Sigma-Aldrich Corp., St. Louis, MO) was present in the hydration solutions at desired concentrations. After BAPC formation in the presence of either dye (60 min) the samples were passed through a 0.2 μm PTFE syringe filter (Millipore Millex FG, Billerica, MA). Fluorescence measurements of the encapsulated contents were carried out by the excitation of Eosin Y at 490 nm and scanning for observed emissions from 495 to 800 nm with a CARY Eclipse fluorescence spectrophotometer (Varian Inc., Palo Alto, CA) (scan rate: 600 nm/min; PMT detector voltage: 600 V; excitation slit: 10 nm; emission slit: 10 nm) using a 0.3 cm path length quartz cuvette. Standard curves examining the concentration and temperature effects on Eosin Y fluorescence were performed and used to correct data obtained for these effects.

For the temperature studies with the different peptide ratios, changes in the fluorescence intensity of the dye Eosin Y were followed as a function of temperature. The dye was used at a concentration that quenches the fluorescence. Any lysis of the BAPCs would result in an increase in fluorescence intensity. For these studies the BAPCs were prepared at 4 °C for at least an hour before washing. The fluorescence was initially measured at 4 °C followed by jumps to 25 °C and then 37 °C followed in some experiments by 10 °C increases up to 95 °C.

Circular Dichroism Experiments. Circular dichroism (CD) experiments were conducted to analyze conformational changes in secondary structures formed by the water-filled 1 mM BAPCs prepared with the different peptide ratios. Data were collected on a Jasco J-815 CD spectrophotometer (Jasco Analytical Instruments, Easton, MD) using a 0.2 mm path length jacketed cylindrical quartz cuvette (Starna Cells Inc., Atascadero, CA). Spectra were scanned from 260 to 190 nm at a scan rate of 50 nm min^{-1} with 1 nm step intervals. All experimental temperatures were maintained using a heating/cooling fluid circulator (IBM Corp.) connected to the jacketed cuvette. CD spectra were measured in "mdeg" using an average of five scans. The raw data were subtracted from blank at the appropriate temperature and smoothed using a Savitsky–Golay filter[26,27] using Spectra Analysis software provided by the manufacturer (Jasco Inc., Easton, MD). Peptide concentrations were determined using the absorbance of phenylalanine as previously described.[17]

Dynamic Light Scattering and Zeta Potential. Branched amphipathic peptides with varying ratios of $(Ac\text{-}FLIVI)_2\text{-}K\text{-}K_4\text{-}CO\text{-}NH_2$ and $(Ac\text{-}FLIVIGSII)_2\text{-}K\text{-}K_4\text{-}CO\text{-}NH_2$ were hydrated at 4 °C to yield BAPCs incorporating a total peptide concentration of 2 mM. These were maintained at 4 °C for 3 h before bringing them to RT prior to analysis. Dynamic light scattering (DLS) and zeta potential (ZP) analysis were performed using a Zetasizer Nano ZS (Malvern Instruments Ltd., Westborough, MA). The accuracy of the instrument was validated using 30 and 90 nm Nanosphere-NIST traceable mean diameter standards (Thermo Fisher Scientific, Waltham, MA).

Cell Culture. HEK-293 cells were kindly donated by Dr. Tao (Auburn University) and maintained as previously described.[21]

Preparation of DNA-BAPCs Nanoparticles. BAPCs (45 μM) were prepared at different ratios of $(Ac\text{-}FLIVI)_2\text{-}K\text{-}K_4\text{-}CO\text{-}NH_2$ and $(Ac\text{-}FLIVIGSII)_2\text{-}K\text{-}K_4\text{-}CO\text{-}NH_2$ and hydrated at different temperatures (4, 25, and 37 °C). Subsequently, they were mixed with 2.5 μg of pEGFP-N3 (Clontech, Mountain View, CA). The charge ratio (N:P) ratio was 26. The N:P charge ratio for a given complex has been previously defined.[20] Solutions were mixed carefully with a pipet and allowed to stand for 10 min at RT before adding $CaCl_2$, 1.0 mM final concentration. After an additional 30 min incubation period, the solution was added to the cell culture. $CaCl_2$ alone at this concentration was analyzed and did not to enhance DNA uptake or expression.

In Vitro Plasmid Transfection. For transfection experiments, cells were seeded as previously described;[21] 24 h later at 60% confluence, all medium was removed from the wells, and 800 μL of Opti-MEM I Reduced Serum Media was added. Next, 200 μL of BAPCs-DNA nanoparticles was added to cells. The BACPs-DNA complexes were incubated with cells for 4–6 h at 37 °C/5% CO_2. After the incubation period, media and transfection reagent were removed and replaced with 1 mL of fresh DMEM containing 10% FBS in each well. The cells were returned to the incubator for 48 h. After this incubation period, transfection efficiency was monitored by fluorescence microscopy and quantified by flow cytometry (Accuri C6 Flow Cytometer, Beckon Dickson, San Jose, CA). Ghost Dye Red 780 (Tonbo Biosciences, San Diego, CA) was used to identify and then exclude dead cells from the analysis. Nontransfected cells containing only DNA and $CaCl_2$ (1 mM) were used as a control. For the positive control, cells were transfected with jetPRIME (PolyPlus, Strasbourg, France) following the manufacturer protocol. Data were analyzed using the FlowJo software V.10.1 (TreeStar, Ashland, OR).

Fluorescence Microscope Images. Images were obtained using an Eclipse Ti2 inverted microcopy system (Nikon, Melville, NY).

RESULTS AND DISCUSSION

Physicochemical and Structural Properties of BAPCS Assembled at Different Temperatures and with Different $(Ac\text{-}FLIVI)_2\text{-}K\text{-}K_4\text{-}CO\text{-}NH_2$: $(Ac\text{-}FLIVIGSII)_2\text{-}K\text{-}K_4\text{-}CO\text{-}NH_2$ Ratios. All of our published studies were performed using the equimolar ratios of $(Ac\text{-}FLIVI)_2\text{-}K\text{-}K_4\text{-}CO\text{-}NH_2$ and $(Ac\text{-}FLIVIGSII)_2\text{-}K\text{-}K_4\text{-}CO\text{-}NH_2$. Early in our deliberations on how best to prepare BAPCs, we made the assumption that an equimolar ratio of the large and small sequences would be a reasonable starting point. It was reasoned that if the branched peptides formed vesicle-like structures, including the shorter $(Ac\text{-}FLIVI)_2\text{-}K\text{-}K_4\text{-}CO\text{-}NH_2$ sequence with the longer $(Ac\text{-}FLIVIGSII)_2\text{-}K\text{-}K_4\text{-}CO\text{-}NH_2$ could ease any strain due to curvature and thereby facilitate assembly. When we examined the actual distribution of the two peptides in the assembled bilayers we observed that the outer leaflet contained both sequences with the larger peptide predominating. Exact ratios were difficult to assess due to the variability involved in the self-assembly process. The ability of this ratio to meet the original design goals left studying the individual peptides as well as all other ratios untested.

In Sukthankar et al.[19] equimolar ratios yielded BAPCs with unusual thermal transitions. Capsules prepared at 25 °C spontaneously fused to form a heterogeneous population of larger spherical structures while those prepared at 4 and 37 °C were uniform spheres with a fixed diameter of 20–30 nm. The secondary structure of the peptides in the assemblies were predominantly random coil or beta-structures for 4° and 37 °C, respectively. The 25 °C peptides were a mixture of the two but transitioned to beta as the capsules grew in size.

In an effort to design BAPCs with new properties, BAPCs (50 μM) were prepared using three different $(Ac\text{-}FLIVI)_2\text{-}K\text{-}K_4\text{-}CO\text{-}NH_2$: $(Ac\text{-}FLIVIGSII)_2\text{-}K\text{-}K_4\text{-}CO\text{-}NH_2$ ratios (1:0, 0.5:0.5, and 0:1). They were annealed at 4 °C and then tested for thermal stability. The dye Eosin Y was encapsulated at a concentration that shows significant quenching (2.1 mM in water). The washed dye encapsulated BAPCs were ramped rapidly to 25 °C and then heated to 95 °C with 10° increments over a period of 2 h. As depicted in Figure 2, the three different BAPC preparations (1:0 (panel A), 0.5:0.5 (panel B), and 0:1 (panel C) clearly trap the dye during capsule formation and remained intact throughout the experiment as judged by the absence of dye release. At the end of each experiment an equal volume of TFE was added to the sample to yield a 50% TFE solution that causes the capsules to disassemble thereby releasing the dye (dotted line), leading to the expected increase in fluorescence intensity. A 0.5× dilution constant was factored in while graphing the increase in fluorescence intensity due to

DOI: 10.1021/acs.langmuir.7b00912
Langmuir 2017, 33, 7096–7104

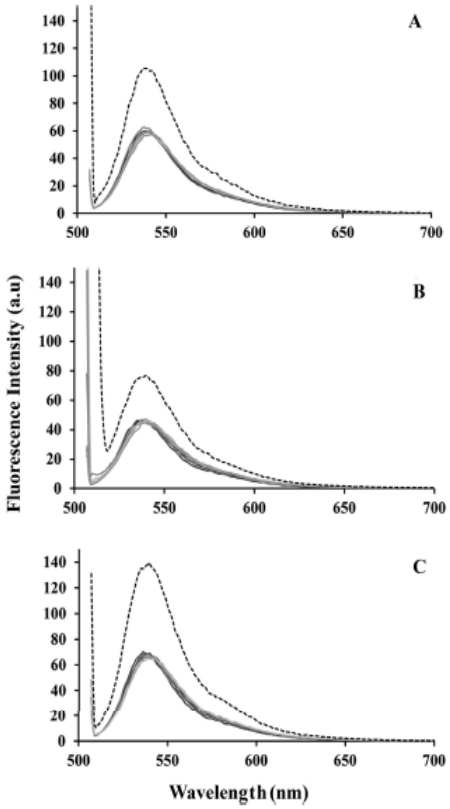

Figure 2. Thermal stability of BAPCs prepared at different peptide ratios. Eosin Y containing BAPCs (50 μM) were prepared at 4 °C using the ratios 1:0 (A), 0.5:0.5 (B), and 0:1 (C). The temperature was then ramped to 95 °C over 2 h. The BAPCs were disassembled in the presence of 50% TFE at the end of the experiment (dashed line).

dye release, to account for the 50% dilution of the sample due to the addition of TFE. This was done for clarity since the released dye curve falls on top of the other spectra. The 50% TFE curve was also corrected for any fluorescence enhancement due to solvent. These results indicate that a mixture of longer and shorter branched peptides is not required for BAPC formation and that encapsulated solutes can be released upon disassembly in 50% TFE solutions.

The peptide and dye concentrations for each ratio were identical; however, the amount of encapsulation was less in the BAPCs prepared with the equimolar peptide ratio. To verify this observation, BAPCs were prepared with the following ratios (1:0, 0.8:0.2, 0.5:0.5, 0.2:0.8, and 0:1). For this experiment the annealing temperatures were included as a second variable. All of the ratios formed BAPCs at the three different temperatures (Figure 3). Previously, Sukthankar et al.[19] showed that encapsulation efficiencies for the equimolar ratio were highest at 4 °C and decreased at higher assembly temperatures. This study reveals a similar pattern with the 4 °C assemblies showing the highest encapsulation values. Over the conditions tested here is roughly a 4-fold difference in the amount encapsulated comparing the highest loading with the 4 °C assembly of just (Ac-FLIVI)-K-K_4-CO-NH_2 compared with

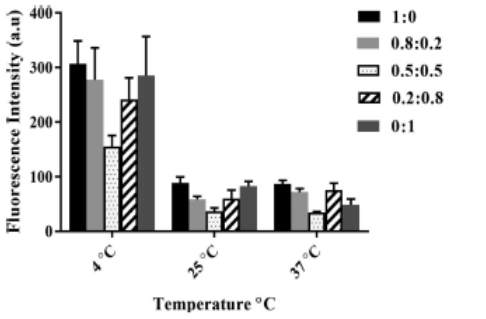

Figure 3. Temperature dependence on dye encapsulation for BAPCs prepared at different peptide ratios for 1 h. Data represent mean values + SEM of three experiments combined.

each temperature grouping the highest values are recorded for the more homogeneous ratios, with the equimolar ratio showing the least amount of trapped solutes during assembly. While the net encapsulation values decreased with increasing temperatures the pattern of increased encapsulation at the more homogeneous ratios was preserved. The trend showing increased encapsulation at the more homogeneous ratios was unexpected. The 0.5:0.5 ratio, which showed the lowest level of dye encapsulation, could be the result of a slower annealing rate or a higher level of precipitation. Examining the Eosin Y encapsulation process carefully we observed tiny colored aggregates in many of the samples. These samples are always filtered using a 0.2 μm PTFE syringe filter. The weights of the dried residue left on the filters showed that the equimolar ratio of peptide showed had the highest level of aggregation, double that of a homomeric ratio. A possible explanation for this is discussed in the section that shows the zeta potential for BAPCs formed with the different peptide ratios. This result supports the idea that lower encapsulation is the result of reduced concentrations of the equimolar ratio peptide assembly in the presence of the Eosin Y.

To further test these results, an encapsulation time-course experiment was performed over 24 h at 4 °C using Rhodamine 6G (Figure 4). This dye is positively charged and does not interact as strongly with the cationic surface of the capsules. No precipitation was observed when this dye (at quenching concentrations 2.0 mM) was mixed with any of the peptide ratios. The dye was also used at a concentration (0.1 mM) that provides maximum fluorescence. Together, these conditions provide for fluorescence intensities that give the best opportunity to identify any changes in encapsulation over time. The $(Ac\text{-}FLIVI)_2$-K-K_4-CO-NH_2 only (Figure 4A) and $(Ac\text{-}FLIVIGSII)_2$-K-K_4-CO-NH_2 only (Figure 4B) BAPCs along with the 0.5:0.5 ratio (Figure 4C) were tested. With each BAPC ratio, self-assembly at 4 °C was essentially complete by 60 min. No significant statistical difference was seen for the times tested. These results supports the idea that the decreased encapsulation efficiency observed for Eosin Y with the equimolar ratio is a consequence of the loss of peptide due to precipitation.

While annealing temperature had no effect on the rates of assembly, earlier studies on BAPCs prepared using an equimolar mixture of $(Ac\text{-}FLIVI)_2$-K-K_4-CO-NH_2 and $(Ac\text{-}FLIVIGSII)_2$-K-K_4-CO-NH_2, the annealing temperature had a profound effect on the secondary structure of the assembled

DOI: 10.1021/acs.langmuir.7b00912
Langmuir 2017, 33, 7096−7104

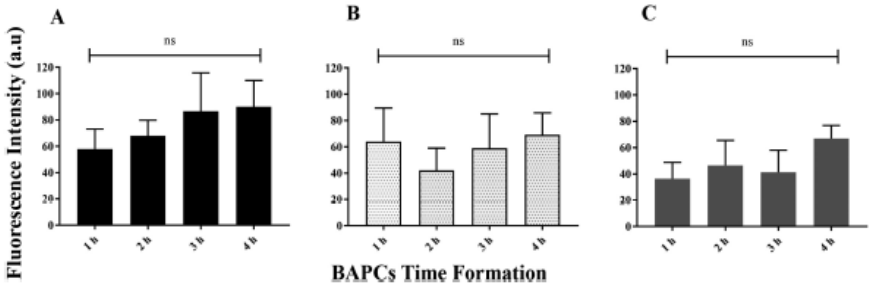

Figure 4. Time dependence at 4 °C for loading of Rhodamine 6G (100 μM) for BAPCs prepared at different peptide ratios (1:0 panel A), 0.5:0.5 (panel B), and 0:1. (panel C). Data represent mean values + SEM of three experiments combined. Differences between values were compared by 2-way ANOVA using Bonferroni as post-test. Nonstatistical significance (ns) was considered when $p > 0.05$.

displayed predominantly random coil at 4 °C, mixed random and beta at 25 °C and beta at 37 °C. To better understand the effects of peptide ratio on structure in the assembled peptides, the secondary structures were analyzed by circular dichroism (CD).

This analysis was repeated for the five different ratios to examine the contributions of the two peptide sequences to the assembled structures. For these CD studies, 1 mM BAPCs were prepared using the five ratios used in Figure 3 assembled at 4, 25, and 37 °C for 75 min before recording the CD spectra at 25 °C (Figure 5). The BAPCs composed of 100% (Figure 5A) and 80% (Figure 5B) $(Ac\text{-}FLIVI)_2\text{-}K\text{-}K_4\text{-}CO\text{-}NH_2$ display mostly random coil secondary structure with a strong minimum at 198 nm at all three temperatures. The 100% $(Ac\text{-}FLIVI)_2\text{-}K\text{-}K_4\text{-}CO\text{-}NH_2$ BAPCs (Figure 5A) shows a minor minimum at 222 nm, suggesting a minor helical component. This structure is absent in the 80% $(Ac\text{-}FLIVI)_2\text{-}K\text{-}K_4\text{-}CO\text{-}NH_2$ BAPCs (Figure 5B). The equimolar ratio (Figure 5C) adopts the random coil conformation only at 4 °C. With increasing temperatures (25 and 37 °C) a mixture of random (198 nm) and beta structures (218 nm) are present. The 20% (Figure 5D) $(Ac\text{-}FLIVI)_2\text{-}K\text{-}K_4\text{-}CO\text{-}NH_2$ BAPCs show increasing amounts of beta with a decrease in random coil at elevated temperatures. The 0% (Figure 5E) $(Ac\text{-}FLIVI)_2\text{-}K\text{-}K_4\text{-}CO\text{-}NH_2$ BAPCs shows essentially only beta structure at all temperatures. Examining all of these data reveals that $(Ac\text{-}FLIVI)_2\text{-}K\text{-}K_4\text{-}CO\text{-}NH_2$ is unstructured while $(Ac\text{-}FLIVIGSII)_2\text{-}K\text{-}K_4\text{-}CO\text{-}NH_2$ adopts beta structure and that mixtures of the two peptides produce BAPCs with both structures present. A summary of this data is shown in Table S1 (Supporting Information). From previous studies[22] only BAPCs showing mix conformations underwent fusion. Those prepared under conditions where random or beta structure predominated, were uniform and size stable 20−30 nm capsules that formed and remained as such when transitioned to higher temperatures.

A composite figure comparing the final spectra for the 4 °C annealing temperature is shown in Figure 6. This figure shows the relative contributions of the two sequences to the final structure of the peptides in the assembled BAPCs.

The BAPC bilayers composed of just unstructured peptides should show a decrease in thermal stability over those where beta-structure interpeptide hydrogen bonding predominates. Over the temperature range tested (up to 95 °C) there was no difference in stability (based on retention of the quenched Eosin Y). Hydrophobic interactions must be providing the cohesive forces that maintain their assembled structures to 95 °C. Perhaps at temperatures above the range we tested, differences in thermal stability will become apparent. The $\pi-\pi$ stacking interactions of the phenylalanines that populate the bilayer interface do not appear to be involved based on atomistic simulations previously reported.[28]

The observation that all of these mixed and more homogeneous structures support assembly and temperature stability imply that these structural arrangements have to be stabilized in different ways. The extended random coil structures would have to form bilayers with a longer cross-sectional distance or as random coils they could have a shorter cross-sectional distance if they interdigitated. Analogously, the predominantly beta-sheet containing BAPCs should have the shortest cross-sectional distance. Differences in the thickness of the bilayer should affect the size of the BAPCs.

To test this hypothesis, BAPC's prepared at 4 °C (3 h) were analyzed at 25 °C by dynamic light scattering (DLS). Under these conditions the BAPCs form uniform stable structures, even when moved to the higher temperature. Three separate preparations were analyzed (Figure 7). This experiment clearly demonstrates that BAPCs prepared with different peptide ratios adopt different sizes to accommodate for aggregate differences in secondary structure. DLS experiments were conducted using 1 mM solutions of the peptides with the five $(Ac\text{-}FLIVI)_2\text{-}K\text{-}K_4\text{-}CO\text{-}NH_2$ to $(Ac\text{-}FLIVIGSII)_2\text{-}K\text{-}K_4\text{-}CO\text{-}NH_2$ ratios (1:0, 0.8:0.2, 0.5:0.5, 0.2:0.8, and 0:1). The average diameters (in nm) observed were 45.9 ± 4.7, 42.2 ± 5.8, 24.0 ± 2.8, 19.5 ± 2.4, and 11.2 ± 2.1, respectively. The DLS value observed for the 0.5:0.5 ratio is in excellent agreement with those observed in our earlier TEM experiments.[19] Prior to performing the experiments described herein, we hypothesized that the longer peptide sequence would yield larger BAPCs. Given the present findings the larger peptide's propensity to form compacted beta-structure prevails, thereby yielding the smallest structures.

Another interesting observation is that despite their size differences, equimolar batches of the different ratios encapsulate the same amount of dye. We observe less than nanomolar concentrations of free peptide by mass spectrometry after filtering BAPCs with a 30 kDa cutoff Amicon cellulose centrifugal filter (Merck). This results points to an extremely low critical association constant. Our best guess is that nearly all of the peptides participate in BAPC assembly or aggregation, with the pure $(Ac\text{-}FLIVIGSII)_2\text{-}K\text{-}K_4\text{-}CO\text{-}NH_2$ yielding a greater number of smaller BAPCs while the shorter $(Ac\text{-}FLIVI)_2\text{-}K\text{-}K_4\text{-}CO\text{-}NH_2$ forming fewer larger BAPCs while the peptides are in an extended conformation. To further investigate the biophysical properties of BAPCs, we analyzed the ZP for the five ratios analyzed by DLS (1:0, 0.8:0.2, 0.5:0.5,

DOI: 10.1021/acs.langmuir.7b00912
Langmuir 2017, 33, 7096−7104

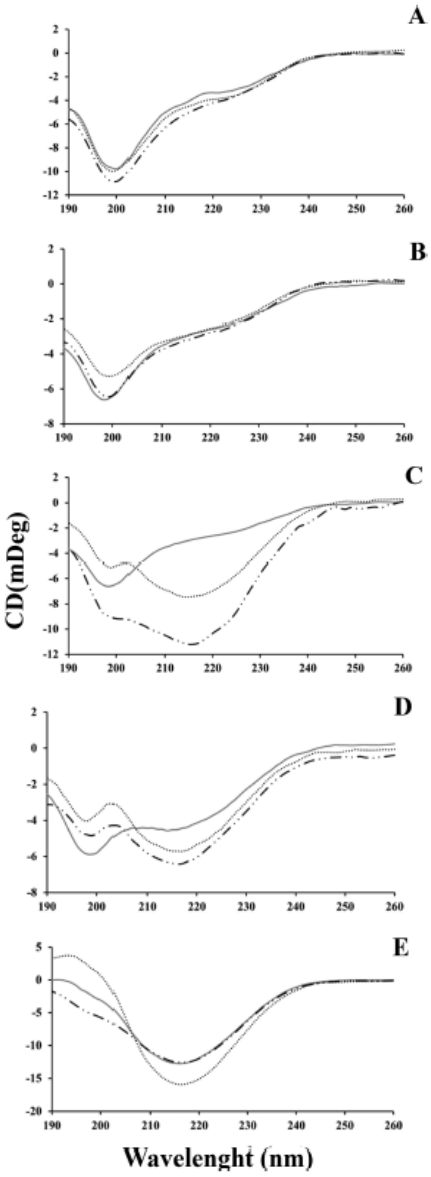

Figure 5. Circular dichroism spectra for five different ratios prepared at 4 °C (gray), 25 °C (dotted), or 37 °C (dot-dashed) for 75 min. All scans were performed at 25 °C. Panels A−E represent the ratios 0:1, 0.8:0.2, 0.5:0.5, 0.2:0.8, and 0:1 of $(Ac\text{-}FLIVI)_2\text{-}K\text{-}K_4\text{-}CO\text{-}NH_2$:$(Ac\text{-}FLIVIGSII)_2\text{-}K\text{-}K_4\text{-}CO\text{-}NH_2$, respectively.

0.2:0.8, and 0:1). The 1:0, 0.8:0.2, 0.2:0.8, and 0:1 ratios showed similar ZP's. The basis for the 0.5:0.5 ratio showing the higher ZP (~57 mV) is unclear. We hypothesized that this higher surface charge at this ratio affects assembly in the presence of Eosin Y leading to precipitation.

In Vitro Transfection Efficiency of BAPCS Assembled at Different Temperatures and with Different $(Ac\text{-}FLIVI)_2\text{-}K\text{-}K_4\text{-}CO\text{-}NH_2$:$(Ac\text{-}FLIVIGSII)_2\text{-}K\text{-}K_4\text{-}CO\text{-}NH_2$ Ratios. In a recent publication we demonstrated the ability of

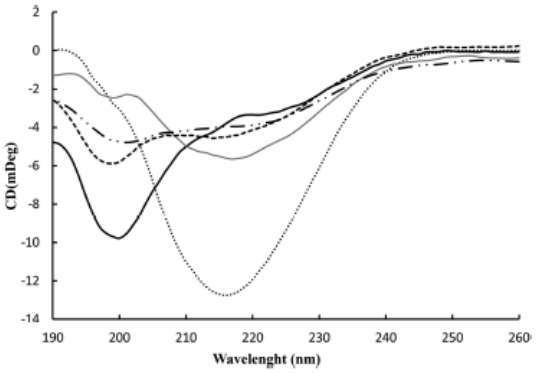

Figure 6. CD spectra of BAPCs composed of different ratios of $(Ac\text{-}FLIVI)_2\text{-}K\text{-}K_4\text{-}CO\text{-}NH_2$:$(Ac\text{-}FLIVIGSII)_2\text{-}K\text{-}K_4\text{-}CO\text{-}NH_2$ assembled at 4 °C. The spectra shown are 1:0 (dark solid line), 0.8:0.2 (dashed line), 0.5:0.5 (dot/dashed line), 0.2:0.8 (light gray line), and 0:1 (dotted line).

nanosized BAPCs to deliver plasmid DNA of different size into cells in culture.[21] Transfection rates of ~55% were achieved with minimal cytotoxicity. The transfection protocol was optimized by testing different BAPCs concentrations and transfection buffers. Cells were also incubated with the BAPCs−DNA complexes for periods ranging from 2 to 12 h. Optimal transfection rates were obtained using BAPCs at 45 μM and 2.5 μg of DNA with an incubation period of 4−6 h in Opti-MEM I Reduced Serum Media.[21] BAPCs were prepared using a equimolar concentration of $(Ac\text{-}FLIVI)_2\text{-}K\text{-}K_4\text{-}CO\text{-}NH_2$:$(Ac\text{-}FLIVIGSII)_2\text{-}K\text{-}K_4\text{-}CO\text{-}NH_2$. They were annealed at 25 °C and subsequently incubated at 4 °C for 1 h and then rewarmed to 25 °C, thereby fixing their size (20−30 nm). In this article, we analyzed how transfection efficiency was affected by preparing BAPCs at different temperatures and different peptide ratios. BAPCs were prepared with the following $(Ac\text{-}FLIVI)_2\text{-}K\text{-}K_4\text{-}CO\text{-}NH_2$:$(Ac\text{-}FLIVIGSII)_2\text{-}K\text{-}K_4\text{-}CO\text{-}NH_2$ ratios −1:0, 0.5:0.5, and 0:1. Also, capsules were annealed at 4, 25, and 37 °C.

HEK-293 cells were incubated with BAPCs associated with a 4.7 kb GFP-encoding plasmid and transfection efficiency was monitored qualitatively by fluorescence microscopy and quantified using fluorescence-activated cell sorting (FACS). Ghost Dye Red 780 was used to identify and then exclude dead cells from the analysis. Dead cells with compromised membranes allow Ghost Dye to permeate and bind amine groups of intracellular proteins resulting in fluorescence much brighter than live cells which are impermeant to Ghost Dye.[29] We selected this dye because the emission peak is 780 nm and do not overlap with the emission peak of GFP (509 nm), thus ensuring the exclusion of false positives. As shown in Figure 9A−D, the percent of dead cells is minimum for all the formulations tested (<1%), proving that BAPCs are extremely biocompatible. Maximal transfection rates were observed for BAPCs annealed at 4 and 37 °C using just $(Ac\text{-}FLIVIGSII)_2\text{-}K\text{-}K_4\text{-}CO\text{-}NH_2$ (0:1 ratio) (Figure 8A), and there was no significant difference between this ratio and the popular commercial transfection reagent (JetPRIME) (Figure 8A). For BAPCs prepared at 4 °C the size decreases from 46 to 25 to 10 nm (Figure 7A), and the transfection rate increases from ~39% to 41% to 70% (Figure 8B). Furthermore, BAPCs

DOI: 10.1021/acs.langmuir.7b00912
Langmuir 2017, 33, 7096−7104

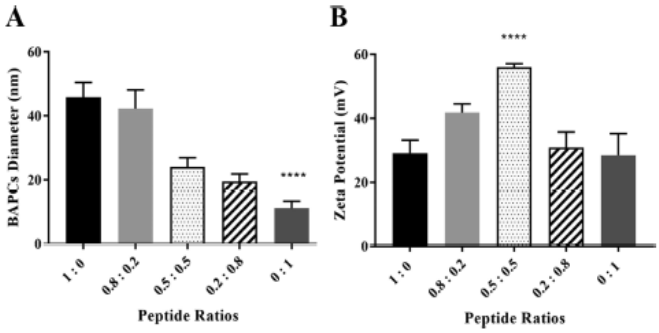

Figure 7. Average diameter (A) and zeta potential (B) of BAPCs formed at five different $(Ac\text{-}FLIVI)_2\text{-}K\text{-}K_4\text{-}CO\text{-}NH_2$:$(Ac\text{-}FLIVIGSII)_2\text{-}K\text{-}K_4\text{-}CO\text{-}NH_2$ ratios. BAPCs solutions (1 mM) were hydrated at 4 °C and scanned at 25 °C. Data represent mean values + SEM of three experiments combined. Differences between values were compared by 2-way ANOVA using Bonferroni as post-test. Statistical significance: (****)$p < 0.0001$, 0:1 vs 0.5:0.5 (A) and 0:1 vs 0.5:0.5 (B).

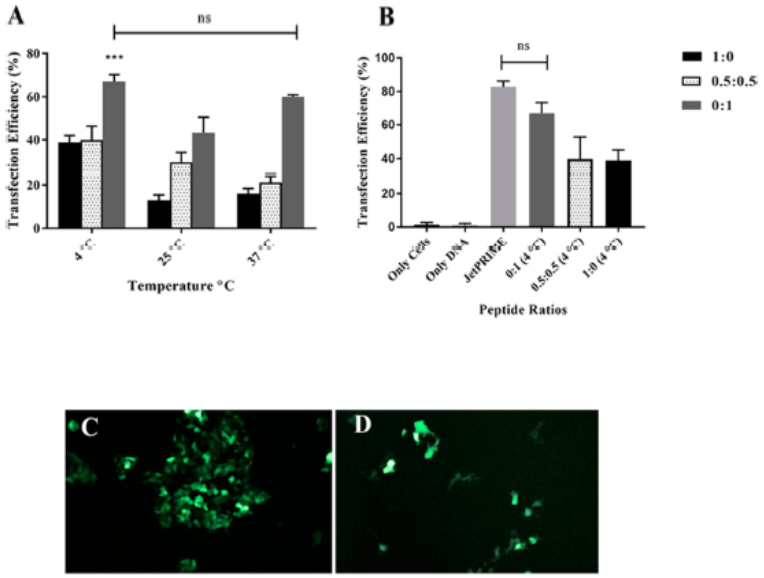

Figure 8. Transfection efficiency of BAPCs-DNA nanoparticles formed at different $(Ac\text{-}FLIVI)_2\text{-}K\text{-}K_4\text{-}CO\text{-}NH_2$:$(Ac\text{-}FLIVIGSII)_2\text{-}K\text{-}K_4\text{-}CO\text{-}NH_2$ ratios and annealed at different temperatures. HEK-293 cells transfected with BAPCs solutions hydrated at 4, 25, and 37 °C and subsequently mixed with 2.5 μg of GFP-encoding plasmid (A). HEK-293 transfected with BAPCs solutions hydrated only at 4 °C and subsequently mixed with 2.5 μg of GFP-encoding plasmid. Positive (JetPRIME) and negative (only DNA) controls were included. (B) Fluorescence microscope images of HEK-293 cells transfected only with $(Ac\text{-}FLIVIGSII)_2\text{-}K\text{-}K_4\text{-}CO\text{-}NH_2$ (C) and only with $(Ac\text{-}FLIVI)_2\text{-}K\text{-}K_4\text{-}CO\text{-}NH_2$ (D). Data represent mean values + SEM of three experiments combined. Differences between values were compared by 2-way ANOVA using Bonferroni as post-test. Statistical significance: (****)$p < 0.0001$, 0:1 vs 0.5:0.5 and 1:0. Nonstatistical significance (ns) was considered when $p > 0.05$.

annealed at 4 and 37 °C displayed beta-structure (Table 1S and Figure 5), suggesting than not only the size but also the secondary structure (beta-structure) are influencing transfection rates.

By exploring this alternative method to assemble BAPCs, we were able to enhance transfection efficiency ~15% (compared with our previous method) while maintaining low cytotoxicity as demonstrated with flow cytometry analysis.

■ CONCLUSIONS

Although our initial assumption has been that BAPC formation required both longer and shorter branched amphipathic peptides, the results presented above show that BAPCs can be prepared from either of the two peptides by themselves or mixtures thereof. The shorter peptide $(FLIVI)_2\text{-}K\text{-}K_4\text{-}CO\text{-}NH_2$ imparts random secondary structure to the BAPCs at each temperature. The larger peptide $(FLIVIGSII)_2\text{-}K\text{-}K_4\text{-}CO\text{-}NH_2$ folds, yielding beta-structure at all temperatures above 4 °C. Combining the peptides generates mixed secondary structures. All ratios resulted in thermally stable constructs. The results of this experiment show that we can now prepare stable, homogeneous BAPCs that can be made to incrementally vary in diameter from ~10 to 45 nm.

Many of our most current applications involve the delivery of dsDNA and dsRNA, which bind to the surface of preformed BAPCs. In this report we demonstrated that the ratio of the two peptides and the annealing temperatures affected the delivery efficiencies of DNA in HEK-293 cells. Previously, we reported that BAPCs (equimolar concentration) annealed at 25 °C and subsequently incubated at 4 °C for 1 h and then

DOI: 10.1021/acs.langmuir.7b00912
Langmuir 2017, 33, 7096−7104

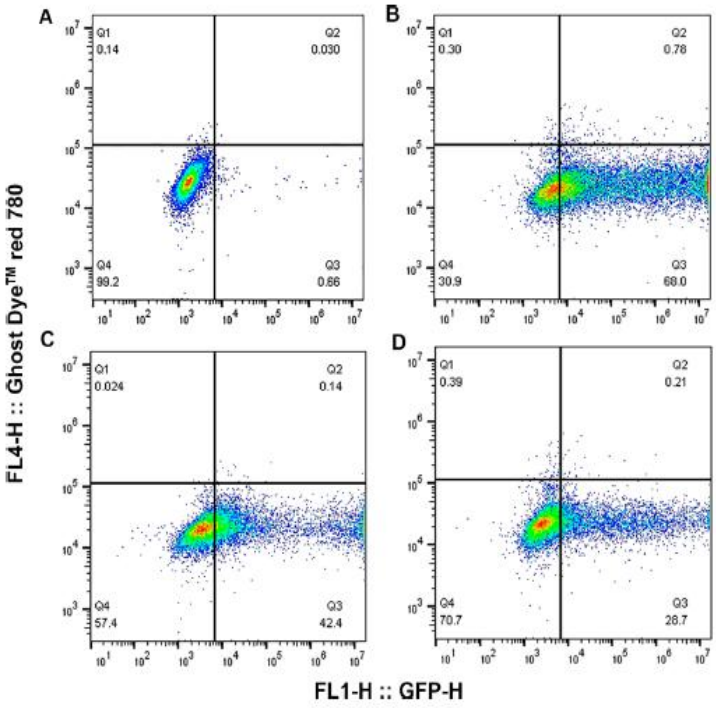

Figure 9. Flow cytometry analysis of GFP-expressing HEK-293 cells after 48 h post-transfection with only cells (A) 1:0, (B) 1:1 (C), and 0:1 (D). BAPCs were hydrated at 4 °C; HEK-293 cells were incubated with the nanoparticles for 4 h in reduced serum media and 1 mM $CaCl_2$.

rewarmed to 25 °C achieved transfection rates of ~55%. Higher transfection rates were observed in this experiments. BAPCs annealed at 4 and 37 °C using just $(Ac\text{-}FLIVIGSII)_2\text{-}K\text{-}K_4\text{-}CO\text{-}NH_2$ (0:1 ratio) displayed efficiencies approaching 70%. It is noteworthy that those annealing temperatures (4 and 37 °C) generated beta secondary structure. The ratio (0:1) generated BAPCs with sizes ~10 nm and ZP (~25 mV). Overall, these results suggested that those parameters are critical factors influencing the BAPCs' ability to deliver nucleic acids into cells. Further studies will consist in studying the morphologies of the BAPCs–DNA complexes that generated the highest delivery rates.

■ ASSOCIATED CONTENT

Supporting Information

The Supporting Information is available free of charge on the ACS Publications website at DOI: 10.1021/acs.langmuir.7b00912.

Fluorescence scans of Rhodamine 6G at different concentrations (Figure **1S**) and a summary of the secondary structures for BAPCs prepared at different ratios and temperatures (Figure **2S**) (PDF)

■ AUTHOR INFORMATION

Corresponding Author

*E-mail jtomich@ksu.edu (J.M.T.).

ORCID

John M. Tomich: 0000-0001-7848-8307

Author Contributions

S.d.M.B. and L.A.A. made equal contributions.

Notes

The authors declare no competing financial interest.

■ ACKNOWLEDGMENTS

This publication is contribution number 16-376-J from the Kansas Agricultural Experiment Station. Partial support for this project was provided by the Terry Johnson Cancer Center at Kansas State University (Innovation Award to J.M.T. and summer graduate research support to S.K.W). L.A.A. acknowledges financial support from Auburn University Cellular and Molecular Biosciences Peaks of Excellence Program. The scholarship award to S.B. was provided by the Coordenação de Aperfeiçoamento de Pessoal de Nível Superior (CAPES) Process number PDSE-99999.007690/2014-02; Affiliation: CAPES Foundation, Ministry of Education, Brasilia, DF, Brazil. We thank Prof. Allan E. David (Samuel Ginn College of Engineering, Auburn University) for his contribution on the ZP assays.

■ REFERENCES

(1) Discher, D. E.; Eisenberg, A. Polymer vesicles. *Science* **2002**, *297*, 967–973.

(2) Bellomo, E. G.; Wyrsta, M. D.; Pakstis, L.; Pochan, D. J.; Deming, T. J. Stimuli-responsive polypeptide vesicles by conformation-specific assembly. *Nat. Mater.* **2004**, *3*, 244–248.

(3) Holowka, E. P.; Pochan, D. J.; Deming, T. J. Charged polypeptide vesicles with controllable diameter. *J. Am. Chem. Soc.* **2005**, *127*, 12423–12428.

(4) Kabanov, A. V.; Batrakova, E. V.; Alakhov, V. Y. Pluronic block copolymers as novel polymer therapeutics for drug and gene delivery. *J. Controlled Release* **2002**, *82*, 189–212.

DOI: 10.1021/acs.langmuir.7b00912
Langmuir 2017, 33, 7096–7104

(5) Ghosh, S.; Reches, M.; Gazit, E.; Verma, S. Bioinspired design of nanocages by self-assembling triskelion peptide elements. *Angew. Chem., Int. Ed.* **2007**, *46*, 2002−2004.
(6) Akter, N.; Radiman, S.; Mohamed, F.; Reza, M. I. Self-assembled potential bionanocarriers for drug delivery. *Mini-Rev. Med. Chem.* **2013**, *13*, 1327−39.
(7) Fletcher, J. M.; Harniman, R. L.; Barnes, F. R.H.; Boyle, A. L.; Collins, A.; Mantell, J.; et al. Self-Assembling Cages from Coiled-Coil Peptide Modules. *Science* **2013**, *340*, 595−599.
(8) Vauthey, S.; Santoso, S.; Gong, H.; Watson, N.; Zhang, S. Molecular self-assembly of surfactant-like peptides to form nanotubes and nanovesicles. *Proc. Natl. Acad. Sci. U. S. A.* **2002**, *99*, 5355−5360.
(9) Matsuura, K.; Murasato, K.; Kimizuka, N. Artificial peptide-nanospheres self-assembled from three-way junctions of β-sheet-forming peptides. *J. Am. Chem. Soc.* **2005**, *127*, 10148−10149.
(10) Matsuura, K.; Watanabe, K.; Sakurai, K.; Matsuzaki, T.; Kimizuka, N. Self-assembled synthetic viral capsids from a 24-mer viral peptide fragment. *Angew. Chem., Int. Ed.* **2010**, *49*, 9662−9665.
(11) Van Hell, A. J.; Costa, C. I.; Flesch, F. M.; Sutter, M.; Jiskoot, W.; Crommelin, D. J. A.; Hennink, W. E.; Mastrobattista, E. Self-assembly of recombinant amphiphilic oligopeptides into vesicles. *Biomacromolecules* **2007**, *8*, 2753−2761.
(12) Reches, M.; Gazit, E. Formation of Closed-Cage Nanostructures by Self-Assembly of Aromatic Dipeptides. *Nano Lett.* **2004**, *4*, 581−585.
(13) Mishra, A.; Panda, J. J.; Basu, A.; Chauhan, V. S. Nanovesicles Based on Self-Assembly of Conformationally Constrained Aromatic Residue Containing Amphiphilic Dipeptides. *Langmuir* **2008**, *24*, 4571−4576.
(14) Naskar, J.; Roy, S.; Joardar, A.; Das, S.; Banerjee, A. Self-assembling dipeptide-based nontoxic vesicles as carriers for drugs and other biologically important molecules. *Org. Biomol. Chem.* **2011**, *9*, 6610−6615.
(15) Koley, P.; Pramanik, A. Multilayer vesicles, tubes, various porous structures and organo gels through the solvent-assisted self-assembly of two modified tripeptides and their different applications. *Soft Matter* **2012**, *8*, 5364−5374.
(16) Barros, S. M.; Whitaker, S. K.; Sukthankar, P. R.; Gudlur, S.; Warner, M.; Beltrão, E. I. C.; Tomich, J. M. A Review of Solute Encapsulating Nanoparticles used as Delivery Systems with Emphasis on Branched Amphipathic Peptide Capsules. *Arch. Biochem. Biophys.* **2016**, *596*, 22−42.
(17) Sukthankar, P.; Gudlur, S.; Avila, L. A.; Whitaker, S.; Katz, B. B.; Hiromasa, Y.; Gao, J.; Thapa, P.; Moore, D.; Iwamoto, T.; Tomich, J. M. Branched Oligopeptides Form Nano-Capsules with Lipid Vesicle Characteristics. *Langmuir* **2013**, *29*, 14648−14654.
(18) Sukthankar, P.; Whitaker, S. K.; Garcia, M.; Herrera, A.; Boatwright, M.; Prakash, O.; Tomich, J. M. Thermally induced conformational transitions in nascent branched amphiphilic peptide capsules. *Langmuir* **2015**, *31*, 2946−2955.
(19) Yan, X.; He, Q.; Wang, K.; Duan, L.; Cui, Y.; Li, J. Transition of Cationic Dipeptide Nanotubes into Vesicles and Oligonucleotide Delivery. *Angew. Chem.* **2007**, *119*, 2483−2486.
(20) Avila, L. A.; Aps, L. R. M. M.; Sukthankar, P.; Ploscariu, N.; Gudlur, G.; Šimo, L.; Szoszkiewicz, R.; Park, Y.; Lee, S. W.; Iwamoto, T.; Ferreira, L.; Tomich, J. M. Alternate supramolecular structures for different ratios of branched amphiphilic cationic peptide /DNA assemblies: Correlation with gene delivery. *Mol. Pharmaceutics* **2015**, *12*, 706−715.
(21) Avila, L. A.; Aps, L. M. M.; Ploscariu, N.; Sukthankar, P.; Guo, R.; Wilkinson, K. E.; Games, P.; Szoszkiewicz, R.; Alves, R. P. S.; Diniz, M. O.; Fang, Y.; Ferreira, L. C. S.; Tomich, J. M. Gene delivery and immunomodulatory effects of plasmid DNA associated with Branched Amphiphilic Peptide Capsules. *J. Controlled Release* **2016**, *241*, 15−24.
(22) Kempe, M.; Barany, G. CLEAR: A Novel Family of Highly Cross-Linked Polymeric Supports for Solid Phase Synthesis. *J. Am. Chem. Soc.* **1996**, *118*, 7083−7093.
(23) Tomich, J. M.; Wallace, D. P.; Henderson, K.; Brandt, R.; Ambler, C. A.; Scott, A. J.; Mitchell, K. E.; Radke, G.; Grantham, J. J.; Sullivan, L. P.; Iwamoto, T. Aqueous solubilization of transmembrane peptide sequences with retention of membrane insertion and function. *Biophys. J.* **1998**, *74*, 256−267.
(24) Chen, R. F. Measurements of absolute values in biochemical fluorescence spectroscopy. *J. Res. Natl. Bur. Stand., Sect. A* **1972**, *76*, 593−606.
(25) Sponer, H. Remarks on the Absorption Spectra of Phenylalanine and Tyrosine in Connection with the Absorption in Toluene and Paracresol. *J. Chem. Phys.* **1942**, *10*, 672.
(26) Savitzky, A.; Golay, M. J. E. Smoothing and Differentiation of Data by Simplified Least Squares *Procedures. Anal. Chem.* **1964**, *36*, 1627−1639.
(27) Gorry, P. A. General least-squares smoothing and differentiation by the convolution (Savitzky-Golay) method. *Anal. Chem.* **1990**, *62*, 570−573.
(28) Jia, Z.; Whitaker, S. K.; Tomich, J. M.; Chen, J. Organization and Structure of Branched Amphipathic Oligopeptide Bilayers. *Langmuir* **2016**, *32*, 9883−9891.
(29) Kaushik, G.; Venugopal, A.; Ramamoorthy, P.; Standing, D.; Subramaniam, D.; Umar, S.; Jensen, R.; Anant, s.; Mammen, J. M. V. Honokiol inhibits melanoma stem cells by targeting notch signaling. *Mol. Carcinog.* **2015**, *54*, 1710−1721.

DOI: 10.1021/acs.langmuir.7b00912
Langmuir 2017, 33, 7096−7104

7 CONCLUSÕES

- Tanto os peptídeos (h_5)-K-K_4 e (h_9)-K-K_4 isoladamente (1:0 e 0:1), quanto nas proporções de 0.2:0.8 e 0.8:0.2 se mostraram eficientes na formação de nanocápsulas peptídicas com manutenção da resitência e habilidade de encapsulamento observados nas BAPCs formadas a 0.5:0.5 de ambos os peptídeos;
- As BAPCs se mostraram resistentes a uma variação de temperatura na faixa de 4 °C - 95 °C sem ruptura ou liberação do conteúdo encapsulado;
- Quando formadas a 4 °C, 25 °C e 37 °C, as BAPCs preparadas a 4 °C exibiram uma maior eficiência de encapsulamento;
- Os melhores resultados de encapsulamento foram observados nas BAPCs formadas pelos peptídeos isoladamente (1:0 e 0:1) sugerindo que tais proporções resultariam em uma maior quantidade de nanocápsulas ou cápsulas de maior tamanho;
- A análise da estrutura secundária evidenciou que as BAPCs formadas apenas por (h_5)-K-K_4 apresentam uma predominância de cadeias aleatórias, as BAPCs formadas por (h_9)-K-K_4 exibem uma predominância de folhas beta, com as formadas pelas demais proporções sendo dirigidas pela conformação caracterítica do peptídeo presente em maior quantidade;
- Os valores obtidos por espalhamento de luz diâmico demonstraram que as BAPCs possuem um diâmetro médio de 45 nm quando na proporção 1:0, de 22 nm quando a 0.5:0.5 e 10 nm a 0:1 dos peptídeos (h_5)-K-K_4 e (h_9)-K-K_4;
- Tais resultados sugerem que os arranjos beta presentes nas BAPCs formadas pela sequência de (h_9)-K-K_4 promovem um arranjo mais compacto das cadeias peptídicas, resultando em cápsulas menores, enquanto que os arranjos aleatórios das sequências de (h_5)-K-K_4 acabam por gerar cápsulas peptídicas de maior tamanho.
- As BAPCs formadas por $(FLIVIGSII)_2$-K-K_4 apresentam a bicamada de menor espessura;
- As BAPCs de menor tamanho apresentaram a maior taxa de transfecção além do menor valor de citotoxicidade observada.
- Os resultados obtidos demonstram que as BAPCs constituem um sistema nanométrico de grande versatilidade, com o potencial de adaptação para o encapsulamento e transporte de um variado número moléculas e potencialmente úteis para uso no transporte de compostos farmacológicos bem como para técnicas de terapia gênica.

8 APÊNDICE

METODOLOGIA DE FORMAÇÃO DAS BAPCS

Para a preparação das nanocápsulas os peptídeos são inicialmente dissolvidos individualmente em 2,2,2-trifluoroethanol (TFE) puro. Na presença desse solvente, os peptídeos adotam uma estrutura helicoidal onde permanecem na forma monomérica, assegurando assim uma mistura completa das duas sequências, quando combinadas.

Ao mesmo tempo, o TFE assegura a permanência das cadeias em conformação de hélice e na forma monomérica mesmo após o processo de secagem. A concentração do peptídeo dissolvido é então determinada usando a absortividade molar (ε) dos resíduos de fenilalanina (195 M^{-1} cm^{-1} a 257.5 nm) (FASMAN et al., 1976). A partir desse ponto, os dois peptídeos são misturados a uma razão equimolar para alcançar a concentração desejada e então secos a vácuo. Partindo do pressuposto de que nenhum dos peptídeos por si só seria capaz de formar nanocápsulas estáveis, todos os experimentos iniciais se limitaram à razão de 1:1 a fim de assegurar uma adequada concentração do peptídeo de cadeia mais curta necessário à adequação das cadeia nos pontos de curvatura da nanocápsula.

Após a secagem, água destilada à temperatura almejada ou solução aquosa contendo o soluto a ser encapsulado é então adicionado gota a gota e a solução mantida em repouso por 30 minutos, para que ocorra a agregação peptídica e formação das nanocápsulas.

Resumo das tapas de formação das nanocápsulas peptídicas (BAPCs)